

DIFFRACTION SCATTERING OF HADRONS:
THE THEORETICAL OUTLOOK*

Henry D. I. Abarbanel†
Stanford Linear Accelerator Center
Stanford University, Stanford, California 94305

ABSTRACT

This is a review of the salient features of high energy diffraction scattering of hadrons. It begins with a summary of the experimental situation for those processes which persist at very high energies—the diffractive processes—and define the underlying exchange mechanism called the Pomeron. A review is made of the key features of the multiperipheral model, since it lies at the beginning of all studies of diffraction. Its virtues and blemishes are exposed. Then we turn to various models which attempt to add unitarity to the multiperipheral model. From the point of view of the direct channel we consider absorptive models, eikonal models and the multiperipheral bootstrap. The t -channel is taken next, and an exposition of the formulation and major results of Reggeon field theory is given.

(Submitted to Rev. Mod. Phys.)

*Work supported by the U. S. Energy Research and Development Administration.
†On leave of absence from Fermi National Accelerator Laboratory, Box 500,
Batavia, Illinois 60510.

"Et fut une digne parole de Julius Brusus aux ouvriers qui lui offraient pour trois mille écus mettre sa maison en tel point que ses voisins n'y auraient plus la vue qu'ils y avaient: 'Je vous en donnerai,' dit-il, 'six mille, et faites que chacun y voie de toutes parts.'"

de Montaigne, M. (1585-88),
"Du repentir"

I. INTRODUCTION

A very striking phenomenon in the collision of strongly interacting particles (hadrons) is the existence of cross sections which are almost independent of the incident energy. Several examples are shown in Fig. 1 (Kycia, 1974) and included is the proton-proton total cross section which has been measured from threshold up to equivalent laboratory momentum $\approx 1.5 \times 10^3$ GeV/c at the Intersecting Storage Ring (ISR) at CERN. Cross sections which remain constant or perhaps grow slowly with the square of the center-of-mass energy, s , are called diffractive. This alludes to the coherence necessary among the multitude of final states allowed in a large s collision in order to produce a cross section which does not decrease rapidly with s . An excellent example of nondiffractive collisions is pion-nucleon charge exchange (Barnes et al., 1974): $\pi^- p \rightarrow \pi^0 n$, which has been measured up to laboratory momentum ~ 150 GeV/c. The cross section for this process behaves as s^{-1} and becomes very small very quickly (Fig. 2). At 100 GeV/c, for example, it is $3.3 \mu\text{b}$ compared to 20-40 mb for typical diffractive cross sections.

This review is concerned primarily with the theoretical work on the problem of diffraction processes. We will begin with a theorist's eye view of the experimental situation and attempt to identify those aspects of diffractive reactions which are amenable to theoretical discussion now and which, equally interesting to be sure, require further and deeper developments. From this discussion we will extract the following signals of diffraction (Leith, 1974):

1. Cross sections (total, elastic, inclusive) are independent of energy up to powers of $\log s$.
2. The amplitude for diffraction scattering is mainly imaginary.

3. Diffraction amplitudes factorize. This means the ratio of amplitudes for $AB \rightarrow A'B'$ and for $CB \rightarrow C'B'$ is independent of B and B'. Formally one writes for the $AB \rightarrow A'B'$ amplitude T

$$T(AB \rightarrow A'B') = (g_{AA'}) (g_{BB'}) \times \text{factors independent of A, A', B, or B'} \quad (1)$$

4. In the differential cross section $d\sigma/dt$ as a function of four momentum transfer, t , there is a sharp forward peak. The evidence is that this peak becomes sharper as the energy s increases.

5. If diffraction is viewed as mediated by an exchange between hadrons, the exchanged object carries the quantum numbers of the vacuum ($I=0, P=C=+, \dots$), but an effective spin of one.

6. At the vertices AA'-exchanged object or BB'-exchanged object the rule $P_A = P_{A'} (-1)^{J_A - J_{A'}}$, where P_A is parity and J_A is spin, seems to hold.

7. The cross section for particle + target is equal to the cross section for antiparticle + target.

With these phenomena in mind we will proceed to the theoretical side of our discussion. Theories divide more or less neatly into two viewpoints: I. The s-channel view and II. the t-channel view (Fig. 3). These views are represented in Fig. 3 where the collision $AB \rightarrow A'B'$ is portrayed. The total collision energy (squared) in the center-of-mass frame is $s = (p_A + p_B)^2$. The four momentum transferred is $t = (p_A - p_{A'})^2$. For proton-proton scattering the physical range of s and t are $s \geq 4m_p^2$, $-s \lesssim t \lesssim 0$. In diffractive processes s becomes large, while t remains finite and small.

Viewpoint I looks in the direction of s and concentrates on the detailed production mechanisms occurring as intermediate states in the transition from initial to final states. In Fig. 4a, for example, we show the initial AB becoming

the final state A'B' via an intermediate state of N=8 particles. The s-channel viewpoint must treat these intermediate states for each N.

Viewpoint II looks in the direction of t and concentrates on the possible set of exchange mechanisms which may mediate the diffractive scattering. In Fig. 4b a wiggly line is shown as representing this exchange. If the wiggly line carries angular momentum J, then the amplitude T is approximately

$$T_{AB \rightarrow A'B'}(s, t) \underset{\substack{s \rightarrow \infty \\ t \text{ fixed}}}{\sim} s^J g_{AA'}(t) g_{BB'}(t) \quad (2)$$

Since the total cross section for AB \rightarrow anything is given by the optical theorem as

$$\sigma_T^{AB}(s) \propto \frac{1}{s} \text{Im } T_{AB \rightarrow AB}(s, 0) \quad (3)$$

we see that energy independence (up to log s) requires $J \approx 1$. The t-channel viewpoint is thus concerned with the spectrum of possible exchanges with angular momentum in the neighborhood of $J=1$.

In each of these points of view unitarity plays a key role. We can see this directly in the s-channel by looking at the unitarity relation for $T_{AB \rightarrow A'B'}(s, t)$. This gives the imaginary part of T in terms of a sum over all possible intermediate states compatible with conservation laws:

$$\text{Im } T_{AB \rightarrow A'B'}(s, t) = \sum_N T_{AB \rightarrow N} T_{A'B' \rightarrow N}^* \quad (4)$$

as portrayed in Fig. 5. The imaginary part of $T_{AB \rightarrow N}$ is itself linked via unitarity to $T_{AB \rightarrow A'B'}$ and a large number of other states since (symbolically to be sure)

$$\text{Im } T_{AB \rightarrow N} = \sum_M T_{AB \rightarrow M} T_{N \rightarrow M}^* \quad (5)$$

So via unitarity all states which can communicate with each other are linked together. Since the s-channel viewpoint focuses on the $T_{AB \rightarrow N}$ as building blocks and these are connected via the nonlinear unitarity relations to the amplitudes of interest, the complexity of the scattering problem from the s-channel point of view is impressive. Fortunately the number of important intermediate states appears to grow only as $\log s$ (Giacomelli, 1974) rather than as \sqrt{s} which is permitted by energy conservation alone. Nevertheless, $\log s$ is 8 at the highest available energies so multiparticle states and the resulting kinematical complexity is an issue. We will discuss the techniques used to study these questions.

In the t-channel point of view unitarity rises to importance because of the possibility of multiple exchanges. In Fig. 6 we show the wiggly line of Fig. 4b being exchanged twice. Just as multiple particle states in the s-channel give rise to an imaginary part of T and link many amplitudes, so do multiple wiggly exchanges give rise to imaginary parts of T, and these are linked by unitarity. The appropriate form for the unitarity relation when viewed through the t-channel is in terms of t-channel partial wave amplitudes. The question of multiple exchanges becomes crucial in diffraction phenomena because the effective angular momentum of the wiggly exchange is one. When we exchange this twice we have a factor s^{1+1} from the product of the exchanges and a factor s^{-1} from the loop integral implied in Fig. 6. The net amplitude is s^1 which is the same order as the initial process in Fig. 4b.

Unitarity, being nonlinear, is a difficult constraint to impose on a theory. One sure way to achieve it is to write a quantum field theory for whatever processes are deemed important and then solve it. Well, that's a fairly tall order. In the case of the s-channel viewpoint, approximation techniques of one

sort or another have been developed. For the t-channel outlook an effective field theory has been developed which does enforce unitarity (Abarbanel and Bronzan, 1974a,b; Gribov, 1968; Migdal et al., 1974). The other attractive enforcer of unitarity (Chew, 1961) studies the analytic structure of amplitudes and writes dispersion relations which connect amplitudes and imaginary parts. This has proven to be an inappropriate tool for investigating diffraction scattering. Dispersion relations are powerful indeed when the number of intermediate states is small. In diffraction, viewed either from the s-channel or the t-channel, the number of relevant amplitudes to be connected by unitarity is always large. Other tools are required.

This review article is not without bias. My preference for the t-channel view will be reflected both in my emphasis during the discussion of theories and in the much larger and more detailed presentation I shall give it. The major portion of this review will be devoted to an explanation of the developments in the t-channel viewpoint which go under the names of Reggeon field theory (Abarbanel and Bronzan, 1974a,b; Abarbanel et al., 1975c; Migdal et al., 1974) or Reggeon calculus (Gribov, 1968). The Reggeon of paramount interest in diffractive processes is that which carries vacuum quantum numbers and is pleasantly named the Pomeron after the Soviet physicist I. Ya. Pomeranchuk who first discussed many of its properties (Pomeranchuk, 1958). From either point of view (s or t) it is the Pomeron whose properties we seek. As promised we begin with the theorist's summary of the experimental facts.

II. REVIEW OF THE EXPERIMENTAL SITUATION

In the introduction we made a list of the features which signal diffractive processes. Now the proposal is to go down this list and discuss each item. After presenting each experimental aspect, I will say a few words about the ease or difficulty in interpreting that observation theoretically. We emphasize that the Pomeron which appears in total cross sections, elastic cross sections, diffractive dissociation, inclusive processes—what have you, where vacuum quantum numbers can be exchanged—is always the same Pomeron. So we are allowed to draw on all these data to illuminate the properties of the Pomeron.

1. Energy Independence

The easiest measurement here is of total cross sections $\sigma_T^{AB}(s)$ (Kycia, 1974). In Fig. 1 are shown the $\sigma^{Ap}(s)$ for collisions of A on protons with $A=p, \bar{p}, \pi^\pm$ and K^\pm . Over a wide range of beam momentum each of these cross sections varies rather slowly. Each is compatible with only logarithmic dependence on $s \approx 2m_p p_{lab}$ after a correction term proportional to $s^{-1/2}$ is removed. Compare this to the very dramatic decrease of the charge exchange cross section (Barnes et al., 1974) shown in Fig. 2.

How do we interpret this? The total cross section is related to the invariant amplitude $T_{AB}(s, t)$ for elastic AB scattering via the optical theorem (Abarbanel et al., 1971a)

$$\sigma_T^{AB}(s) = \text{Im } T_{AB}(s, 0) / \Delta^{1/2}(s, m_A^2, m_B^2) \quad (6)$$

where

$$\Delta(x, y, z) = (x + y - z)^2 - 4xy \quad (7)$$

is the usual flux factor. If we make the ansatz

$$T_{AB}(s, t) = s (\log s)^\beta f_{AB}(t) \quad , \quad (8)$$

with β small, we have a representation of the amplitude which gives $\sigma_T^{AB}(s) \approx (\log s)^\beta$. The Froissart bound (Froissart, 1961a; Martin, 1963; Martin and Cheung, 1970) on the growth of $\sigma_T(s)$ limits $\beta < 2$. In terms of a t-channel point of view the amplitude (8) represents the exchange of a spin one object with a little bit of logarithmic dependence.

As another example of cross sections becoming energy independent we look at the elastic cross sections (Fermilab Single Arm Spectrometer Group, 1975; Leith, 1974) in Fig. 7. Again after the disappearance of a term behaving more or less as $s^{-1/2}$ in the elastic amplitude,

$$\sigma_{el}(s) \propto \frac{1}{s^2} \int_{-\infty}^0 dt |T_{AB}(s, t)|^2 \quad (9)$$

is almost constant in s .

Finally we look at the cross sections for $pp \rightarrow A + \text{anything}$ with $A = p, \bar{p}, \pi^\pm, K^\pm$ as shown in Fig. 8 (Giacomelli, 1974). Plotted here is the differential cross section

$$\frac{d^2\sigma(pp \rightarrow A + \text{anything})}{\pi dy_A dp_T^2} \quad (10)$$

for fixed momentum p_{T_A} of A transverse to the beam direction as a function of the rapidity of A (De Tar, 1971) when y_A is near its maximum value. Rapidity is defined as

$$y = \frac{1}{2} \log \frac{E + p_{\parallel}}{E - p_{\parallel}} \quad (11)$$

where p_{\parallel} is the momentum along the beam direction and $E = (p_T^2 + p_{\parallel}^2 + m^2)^{1/2}$ is the particle energy. The cross sections are given for \sqrt{s} from ≈ 6.8 GeV [$p_{lab} = 24$ GeV/c] to $\sqrt{s} \approx 53$ [$p_{lab} \approx 1400$ GeV/c]. In each of these processes vacuum quantum numbers can be exchanged in generalized t-channels. The resulting constancy of the cross sections is impressive.

The theoretical status of this energy independence of cross sections or s^1 behavior of amplitudes is that there is no fundamental explanation for approximate spin one exchange. There are many conjectures and many suggestive formulae. We will see some of these. It is true that if $T_{AB}(s, 0) \sim s^\alpha$ then the Froissart bound requires $\alpha \leq 1$, and experiment saturates the bound. It is hard to know what precisely to make of that. Recent work in diffraction physics has retreated from "explaining" why $\alpha=1$ and focused attention on the consequences thereof; for example, if $T_{AB}(s, 0) \sim s^\alpha (\log s)^\beta$, perhaps β is predictable given $\alpha=1$. Caveats aside there are suggestions, and we will come to them.

2. Diffraction Amplitudes are Almost Imaginary

Figure 9 shows the best evidence for this statement (Leith, 1974). The ratio $\rho(s) = \text{Re } T(s, 0)/\text{Im } T(s, 0)$ is shown for proton-proton scattering from laboratory energies of 1 GeV to 1000 GeV. Note that in the neighborhood of 120 GeV this ratio becomes positive, while remaining small. If the cross section grows as $(\log s)^\beta$, then analyticity arguments (Leith, 1974) tell us that

$$\rho(s) \sim \frac{\pi\beta}{2} \frac{1}{\log s} \quad (12)$$

for large s . So eventually $\rho(s)$ must be small and positive for large s .

The imaginary nature of the diffraction amplitude represents absorption out of the elastic channel. Indeed, if the amplitude is pure imaginary, then in some loose sense the competing inelastic channels have become as strong as possible in soaking up probability. The imaginary nature of the diffraction amplitude can be connected with $\alpha \approx 1$ and sufficient analyticity (Eden, 1967). In several of the models to be discussed, notably the multiperipheral model, it is also rather natural. We may now update our ansatz (8) to exhibit the imaginary amplitude

$$T_{AB}(s, t) = is (\log s)^\beta f_{AB}(t) \quad (13)$$

near $t=0$. $f_{AB}(t)$ is real.

3. Diffraction Amplitudes Factorize

As explained above this means that the amplitude for the process $AB \rightarrow A'B'$ can be written as

$$T_{AB \rightarrow A'B'}(s, t) = g_{AA'}(t) g_{BB'}(t) \times \text{function of } s \text{ independent of } A, A', B, B' \quad . \quad (14)$$

If this is the case, then

$$\frac{T_{AB \rightarrow A'B'}(s, t)}{T_{CB \rightarrow C'B'}(s, t)} = \frac{g_{AA'}(t)}{g_{CC'}(t)} = \text{independent of } B, B' \quad . \quad (15)$$

Furthermore this independence must hold for all s as a function of t . Clearly this is a stringent requirement.

Before revealing the evidence for factorization, a few theoretical words are in order. If the wiggly exchange diagram of Fig. 4b were correct, factorization would be elementary. It would represent the locality of the acts $A \rightarrow A' + \text{wiggly}$ and $B + \text{wiggly} \rightarrow B'$. Indeed, if the wiggly is an elementary particle or a simple pole in angular momentum, one can demonstrate using unitarity (Arbab and Jackson, 1968) that the amplitude must factorize.

Alas for the simplest picture, multiple exchange graphs as in Fig. 6 in general have no factorization but are superficially as important as the factorized contribution. Factorization is an important challenge to theories of diffraction.

We give two examples to show the quality of factorization in experimental results. Others are discussed by Leith (Leith, 1974). First, in the set of reactions $A_p \rightarrow A_p$ and $A_p \rightarrow AN^*(1688)$ with $A = \pi^-, K^-, \text{ or } \bar{p}$ the ratio of these amplitudes should be independent of A , if factorization holds true. The process $A_p \rightarrow AN^*(1688)$ is called diffractive dissociation and involves an energy independent cross section and the other attributes of diffraction. In Fig. 10 (Leith, 1974) is shown the ratio of the differential cross sections for these diffractive

processes as a function of t . The independence of beam required for factorization holds remarkably well.

Second we turn to the results of an inclusive experiment at Serpukhov. The CERN-IHEP collaboration measured

$$\pi^- p \rightarrow X+p \quad \text{and} \quad K^- p \rightarrow X+p \quad (16)$$

at beam momenta 25 GeV/c and 40 GeV/c. These reactions are shown in Fig. 11.

If the Pomeron factorizes, then the ratio of these cross sections should be independent of beam momentum, momentum transfer t between the protons, and x , the fraction of beam momentum carried off by the recoil proton. The experimental results are shown in Fig. 12 (Leith, 1974). Indeed we must have

$$\frac{\frac{d\sigma}{dt dx} (\pi^- p \rightarrow X+p)}{\frac{d\sigma}{dt dx} (K^- p \rightarrow X+p)} = \frac{\sigma_{\text{total}}(\pi^- p)}{\sigma_{\text{total}}(K^- p)} \quad (17)$$

Integrating over t , the left-hand side here is 1.20 ± 0.09 and the right is 1.18 ± 0.04 .

There are, as mentioned, several other (better) examples of factorization. I choose these two rather diverse examples to stress the point that Pomeron amplitudes must factorize everywhere, not just sometimes, since the same wiggly t -channel or s -channel object is involved.

We may now further update our model amplitude for diffraction to read

$$T_{AB \rightarrow A'B'}(s, t) = is (\log s)^\beta g_{AA'}(t) g_{BB'}(t) \quad (18)$$

4. The Diffraction Differential Cross Section Has a Sharp Forward Peak Which Gets Sharper as s Increases

The most comprehensive measurements of elastic cross sections are for proton-proton scattering. From Fermilab and the CERN-ISR we have good data

for $s \sim 100 \text{ (GeV)}^2$ up to $s \sim 3000 \text{ (GeV)}^2$ that show for $|t| < 0.15 \text{ (GeV/c)}^2$ that

$$\frac{d\sigma}{dt}(s, t) = \frac{d\sigma}{dt}(s, 0) \exp -b(s) |t| \quad , \quad (19)$$

with

$$b(s) = b_0 + 2\alpha' \log \left[s/1 \text{ (GeV)}^2 \right] \quad (20)$$

and

$$b_0 = 8.3 \text{ (GeV)}^{-2} \quad , \quad (21)$$

and

$$\alpha' = 0.28 \text{ (GeV)}^{-2} \quad . \quad (22)$$

There is other evidence for a shrinking of the sharp forward peak in elastic diffractive scattering, but none of it covers so large an energy range as the p-p data. The most recent data comes from Fermilab (Fermilab, 1975) and is shown in Fig. 13 where the parameter $b(s)$ is given.

We must modify our model amplitude again to take account of the shrinking peak

$$T_{AB \rightarrow A'B'}(s, t) = i s^{\alpha(t)} (\log s)^\beta g_{AA'}(t) g_{BB'}(t) \quad , \quad (23)$$

where $\alpha(t) = 1 + \alpha't$ and $g_{ij}(t)$ falls rapidly with increasing $|t|$. β here may depend on t ; experiments are not yet sensitive to it.

5. Vacuum Quantum Numbers Exchanged

The evidence here is simple to state. Any process which carries non-vacuum quantum numbers in the t-channel has a cross section which falls rapidly (as a power of s) in energy. A beautiful example is pion-nucleon charge exchange which has $I=1$, $Q=1$, $C=-1$ quantum numbers flowing in the t-channel. The dominant πN amplitude is the spin nonflip $I=0$ t-channel amplitude. It has an energy independent cross section and is diffractive.

We may also examine the cross sections for the processes $K^- p \rightarrow \bar{K} + (N\pi\pi)$ shown in Fig. 14 (Leith, 1974). In the $(N\pi\pi)^+$ configuration there are enhancements in the $N\pi\pi$ mass due to diffractive excitation of a nucleon excited state. There are none in the $(N\pi\pi)^0$ spectrum. As Leith notes, this experiment is evidence for the $Q=0$ and $C=+1$ nature of the Pomeron.

There is no known theoretical "explanation" of vacuum quantum numbers for the Pomeron. However, from the t -channel exchange viewpoint it has been shown (Pomeranchuk and Okun, 1956) and generalized (Amati et al., 1964) that if amplitudes are dominately imaginary, then exchange of vacuum quantum numbers gives larger cross sections than exchange of nonvacuum quantum numbers. Of course, they could both have the same s -dependence but the vacuum exchange the larger numerical amplitude. It seems profitable to set aside this issue and accept for the moment that vacuum quantum number exchange amplitudes is where we look for energy independent cross sections.

There is a little analogy which is useful, if not rigorous, in helping to understand how vacuum quantum number exchanges might remain larger than nonvacuum quantum number exchange. In the wiggly exchange graph of Fig. 15 we can imagine a flow of some current (isospin current, charge current, ...) along each line. If the current must carry charge or isospin or whatever, then the quantity carried must accelerate very rapidly to go from the direction of travel of particles A and A' to the direction of travel of particles B and B'. In this acceleration, stuff is radiated as in electrodynamics when charge is accelerated. The faster A and B pass by each other, the higher s is, the more rapid the acceleration of the quantity must be, and the more radiation of the quanta of the stuff must occur. Radiation of quanta opens up more channels for the scattering to go into and decreases the amplitude in the $AB \rightarrow A'B'$ channel. Only if the

quantum numbers of the vacuum are carried across is nothing accelerated, and there is no accompanying amplitude decreasing radiation.

6. At the Vertices $A \rightarrow A' + \text{Pomeron}$, the Rule Parity of $A = \text{Parity of } A' \times (-1)^{(\text{spin of } A) - (\text{spin of } A')}$ Holds

This is at best a rule (Leith, 1974) which has no substantial theoretical footing but seems to be empirically true. To study this rule one must examine the overlap of the wave function of A with the wave function of A' with the operator which represents the emission or absorption of the Pomeron:

$$g_{AA'} \propto \int \psi_{A'}^* (\text{Pomeron operator}) \psi_A \quad (24)$$

The theoretical lack of knowledge about the hadronic wave functions ψ_A is legendary; the same holds for the Pomeron operator. It is my opinion that keen insight into the structure of hadrons will be necessary before one can address the spin-parity rules for the A - A' -Pomeron vertex. It is an important problem which will not be touched on further in this review.

7. The Cross Section for AB Equals the Cross Section for $\bar{A}\bar{B}$

In Fig. 15 (Leith, 1974) is shown data for the total cross sections $A p$ with $A = \pi^\pm, K^\pm, p^\pm$ and the $K^\pm n$ total cross sections plotted versus $(p_{\text{lab}})^{-1/2}$ for p_{lab} up to 25 GeV/c. Each of the pairs AB and $\bar{A}\bar{B}$ become equal at very large p_{lab} . Since the difference between the $AB \rightarrow AB$ amplitude and the $\bar{A}\bar{B} \rightarrow \bar{A}\bar{B}$ amplitude is some nonvacuum quantum number exchange, these data are consistent with the remarks above.

This ends our review of the experimental situation in diffraction scattering of hadrons. For more detail the lectures of Leith (Leith, 1974) from which we have generously drawn should be consulted. We turn now to the theoretical structure which has grown up around and with these experimental results. First

we look at the s-channel viewpoint and then examine at some length the t-channel point of view.

III. BASIC THEORETICAL IDEAS

Almost all thinking about high energy scattering at small momentum transfer is an extension in some form of the multiperipheral model (Abarbanel et al., 1971a; Amati et al., 1962; Bertocchi et al., 1962; Fubini, 1963). Diffraction scattering is no exception. We will review here very briefly the fundamentals of multiperipheralism, its key content, and its major implications.

Multiperipheral scattering amplitudes are generalizations of the exchange processes familiar from quantum field theory (Drell and Hearn, 1966). Suppose we have two-to-two scattering of spinless equal mass (m) particles. At low energies the amplitude for this will be dominated by resonances when they can occur. These are poles in s (Chew, 1961; Eden, 1967; Frautschi, 1963) (Fig. 17)

$$T(s, t) = \sum_R \frac{P_{J_R}(\cos \mathcal{J}_s)}{M_R^2 - s} g_R^2 \quad (25)$$

where the resonance is at the (complex) value M_R^2 . The center-of-mass scattering angle \mathcal{J}_s is related to t by

$$t = -2 (s/4 - m^2)(1 - \cos \mathcal{J}_s) \quad , \quad (26)$$

and the spin J_R of the resonance enters via the Legendre polynomial P_{J_R} .

When the energy s is increased, one leaves the resonance region and cross sections become very smooth. The number of partial waves is about $(\sqrt{s}) \times$ (impact parameter ≈ 1 fermi) and becomes quite large. Now a finite set of resonances give an amplitude which falls as s^{-1} . Diffractive amplitudes rise

approximately as s^1 and charge exchange amplitudes as $s^{1/2}$, so a finite set of s-channel resonances cannot be enough.

In field theory (Bjorken and Drell, 1964) one may also exchange resonances in the t channel as in Fig. 18 giving rise to the amplitude

$$T(s, t) = \sum_R g_R^2 \frac{P_{J_R}(\cos \mathcal{A}_t)}{M_R^2 - t} \quad (27)$$

with

$$s = -2\left(\frac{t}{4} - m^2\right)(1 - \cos \mathcal{A}_t) \quad (28)$$

Now for fixed t and $s \rightarrow \infty$ which is the limit we are concerned with each term in (27) behaves as s^{J_R} . A finite sum of t-channel resonances will give amplitudes growing faster than s^1 , if any of those resonances has $J_R > 1$. Such a growth violates the Froissart bound, not to mention experiment. Does this mean we cannot allow resonances with spin > 1 ? No, it means that a finite set of resonances won't do, and the sum in (27) must diverge. More of this later.

The peripheral model (Drell and Hearn, 1966) in its crudest form approximates the t-channel resonance sum by the term with the lowest mass or longest range in impact parameter (thus the name peripheral). This term is usually the pion or another (fictitious) spin 0 meson giving the peripheral amplitude (Fig. 19)

$$T_P(s, t) = g^2 (m^2 - t)^{-1} \quad (29)$$

In itself this amplitude won't do. It is pure real and behaves as s^0 .

The multiperipheral model (Fubini, 1963) attempts to approximate the imaginary part of the $AB \rightarrow A'B'$ amplitude by making a peripheral amplitude ansatz for each possible t-channel like exchange. The unitarity relation (4)

(Zachariasen, 1971) gives $\text{Im } T(s, t)$ as

$$\begin{aligned} & \text{Im } T_{AB \rightarrow A'B'}(p_A + p_B \rightarrow p_{A'} + p_{B'}) \\ &= \sum_{N=2}^{\infty} \prod_{j=1}^N \int \frac{d^3 p_j}{(2\pi)^3 2E_j} (2\pi)^4 \delta^4 \left(p_A + p_B - \sum_{j=1}^N p_j \right) T_{AB \rightarrow N}(p_A + p_B \rightarrow p_1 \cdots p_N) \\ & \quad \times T_{A'B' \rightarrow N}^*(p_{A'} + p_{B'} \rightarrow p_1 \cdots p_N) \quad . \end{aligned} \quad (30)$$

Now one makes a peripheral approximation to $T_{AB \rightarrow N}$ (Fig. 20)

$$T_{AB \rightarrow N}(p_A + p_B \rightarrow p_1 \cdots p_N) = g^N \prod_{j=1}^{N-1} \frac{1}{m^2 - Q_j^2} \quad , \quad (31)$$

where

$$Q_j = p_A - p_1 - \cdots - p_j \quad (32)$$

and is the momentum transfer between links along the particle emission chain.

In the peripheral approximation $T_{AB \rightarrow N}$ is related to $T_{AB \rightarrow N-1}$ by multiplication with $g/(m^2 - Q_{N-1}^2)$, so one may write a recursion relation for

$\text{Im } T_{AB \rightarrow A'B'}$ (Fig. 21)

$$\begin{aligned} & \text{Im } T(p_A + p_B \rightarrow p_{A'} + p_{B'}) = K(p_A + p_B \rightarrow p_{A'} + p_{B'}) \\ & \quad + \int \frac{d^4 Q_1 d^4 Q_1' \delta^4(Q_1 - Q_1' - p_A + p_{A'})}{(m^2 - Q_1^2)(m^2 - Q_1'^2)} K(p_A - Q_1 \rightarrow p_{A'} - Q_1') \\ & \quad \times \text{Im } T(Q_1 + p_B \rightarrow Q_1' + p_{B'}) \quad , \end{aligned} \quad (33)$$

with

$$K(p_A + p_B \rightarrow p_{A'} + p_{B'}) = \pi g^2 \delta \left((p_A + p_B)^2 - m_0^2 \right) \quad . \quad (34)$$

If we call $A = \text{Im } T(p_A + p_B \rightarrow p_A' + p_B')$ and the propagators $(m^2 - Q_1^2)^{-1} \times (m^2 - Q_1^2)^{-1} = G_0$, we may cast (33) into the symbolic form

$$A = K + KG_0A \quad (35)$$

which reveals it to be just the Schrödinger equation (well, really the Bethe-Salpeter equation), for two particle scattering in the t-channel. This equation can be partly diagonalized by the Mellin transform (Abarbanel et al., 1971a)

$$A(\ell, t) = \int_{s_0}^{\infty} ds s^{-\ell-1} A(s, t) \quad (36)$$

whose inverse

$$A(s, t) = \int_{c-i\infty}^{c+i\infty} \frac{d\ell}{2\pi i} s^\ell A(\ell, t) \quad (37)$$

represents $A(s, t)$ as a "sum" over powers of s . What we have done in this transform is trade off the variable $\log s$ for its conjugate variable ℓ . (Conjugate because s^ℓ is $e^{\ell \log s}$.)

The resulting equation is two dimensional, and if we assign two vectors to each momentum (Fig. 22), we are able to write

$$A(\ell, t) = A(\ell, \vec{p}, \vec{q}, \vec{k}) = K(\ell, \vec{p}, \vec{q}, \vec{k}) + \int d^2 p' K(\ell, \vec{p}, \vec{q}, \vec{k}') G_0(\vec{p}', \vec{q}) A(\ell, \vec{p}', \vec{q}, \vec{k}) \quad (38)$$

where $t = -|\vec{q}|^2$. The equation is two dimensional because in integrating over s we had to specify two components of each four vector: the energy and the momentum in the beam direction. The two remaining momenta are the conjugate variables to the impact parameter vectors \vec{b} . All the dynamics resides in the two degrees of freedom perpendicular to the beam direction. This two dimensional dynamic space is not particular to the multiperipheral approximation. It is pervasive in very high energy processes.

The solution to (38) is given in terms of the eigenfunctions of the homogeneous equation

$$\lambda_n(\ell, t) \psi_n(\ell, \vec{p}, \vec{q}) = \int d^2 p' K(\ell, \vec{p}, \vec{q}, \vec{p}') G_0(\vec{p}', \vec{q}) \psi_n(\ell, \vec{p}', \vec{q}) \quad (39)$$

in the usual fashion

$$A(\ell, \vec{p}, \vec{q}, \vec{k}) = \sum_n \psi_n(\ell, \vec{p}, \vec{q}) \frac{k_n(\ell, t)}{1 - \lambda_n(\ell, t)} \psi_n^*(\ell, \vec{k}, \vec{q}) \quad , \quad (40)$$

where

$$K(\ell, \vec{p}, \vec{q}, \vec{k}) = \sum_n k_n(\ell, t) \psi_n(\ell, \vec{p}, \vec{q}) \psi_n^*(\ell, \vec{k}, \vec{q}) \quad . \quad (41)$$

For doing the Mellin inversion of (37) to reconstruct the absorptive part of $T_{AB \rightarrow A'B}$, we need to know the analytic structure of $A(\ell, t)$ in ℓ . For our particular K , and for most smooth enough potentials K , $K(\ell)$ is analytic in ℓ to the right of $\ell = -1$. Also the $\psi(\ell, \vec{p}, \vec{q})$ are smooth in ℓ . The interesting structure comes when $\lambda_n = 1$, this occurs at $\ell = \alpha_n(t)$:

$$\lambda_n(\alpha_n(t), t) = 1 \quad . \quad (42)$$

Furthermore when K is "smooth enough", that is to say usually, λ_n is analytic near $\ell = \alpha_n(t)$ so the singularity in $A(\ell, t)$ is a set of poles

$$A(\ell, t) = \sum_n \frac{\psi_n \psi_n^* k_n \left[\frac{\partial \lambda_n}{\partial \ell} \Big|_{\ell = \alpha_n(t)} \right]}{\ell - \alpha_n(t)} \quad , \quad (43)$$

and for $A(s, t)$, we find

$$A(s, t) = \sum_n s^{\alpha_n(t)} \beta_n(\vec{p}, t) \beta_n(\vec{k}, t) \quad . \quad (44)$$

This is the key result of the multiperipheral model: there are poles in the variable ℓ conjugate to $\log s$, the position of these poles varies with t ; $\ell = \alpha_n(t)$.

The large s , fixed t behavior of $A(s, t)$ is given by the $\alpha_n(t)$ with the largest

Re $\alpha_n(t)$, call it $\alpha(t)$ so

$$A_{MP}(s, t) \underset{\substack{s \rightarrow \infty \\ t \text{ fixed}}}{\sim} s^{\alpha(t)} \beta_{AA'}(t) \beta_{BB'}(t) \quad , \quad (45)$$

whose similarity to Eq. (23) is notable.

If $\alpha(t) \leq 1$ for $t \leq 0$, then this result of the multiperipheral model answers most of the questions we ask about high energy scattering. Furthermore, if we find an $\alpha(t)$ such that $\alpha(0)=1$, then we have a total cross section which is constant since by the optical theorem

$$\sigma_T^{AB}(s) \sim \frac{1}{s} A(s, 0) = s^{\alpha(0)-1} \beta_{AA'}(0) \beta_{BB'}(0) \quad . \quad (46)$$

A nice interpretation can be given to this power of s , $\alpha(t)$, by thinking again of the multiperipheral integral equation as a Schrödinger equation. When looking for the eigenstates we are essentially looking for the two particle bound states (or resonances) whose position $\alpha_n(t)$ depends on the parameter t . Just as we had a peripheral amplitude in (27) which behaved as s^{J_R} for a spin J_R resonance in the t -channel, so we may interpret the multiperipheral $s^{\alpha_n(t)}$ as coming from a resonance with "spin" $\alpha_n(t)$. This "spin" depends on t and may even be complex. The behavior $s^{\alpha(t)}$ represents the sum

$$\sum_R \frac{s^{J_R} g_R^2}{m_R^2 - t} \sim s^{\alpha(t)} \quad (47)$$

outside its region of convergence.

Unfortunately the multiperipheral result has its fatal flaws. These are a signal of the inadequate representation of the unitarity relation, and all attempts to go beyond multiperipheralism have basically had the goal of the restoration of unitarity or the addition of more unitarity. The first flaw is that nothing

prevents $\alpha(0)$ from becoming larger than 1 (the unitarity bound), if the strength of the potential K is made large enough. Take our particular "potential" (34) with $m_0=0$. Then explicitly one has (Wick and Cutkosky, 1954)

$$\alpha(0) = -\frac{3}{2} + \sqrt{\frac{1}{4} + \frac{g^2}{16\pi^2 m^2}} \quad , \quad (48)$$

and we may easily arrange that $\alpha(0) > 1$. Somewhere we didn't get enough unitarity.

The second flaw is experimental. If we only have poles in ℓ at $\alpha_n(t)$, then even if $\alpha(0)=1$ we can at most have constant total cross sections. We have seen in our experimental review that total cross sections appear not to be constants, but rise as a small power of $\log s$.

The third flaw is subtler. We have evaluated only $\text{Im } T$. If we imagine that $T(s, t)$ near $t=0$ is pure imaginary, then the sign of the contribution to $T(s, t)$ of the double scattering correction depicted in Fig. 6 is positive in multiperipheral models (Abarbanel, 1972b). This occurs because such corrections are determined from unitarity which is more or less $\text{Im } T \propto T^*T > 0$. Now if pure imaginarity represents absorption from the initial channel, as it must, then double exchange represents absorption of amplitude from the simple exchange and should subtract from it not add to it. It can hardly be a secret any longer that this flaw is fixed up by unitarity as well. What's missing is even more absorption, multiple scattering if you like, that results in the appropriate sign of the correction term.

The fourth flaw, if one more is even needed, is a consistency problem with the multiperipheral model pole with $\alpha(0)=1$. For good kernels K this pole will be isolated and $\alpha(t)$ will be regular at $t=0$. In such a case one may prove, beginning with properties of inclusive reactions (Abarbanel et al., 1971b) like

$pp \rightarrow p + \text{anything}$, and on through some weighty analysis (Brower and Weis, 1972; Jones et al., 1972) that the Pomeron so defined does not contribute to total cross sections at all! In particular quantities like $\beta_{AA}(0)$ as in Eq. (46) must be zero. Again this is a price one pays for ignoring unitarity. This time the avoidance of unitarity comes from not considering complicated potentials or kernels K which contain the poles at $\alpha_n(t)$ themselves. When this is done, the resulting K 's are not "smooth enough", and poles alone do not emerge.

It would be unfortunate indeed to end our comments about the multi-peripheral model on this sour note, for it actually provides a very excellent description of an enormous amount of data and is certainly a very rational starting point for refined theories of diffraction (Bøggild and Ferbel, 1974; DeTar, 1971). After all, it does possess power behaved amplitudes whose power varies with t . These amplitudes factorize. Just these results with the ansatz that $\alpha(0)=1$ gives constant cross sections, and cross sections are almost constant. It gives inclusive cross sections that are essentially independent of produced particle rapidity for produced particles slow in the center-of-mass of the collision (pionization region). The view, then, of the multiperipheral model I feel one ought to take is that it yields a very attractive beginning point for theoretical fine tuning in the study of diffraction. It identifies most of the important degrees of freedom one needs to focus on and provides the "unperturbed problem" from which deviations are to be treated as perturbations.

There is a fruitful analogy in many body theory to this use of the multiperipheral model. In the theory of second order phase transitions (Fisher, 1974; Stanley, 1971; Wilson and Kogut, 1974) one begins the study of the correlation functions of spins or whatever with a mean field theory which has only poles in Green's functions. These poles are just like those in the multiperipheral model.

They represent effective resonances or mean fields. The mean field theory with only poles is an accurate description of systems with a phase transition far enough away from the transition. Close to the transition the Green's functions deviate in small but striking ways from the poles only behavior. Poles only, however, remain an excellent starting point. From that point the fine tuning begins.

IV. ABSORPTION MODELS

The s-channel approach to correcting the multiperipheral model concentrates on the modification of the production amplitudes $T_{AB \rightarrow N}$ in their contribution to $T_{AB \rightarrow A'B'}$ via the unitarity relation. The requirements of unitarity are imposed through rescattering of the produced particles after the basic production mechanism has operated. Typically this rescattering is taken to occur only between pairs of particles so only the elastic S-matrix, S_{AB} , need be considered (Blankenbecler and Sachrajda, 1975; Ciafaloni and Marchesini, 1975; Schwimmer, 1974). Some more ambitious models use two very fast particles as a c-number source for secondaries and are able to take into account many more rescatterings (Auerbach et al., 1972; Aviv et al., 1972).

The statement of rescattering is best made in rapidity $y = \log s$ and impact parameter \vec{b} space. To see why this is so consider the two-to-two process $AB \rightarrow A'B'$ as shown in Fig. 23 taking place by the "exchange" of a potential V_1 and then V_2 . To leading order in s the product scattering is diagonal in s (or $\log s$), \vec{b} space

$$T_{AB \rightarrow A'B'}(s, \vec{b}) = V_1(s, \vec{b}) V_2(s, \vec{b}) \quad , \quad (49)$$

because at very high energy there is a two dimensional subgroup of the full Lorentz group which remains as a symmetry. This resides in the two dimensional impact parameter space. Products of amplitudes are just group multiplication. Another way to view this is to remember that the angular momentum l is related

to impact parameter $|\vec{b}|$ by $\ell \approx \sqrt{s} |\vec{b}|$ and going over to impact parameter space by

$$T_{AB \rightarrow A'B'}(s, \vec{b}) = \int_{-\infty}^0 dt J_0(b\sqrt{-t}) T_{AB \rightarrow A'B'}(s, t) , \quad (50)$$

is just a slick partial wave projection.

Now imagine an amplitude for $T_{AB \rightarrow N+1}$ as a function of the rapidities y_k and impact parameters \vec{b}_k of the produced particles and let the amplitude be represented as in the multiperipheral like configuration of Fig. 24:

$$T_{AB \rightarrow N+1}(y_k, \vec{b}_k) = \prod_{j=1}^N T(Y_j, \vec{B}_j) \quad (51)$$

where the exchanges are themselves elastic T matrices depending on the rapidity differences $Y_j = y_{j+1} - y_j$ and impact parameter differences $\vec{B}_j = \vec{b}_{j+1} - \vec{b}_j$ along the production chain. A pure pole exchange with $s^{1+\alpha't}$ gives

$$T(Y, \vec{B}) = e^{-|\vec{B}|^2/4\alpha'Y/4\alpha'Y} , \quad (52)$$

and insertion of this in (51) gives back the multiperipheral model.

Now rescattering is introduced by allowing the initial particles and pairs of outgoing particles to interact as if they were elastic and thus each pair picks up the phase (Finkelstein and Zachariasen, 1971; Gottfried and Jackson, 1964; Schwimmer, 1974) $\exp i\delta(Y_j, \vec{B}_j) = \sqrt{S(Y_j, \vec{B}_j)}$ corresponding to its y and \vec{b} gap. One modifies (51) then

$$T_{AB \rightarrow N+1}^{\text{absorbed}}(y_k, \vec{b}_k) = \sqrt{S(y, \vec{b})} \prod_{j=1}^N T(Y_j, \vec{B}_j) \times \prod_{1 \leq \underline{\ell} < \underline{k} \leq N+1} \left\{ S(y_k - y_{\underline{\ell}}, \vec{b}_k - \vec{b}_{\underline{\ell}}) \right\}^{1/2} \quad (53)$$

as shown in Fig. 25.

Before we go any further it is clear that the full content of s-channel unitarity has not been employed. Possible many particle interactions as shown in

Fig. 26 are clearly absent. This means we may well have not put in enough unitarity by this elastic rescattering approximation.

If we take just the multiperipheral amplitude of (52) with no rescattering, then the resulting total cross section violates the Froissart bound. Even if we take (52) and the rescattering in (53), the total cross section grows faster than any power of $\log s$ (Schwimmer, 1974). Unitarity requires $\sigma_{\text{total}}(s) < (\log s)^2$. So clearly another tack is needed.

One is a self-consistency approach (Caneschi and Schwimmer, 1972; Finkelstein and Zachariasen, 1971; Schwimmer, 1974): let the $T(y, \vec{b})$ in (53) determine itself via the unitarity relation

$$2 \text{Im } T(y, \vec{b}) = |T(y, \vec{b})|^2 + \sum_{N=2}^{\infty} |T_{N+1}(y_k, \vec{b}_k)|^2 . \quad (54)$$

This yields a $T(y, \vec{b})$ which is a black disc

$$T(y, \vec{b}) = is \theta(R_0^2 y^2 - \vec{b}^2) + \text{lower order terms} . \quad (55)$$

In the very high energy limit there is no scattering outside an impact parameter $|\vec{b}| = R_0 \log s$ and total absorption within. Since impact space is two dimensional the total cross section coming from this amplitude

$$\sigma_{\text{total}}(s) = \frac{1}{s} \int d^2b \text{Im } T(s, \vec{b}) \quad (56)$$

$$\sim (\log s)^2 \quad (57)$$

and in the elastic amplitude $T(s, t)$ structure in t varies as $(\log s)^2$ in contrast to $\log s$ characteristic of the multiperipheral model (and experiment). This behavior is also found in various eikonal models which we'll discuss soon. An amusing result in such self-consistent models comes when one allows the Pomeron here called \sqrt{s} to act in other channels; that is, allows diffraction

dissociation. Then one demonstrates (Schwimmer, 1974)

$$\sigma_{\text{elastic}} + \sigma_{\text{diff. dissoc.}} = \frac{1}{2} \sigma_{\text{total}} \quad (58)$$

A second interesting approach is iterative (Ciafaloni and Marchesini, 1975). It chooses a zeroth step Pomeron and then creates a first step Pomeron by adding zeroth step Pomeron rescattering corrections as in Fig. 27 using the rescattering prescription in Eq. (53), elastic scattering only. An amplitude of the scaling form

$$T(y, \vec{b}) = y^{\eta-\nu} f(\vec{b}^2/y^\nu) \quad (59)$$

emerges from this, where

$$\eta \approx 1/2 \quad (60)$$

$$\nu \approx 3/2 \quad (61)$$

in first approximation. The total cross section grows as

$$\sigma_{\text{total}}(s) \sim (\log s)^\eta \quad (62)$$

and the structure in t is correlated with $(\log s)^\nu$. This is certainly better than the self-consistency program from an experimental point of view. Where multiple iterations lead is not established.

We have seen in two approximate approaches to adding unitarity to the multi-peripheral amplitude, $s^{\alpha(t)}$, two characteristic features:

1. The amplitude is multiplied by powers of $\log s$. This is the fine tuning alluded to in the introductory remarks. The power behavior is taken as more or less given, and the structure in $\log s$ is determined.

2. The $\alpha(t)$ functional dependence is modified from $\alpha(t) = 1 + \alpha't$ to $1 + \alpha't^{1/\nu}$. In our discussions from the t -channel point of view, much the same fine tuning will occur when a much vaster set of absorptive corrections are accounted for.

V. EIKONAL MODELS

There is another class of models which enforce unitarity in the s-channel by iterating the basic Pomeron exchange. The underlying idea is the eikonal approximation (Abarbanel and Itzykson, 1969; Blankenbecler and Sugar, 1969; Chang and Ma, 1969; Cheng and Wu, 1969; Glauber, 1959; Levy and Sucher, 1969) which is taken over, with appropriate window dressing, from potential scattering theory. Recall that a particle of mass m scattering in a potential $V(\vec{r})$ has the eikonal scattering matrix from initial momentum \vec{k}_i to final momentum \vec{k}_f

$$T(\vec{k}_i \rightarrow \vec{k}_f) = \frac{ik}{m} \int d^2b \left\{ e^{+i\chi(\vec{b}, k)} - 1 \right\} e^{-i\vec{\Delta} \cdot \vec{b}} \quad (63)$$

in the limit $|\vec{k}_i| = |\vec{k}_f| = k \rightarrow \infty$ and momentum transferred $t = (\vec{k}_i - \vec{k}_f)^2 = |\vec{\Delta}|^2 + 0\left(\frac{1}{k}\right)$ is fixed. The vector \vec{b} is a two dimensional vector transverse to some appropriate linear combination of unit vectors $\hat{k}_i = \vec{k}_i / |\vec{k}_i|$ and \hat{k}_f . The eikonal phase is

$$\chi(\vec{b}, k) = -\frac{m}{k} \int_{-\infty}^{+\infty} dz V(\vec{b}, z) \quad , \quad (64)$$

and z represents the line perpendicular to \vec{b} . This phase is just that phase picked up by the particle as it traverses the scattering potential. If we replace $\frac{k}{m}$ by $\frac{s}{m}$ and $V(\vec{b}, z)$ by an integral over the exchanged object or the born approximation, then the eikonal formula may be taken over to quantum field theory (more or less). So

$$\chi(\vec{b}, s) = +\frac{m^2}{s} \int \frac{d^2q}{(2\pi)^2} e^{iq \cdot \vec{b}} T_{\text{Born}}(s, t = -|q|^2) \quad (65)$$

and

$$T(s, t) = \frac{is}{m} \int d^2b e^{-i\Delta \cdot b} \left[e^{+i\chi(b, s)} - 1 \right], \quad t = -|\Delta|^2. \quad (66)$$

Formally this representation of T is unitary as the S matrix in b, s space is precisely

$$S(b, s) = \exp i \chi(b, s) \quad . \quad (67)$$

Next is needed a rationale for selecting a $\chi(b, s)$. Several approaches have been tried. If $T_{\text{Born}}(s, t)$ is taken to be the exchange of an elementary spin J particle, then

$$T_{\text{Born}}(s, t = -|q|^2) = g^2 s^J / (m^2 + |q|^2) \quad (68)$$

and

$$\chi(b, s) = \frac{g^2 s^{J-1}}{m^2} \int d^2q e^{iq \cdot b} / (m^2 + |q|^2) \quad . \quad (69)$$

If $J=0$, scalar meson exchange, then for large s , fixed t , the behavior of the eikonal T matrix is just T_{Born} ; clearly an uninteresting case. If $J=1$, $\chi(s, b)$ is independent of s , and $T(s, t)$ is

$$T(s, t) = i s f(t) \quad . \quad (70)$$

Now this is much better. It comes very close to our ansatz a long time ago, but lacks a power of s which changes with t .

Now suppose $J>1$. In our earliest discussions above we noted that multiple exchanges of this would violate unitarity more and more. Here, however, the eikonal phase grows with s and the integrand oscillates. The phase is stationary when $b \propto \log s$, and since transverse space is two dimensional

$$T(s, t) \sim i s (\log s)^2 \quad , \quad (71)$$

and

$$\sigma_T(s) \sim (\log s)^2, \quad (72)$$

saturating the Froissart unitarity bound.

The eikonal formula is then an attractive framework into which one may put her or his dynamics and rest assured that significant aspects of s-channel unitarity will be respected. If one has a more complex T_{Born} than (68), for example $s^{1+\alpha't}$ or additional logarithms, then very much the same qualitative features as far as s dependence goes emerges (Chou and Yang, 1968; Durand and Lipes, 1968; Frautschi and Margolis, 1968). In pictorial language one is summing via (66) the exchange graphs of Fig. 28 in which the particle-particle-N Pomeron couplings g_N are

$$g_N = (-g_1)^N / N!, \quad (73)$$

which is quite special to the eikonal approximation. One of the obvious missing ingredients in the eikonal model is a process such as appears in Fig. 29. Here the Pomerons emitted by the particles are allowed to interact and, since Pomeron exchange is absorptive, further shield the original exchange. One may organize the complicated exchange on the left of Fig. 29 to look like an eikonal like exchange, but barring miracles the eikonal condition (73) on the modified couplings H_N will not transpire.

One could go on at some length about eikonal formulations of very high energy scattering (Abarbanel, 1972a; Blankenbecler et al., 1974; Sugar, 1972). Indeed one may eikonalize not only the elastic amplitude but also the $N \rightarrow M$ amplitudes (Baker and Blankenbecler, 1962; Dash and Pignotti, 1970; Dash et al., 1970) and construct explicitly s-channel unitary models of production. When we have introduced and explained Reggeon Field Theories in the t-channel

sections, it will be fairly clear that eikonal formulae do not respect t-channel unitarity, at least for $s \rightarrow \infty$, $t \approx 0$, so the peculiarities of the production models are perhaps just that.

VI. MULTIPERIPHERAL BOOTSTRAP MODELS

If the basic multiperipheral model amplitudes are not good enough, it seems natural enough to modify the original multiperipheral equation to alter its failures (Ball and Zachariasen, 1974; Zachariasen, 1974). In the spirit of multiperipheralism the only place where one has freedom to enlarge the game is in the potential or kernel of Eq. (33). We took K to be just single particle production as in Fig. 21, but suppose we imagine that instead two particle production is significant and single particle states arise as resonances of the produced two particle states. Since K is just the phase space integral over the two particle scattering amplitudes, we have (Fig. 30)

$$\begin{aligned}
 K(\ell, t) = & \int_{s_0}^{\infty} ds s^{-\ell-1} \int \frac{d^3 p_1}{2E_1} \frac{d^3 p_2}{2E_2} \frac{\delta^4(p_A + p_B - p_1 - p_2)}{(2\pi)^2} \times \\
 & \times T_{AB \rightarrow 12}(p_A + p_B \rightarrow p_1 + p_2) T_{A'B' \rightarrow 12}^*(p_{A'} + p_{B'} \rightarrow p_1 + p_2) .
 \end{aligned}
 \tag{74}$$

In the case that T is primarily imaginary, one arrives at a nonlinear integral equation for $A(\ell, t)$ by combining the ansatz for K with the integral equation (38).

Now any progress in solving this is certainly impressive. Putting aside one's justified astonishment at the boldness of the approximations, one expands the integral equation into pieces singular at $\ell=1$ and $t=0$ and pieces regular there.

When we finish, there emerges a solution

$$\begin{aligned} \text{Im } T(s, t) = & \beta_1(t) \left(\frac{s}{s_0}\right)^{\alpha(t)} \log \frac{s}{s_0} \times J_1 \left[\frac{(R_0 \log s + R_1) \sqrt{-t}}{(R_0 \log s + R_1) \sqrt{-t}} \right] \\ & + \beta_0(t) \left(\frac{s}{s_0}\right)^{\alpha(t)} J_0 \left[(R_0 \log s + R_1) \sqrt{-t} \right] + o\left(\frac{1}{\log s}\right), \end{aligned} \quad (75)$$

where $J_\nu(z)$ is the usual Bessel function, $\alpha(t) = 1 + \alpha't$, $\beta_\nu(t)$ is an arbitrary function of t , and s_0 , R_0 , and R_1 are some constants. The total cross section here rises as $\log s$, while the structure in t is a mixture of $\log s$ and $(\log s)^2$ behavior coming from the combination of Bessel functions and $s^{1+\alpha't}$. The appearance of $\log s$ as the expansion parameter rather than, say, $(\log s)^p$, p noninteger, comes from the assumption of a Taylor series in the conjugate variable ℓ around $\ell=1$. In solving the bootstrap equation a series like $(\ell-1)^p \sum_{N=1}^{\infty} C_N (\ell-1)^N$, would significantly alter the details.

We may understand the leading term emerging from the multiperipheral bootstrap by going over to the ever popular impact parameter space, where

$$T(s, b) \propto \frac{is}{\log s} \theta(R_0 \log s - |b|) \quad (76)$$

which is close to the absorption models we studied above. This satisfied elastic unitarity (more or less)

$$\text{Im } \frac{T(s, b)}{s} = \left| \frac{T(s, b)}{s} \right|^2 + o\left(\frac{1}{s}\right), \quad (77)$$

which, strictly speaking, is the only feature which has been built in by the choice of kernel (74).

VII. BRIEF SUMMARY OF s-CHANNEL MODELS

We have quickly reviewed the chief features and underlying ideas of attempts to impose unitarity on a multiperipheral model. The almost insurmountable problem with the s-channel approach is the large number of variables involved in the determination of a $T_{AB \rightarrow N}$ amplitude, namely $3N-4$. Indeed one must make, as N grows, evidently stronger and stronger statements about production amplitudes which are the ingredients in the unitarity recipe for $\text{Im } T_{AB \rightarrow A'B'}$. As we saw from the initial discussion of the multiperipheral model a remarkably simple ansatz led to $s^{\alpha(t)}$ behavior and most of the major features of the experimental data. How one corrects this elementary behavior to restrict $\alpha(0) \leq 1$, for example, is where the many body final state complications enter without relief. In the study of full s-channel unitarity for $T_{N \rightarrow M}$ as well as $T_{2 \rightarrow 2}$ and $T_{2 \rightarrow N}$, the variable problem only magnifies.

The simplifying assumption that only two body interactions (initial and final state) are important can hardly be said to be grounded very strongly, but without it it is almost impossible to proceed. Even accepting this bold step, it was necessary to guess at self-consistent Pomeron formulae to highly nonlinear equations (as in absorption models and multiperipheral bootstrap models) or to ignore Pomeron-Pomeron interactions as in the eikonal models.

A feature of these self-consistent models which recurs persistently is that the differential cross section depends on the combination $\sqrt{-t} \log s$ or equivalently has impact parameters growing as $\log s$. This would mean the differential cross section $d\sigma/dt$ would shrink as $(\log s)^2$ which is not what the evidence from the CERN-ISR or from Fermilab (Fig. 13) tells us. The multiperipheral model in contrast gives $d\sigma/dt$ shrinking as $\log s$ and impact parameters $\sim \log s$, in accord with the present day experimental observations, but no very dramatic conclusions ought to be drawn from that.

At the risk of turning this review into an exposé of my opinions, I feel it is fair to state that the s-channel approach to unitarizing the multiperipheral or

other "underlying" production mechanism has been artfully carried out but less than successful in producing a convincing and coherent account of very high energy diffraction scattering. I believe the basic physics of absorption coupled with the multiperipheral amplitude, $s^{\alpha(t)}$, is the correct approach. Unfortunately, despite very clever efforts, posing the problem in the language where many body effects are unavoidable and intractable has proven a serious barrier.

VIII. t-CHANNEL VIEWPOINTS AND REGGEON FIELD THEORY

We now begin the parts of this article which constitute the heart of recent developments in the theory of diffraction scattering (Abarbanel et al., 1975c). The discussion is couched in terms of the two dimensional impact parameter \vec{b} and its conjugate variable \vec{q} (four momentum transfer in elastic processes = $-|\vec{q}|^2$) and of the rapidity $y = \log s$ and its conjugate variable J (called l above). This variable J will turn out to be none other than the complex angular momentum, so we'll start with a pedestrian review of facts about complex angular momentum (Brower et al., 1974; Chiu, 1972; Collins, 1971; Eden, 1967; Frautschi, 1963).

The angular momentum referred to is that in the t-channel. It is defined by the partial wave expansion (Goldberger and Watson, 1964) of the elastic amplitude (for equal mass, m , spinless particles)

$$T(s, t) = \sum_{J=0}^{\infty} P_J(\cos \mathcal{J}_t) (2J+1) F_J(t) \quad , \quad (78)$$

$$F_J(t) = \frac{1}{2} \int_{-1}^{+1} d(\cos \mathcal{J}_t) P_J(\cos \mathcal{J}_t) T(s, t) \quad , \quad (79)$$

$$s = -2 \left(\frac{t}{4} - m^2 \right) (1 - \cos \mathcal{J}_t) \quad . \quad (80)$$

These definitions hold for integer J in the physical region of the t-channel: $t \geq 4m^2$, $s \leq 0$. We wish to continue the expansion to $t \leq 0$, $s \geq 4m^2$, the physical

region of the s -channel, and any J . Books are available on how one does this in detail (Eden, 1967; Omnès and Froissart, 1963). We imagine a dispersion relation in s , for fixed t , may be written for $T(s, t)$:

$$T(s, t) = \frac{1}{\pi} \int_{4m^2}^{\infty} \frac{ds' \operatorname{Im} T(s', t)}{s' - s - i\epsilon} + \frac{1}{\pi} \int_{4m^2}^{\infty} \frac{du' \operatorname{Im} T(u', t)}{u' - u - i\epsilon} , \quad s+t+u=4m^2 , \quad (81)$$

and using this in the definition of $F_J(t)$ we have

$$F_J(t) = \frac{1}{\pi} \int_{z_0(t)}^{\infty} dz' Q_J(z') \left[\operatorname{Im} T(z', t) - (-1)^J \operatorname{Im} T(-z', t) \right] , \quad (82)$$

where

$$z_0(t) = 1 + \frac{4m^2}{2\left(\frac{t}{4} - m^2\right)} , \quad z = \cos \mathcal{A}_t \quad (83)$$

and $Q_J(z)$ is the Legendre function of the second kind. This formula due to Froissart and Gribov (Froissart, 1961b; Gribov, 1962) allows one to define signed partial wave amplitudes

$$F^\tau(J, t) = \int_{z_0(t)}^{\infty} \frac{dz'}{\pi} Q_J(z') \left[\operatorname{Im} T(z', t) \mp \tau \operatorname{Im} T(-z', t) \right] , \quad (84)$$

with $\tau = \pm 1$. This is the appropriate formula for continuing to complex J . The full amplitude $T(s, t)$ is recovered by the Sommerfeld-Watson transform (Collins, 1971; Frautschi, 1963)

$$T(s, t) = - \int \frac{dJ}{2i} \sum_{\tau} \frac{(P_J(-z_t) + \tau P_J(z_t))}{\sin \pi J} F^\tau(J, t) , \quad (85)$$

where the contour in the J plane runs to the right of singularities in $F^\tau(J, t)$.

We are interested in very high energies which formally means z_t large.

For this regime we may use

$$P_J(z) \sim z^J \quad (86)$$

and

$$Q_J(z) \sim z^{-J-1} \quad (87)$$

to rewrite our expressions for $F^\tau(J, t)$ and $T(s, t)$

$$F^\tau(J, t) = \int_{4m^2}^{\infty} ds' s'^{-J-1} \left[\text{Im } T(s', t) + \tau \text{Im } T(-s', t) \right] \quad , \quad (88)$$

and

$$T(s, t) = \int_{c-i\infty}^{c+i\infty} \frac{dJ}{2\pi i} s^J \sum_{\tau} \xi_J^\tau F^\tau(J, t) \quad , \quad (89)$$

with

$$\xi_J^\tau = (\tau + e^{-i\pi J}) / \sin \pi J \quad . \quad (90)$$

Now one may verify by elementary integration that when $\text{Im } T(s, t) \sim s^{\alpha(t)}$ as in the multiperipheral model

$$F^\tau(J, t) = (J - \alpha(t))^{-1} \quad \text{for } \tau = +1 \text{ or } \tau = -1 \quad . \quad (91)$$

If $\tau = \pm 1$, then the partial wave amplitude has physical poles in even (odd) angular momentum. We wish to examine the $F^\tau(J, t)$ which is relevant for $J \approx 1$, $t \approx 0$ and do not wish any poles or other singularities to represent actual singularities or equivalently particles, since there are no zero mass particles of spin one in pure hadron physics. So we are interested in the $\tau = +1$ amplitude, and unless further warning is made, we will discuss it alone. Call it simply $F(J, t)$

$$F(J, t) = \int_{s_0=4m^2}^{\infty} ds s^{-J-1} \text{Im } T(s, t) \quad , \quad (92)$$

and

$$T(s, t) = \int_{c-i\infty}^{c+i\infty} \frac{dJ}{2\pi i} \xi_J s^J F(s, t) \quad , \quad (93)$$

$$\xi_J = (1 + e^{-i\pi J}) / \sin \pi J \quad . \quad (94)$$

Notice that the representation (92) is just the Mellin transform needed to partially diagonalize the multiperipheral integral equation. This is not a coincidence. The poles of the multiperipheral model are known as Regge poles (Blankenbecler and Goldberger, 1962; Chew and Frautschi, 1961). Regge first discussed J-plane poles in potential scattering (Regge, 1960).

Now we are ready to consider the question of unitarity coupled with the multiperipheral model. In our present language, we wish to ask: What happens to the pole in J when it rescatters? Our approach will be to take a Feynman graph from a conventional ϕ^3 like field theory and analyze it at large s, fixed t. We want this graph to have double Reggeon $s^{\alpha(t)}$ or $(J - \alpha(t))^{-1}$ exchange. The simplest such graph one would consider writing is shown in Fig. 30. However, one can give a physical argument why it will be dominated for large s by the more complicated graph in Fig. 31. It goes like this: the scattering is caused during the very rapid passage of particles A and B by each other via the exchange of two objects (Reggeons here) in the two dimensional plane perpendicular to their relative motion. As s is increased, the time which A and B spend in each other's vicinity during which they must make the exchange decreases rapidly. In Fig. 30 particle A emits a Reggeon (wiggly line) and later emits a second Reggeon. B absorbs one at a time; this also involves a time delay. In Fig. 31 particle A breaks up into two other particles and each of these emits a Reggeon at the same time. B does the same in order to receive the Reggeons at the same

time. Particle A reconstitutes itself from the particles it emitted, but it does this at its leisure in its own rest frame no longer caring about the brief encounter with B.

There is a fancy defense for this little argument. Figure 31 was first studied by Mandelstam (Mandelstam, 1963) who showed it dominated Fig. 30 as a Feynman graph for $s \rightarrow \infty$. Figure 30 was first considered by Amati et al. (Amati et al., 1962) as a contribution to $\text{Im } T(s, t)$ through elastic unitarity (Fig. 32). When one understands that there are additional contributions to $\text{Im } T(s, t)$ from two Reggeon exchange, the two seemingly disparate calculations are easily reconciled.

After some straightforward algebra the contribution of Fig. 31 to the partial wave amplitude $F(J, t)$ arising from the double exchange of s^α is (Fig. 33)

$$F(J, t) = \int d^2 q_1 d^2 q_2 \delta^2(\vec{q} - \vec{q}_1 - \vec{q}_2) N_2(J, \vec{q}_1, \vec{q}_2)^2 / J - \alpha(\vec{q}_1) - \alpha(\vec{q}_2) + 1 \quad , \quad (95)$$

with $t = -|\vec{q}|^2$, as usual, $\alpha(\vec{q}) = \alpha(t = -|\vec{q}|^2)$, and $N_2(J, \vec{q}_1, \vec{q}_2)$ is a complicated integral over the crossed box graph shown in Fig. 34. N_2 is a smooth function in J for $\vec{q}_i \approx 0$, so the only singularity in J from (95) is a branch point due to the denominator. This branch point occurs at

$$J_{\text{branch point}} = \alpha^{(2)}(t) = 2 \left[\alpha\left(\frac{t}{4}\right) - 1 \right] + 1 \quad . \quad (96)$$

Note that this branch point occurs at $J=1$ when $t=0$, if $\alpha(0)=1$.

From the exchange of K Reggeons one finds a contribution to $F(J, t)$

$$F(J, t) = \int \prod_{j=1}^K d^2 q_j \delta^2 \left(\vec{q} - \sum_{j=1}^K \vec{q}_j \right) N_K(J, \vec{q}_1, \dots, \vec{q}_K)^2 \left[J - \sum_{j=1}^K \alpha(\vec{q}_j) + K - 1 \right]^{-1} \quad . \quad (97)$$

This gives rise to a branch point in J at

$$J-1 = \alpha^{(K)}(t) - 1 = K \left[\alpha(t/K^2) - 1 \right] . \quad (98)$$

Note that this branch point occurs at J=1 when t=0, if $\alpha(0)=1$.

Return to (95) now and take the discontinuity in J across the branch line.

Since $N_2(J)$ is regular, this amounts to replacing the denominator by a delta function

$$\begin{aligned} \text{disc}_J F(J, \vec{q}) &= 2\pi i \int d^2 q_1 d^2 q_2 \delta^2(\vec{q} - \vec{q}_1 - \vec{q}_2) \delta(1-J - (1-\alpha(\vec{q}_1)) - (1-\alpha(\vec{q}_2))) \\ &\quad \times N_2(J, \vec{q}_1, \vec{q}_2)^2 \end{aligned} \quad (99)$$

or writing $E=1-J$ (the Reggeon energy)

$$\text{disc}_E F(E, \vec{q}) = -2\pi i \int d^2 q_1 d^2 q_2 \delta^2(\vec{q} - \vec{q}_1 - \vec{q}_2) \delta(E - \epsilon(\vec{q}_1) - \epsilon(\vec{q}_2)) N_2(E, \vec{q}_1, \vec{q}_2)^2 , \quad (100)$$

with

$$\epsilon(\vec{q}) = 1 - \alpha(\vec{q}) , \quad (101)$$

which is shown in Fig. 35.

We read this formula as follows: two particles create two Reggeons, $\alpha(\vec{q}_1)$ and $\alpha(\vec{q}_2)$, with an amplitude $N_2(E, \vec{q}_1, \vec{q}_2)$. These two Reggeons are "on shell": $\epsilon(\vec{q}) = 1 - \alpha(\vec{q})$ and their momentum coordinates \vec{q}_i are integrated over, $d^2 q_1 d^2 q_2$, subject to the constraints of momentum conservation, $\delta^2(\vec{q} - \vec{q}_1 - \vec{q}_2)$, and "energy" conservation, $\delta(E - \epsilon(\vec{q}_1) - \epsilon(\vec{q}_2))$. Finally the two Reggeons become two particles with an amplitude N_2 . It is instructive to compare this to the N=2 contribution to the unitarity relation for $T_{AB \rightarrow AB}(s, t)$ (Eq. 30):

$$\begin{aligned} \text{disc}_s T_{AB \rightarrow AB}(s, t) &= \frac{2i}{(2\pi)^2} \int \frac{d^3 p_1}{2E_1} \frac{d^3 p_2}{2E_2} \delta^3(\vec{p}_A + \vec{p}_B - \vec{p}_1 - \vec{p}_2) \delta(E_A + E_B - E(\vec{p}_1) - E(\vec{p}_2)) \\ &\quad \times T_{AB \rightarrow 12}(p_A + p_B \rightarrow p_1 + p_2) T_{AB \rightarrow 12}^*(p_A + p_B \rightarrow p_1 + p_2) . \end{aligned} \quad (102)$$

Except for uninteresting factors of 2π and i , this formula is to be read almost identically to the Reggeon discontinuity formula (100). Some differences are elementary: phase space has three momentum coordinates and one energy coordinate. $E(\vec{p}) = (m^2 + |\vec{p}|^2)^{1/2}$. The appearance of $T T^*$, however, is important. It announces the presence of an imaginary part in $T_{AB \rightarrow 12}$ itself. If we generalize the set of graphs entering N_2 to include diagrams like Fig. 36, then (100) reads

$$\text{disc}_E F(E, \vec{q}) = 2i \int d^2 q_1 d^2 q_2 \delta^2(\vec{q} - \vec{q}_1 - \vec{q}_2) \delta(E - \epsilon(\vec{q}_1) - \epsilon(\vec{q}_2))$$

$$N_2(E+i\epsilon, \vec{q}_1, \vec{q}_2) N_2(E-i\epsilon, \vec{q}_1, \vec{q}_2) \quad , \quad (103)$$

and the correspondence with usual unitarity is complete. The $\pm i\epsilon$ refers to the two Reggeon branch point in N_2 .

From the Reggeon unitarity relation we abstract the following view of a Reggeon: it is a quasi-particle living in one time and two space dimensions, τ and \vec{x} , which are the conjugate variables to the Reggeon energy E and Reggeon momentum \vec{q} . In the unitarity relation when the Reggeons are on shell, the energy-momentum relation is $E(\vec{q}) = 1 - \alpha(\vec{q})$, where $\alpha(\vec{q}) = \alpha(t = -|\vec{q}|^2)$ is the familiar function describing the s dependence of the multiperipheral model. If $\alpha(0)=1$, then $E(0)=0$, which is the energy-zero momentum relation for a massless particle. The Pomeron is a massless particle in E, \vec{q} space.

Away from $\vec{q}=0$, the exchange of various numbers of Reggeons gives rise in $F(E, \vec{q})$ to, first a pole at $E = \epsilon(\vec{q})$, then various branch points associated with many Reggeon states in the unitarity relation. Figure 37 shows this. At $\vec{q}=0$, the pole is at $\epsilon(0)$; the N Reggeon branch point is at $N \epsilon(0)$. When $\epsilon(0)=0$, all the cuts and the pole coalesce, just as one expects from experience with massless particles, such as photons.

One may write discontinuity or unitarity relations for $N_K(E, \vec{q}_1)$ as well (Abarbanel, 1972b; Gribov et al., 1965; White, 1972). These are shown in Fig. 38 for the 2 Reggeon discontinuity of N_2 . This involves the four Reggeon amplitude M_4 . Of course, a discontinuity relation for M_4 may be written. It involves M_4 itself and is depicted in Fig. 39.

The status of these unitarity relations is quite general. They have been derived from the structure of hybrid Feynman graphs (Gribov, 1968), from the dual resonance model (Lovelace, 1971), in a very wide class of multiperipheral models (Abarbanel, 1972b), and directly from analytically continued multi-particle t-channel unitarity (Gribov et al., 1965; White, 1972). Any theory that satisfies them for n Reggeons \rightarrow m Reggeons will satisfy t-channel unitarity in the same regime.

If $\alpha(0) < 1$, so $\epsilon(0) > 0$, for the Reggeons, then the pole and its associated branch points are separated in the E plane. The study of $F(E)$ or $N_K(E)$ or $M_K(E)$ would then be adequately carried out by a dispersion relation in E which utilized the nearby singularities (Abarbanel, 1972b). For $\epsilon(0)=0$, this is clearly inadequate in the neighborhood of $E=0$. The technique which has been more fruitful has been to write a Reggeon field theory treating the Reggeon as a quasi-particle in the τ, \vec{x} space described before (Abarbanel et al., 1975c; Gribov, 1968). This guarantees the phase space structure of the Reggeon unitarity relations and provides a constructive method for determining the M_K or N_K functions. A solution of the field theory in any consistent scheme yields the M_K or N_K within the limitations of that scheme and satisfies t-channel unitarity.

So we introduce a field $\phi(\vec{x}, \tau)$ and take the multiperipheral model for our "bare" Reggeon

$$\alpha(t) = \alpha_0 + \alpha'_0 t \quad , \quad (104)$$

$$\epsilon(\vec{q}) = \alpha_0' \vec{q}^2 + \Delta_0 \quad , \quad (105)$$

$$\Delta_0 = 1 - \alpha_0 \quad . \quad (106)$$

The Lagrange density for this energy-momentum relation is

$$\mathcal{L}(\vec{x}, \tau) = \frac{i}{2} \phi^+(\vec{x}, \tau) \frac{\overrightarrow{\partial}}{\partial \tau} \phi(\vec{x}, \tau) - \alpha_0' \nabla \phi^+ \cdot \nabla \phi - \Delta_0 \phi^+ \phi \quad . \quad (107)$$

Reggeons will interact and this we must account for. The study of more complicated graphs which are the generalization of Fig. 31 shows that for the Pomeron, which has vacuum quantum numbers, graphs with n Pomerons \rightarrow m Pomerons exist. Figure 40 shows examples of $1 \rightarrow 2$, $2 \rightarrow 2$, and $1 \rightarrow 3$. Each of these transitions is described by a function $M^{(n, m)}(E_i, \vec{q}_i)$ depending on the energies and momenta of all the Reggeons. Reggeons carrying quantum numbers may have restrictions as to which n may go to which m , but all that are so allowed can be found in the graphical analysis.

If we had to face this terrible infinity of nonlocal couplings, there would be little hope of achieving anything. We are interested in a restricted set of questions, however, having to do with diffraction scattering as $s \rightarrow \infty$, t fixed. First we will argue that we need only consider the Pomeron, then that we need only consider the regime $E \approx 0$, t small, and finally that only the triple Pomeron coupling will be important (Abarbanel and Bronzan, 1974a, b; Migdal et al., 1974).

Let us take the Green's function for the Lagrangian (107). In E, \vec{q} space it is

$$G(E, \vec{q}) = i \left(E - \alpha_0' \vec{q}^2 - \Delta_0 + i\epsilon \right)^{-1} \quad (108)$$

and in $\tau = -i \log s = -iy$, \vec{x} space it is

$$G(y, \vec{x}) = \int \frac{d^2 q dE}{(2\pi)^3} e^{i(\vec{q} \cdot \vec{x} - E\tau)} G(E, \vec{q}) \quad (109)$$

$$= \theta(y) e^{-y\Delta_0} \frac{1}{4\pi\alpha'_0 y} e^{-|\vec{x}|^2/4\alpha'_0 y}, \quad (110)$$

which represents the probability amplitude for a source (particles) to emit a Reggeon ($\alpha(t) = \alpha_0 + \alpha'_0 t$) at zero rapidity, zero impact parameter and for another source to absorb it at y, \vec{x} . This is shown in Fig. 41. This amplitude represents the diffusion of the Reggeon over the time interval y and space interval $|\vec{x}|$. If two Reggeons depart the initial source and arrive at the sink, Fig. 42 represents that possibility. Each line carries a factor like (110). Along the way from $(0, 0)$ to (y, \vec{x}) the Reggeons may choose to interact. Figure 43 shows this.

This space-"time" picture is borne out experimentally to a very reasonable approximation. The latest results on elastic scattering (Fermilab, 1975) show that, indeed, the average "size" of a hadron as probed by Pomerons is $\propto \sqrt{\log s}$ and that the "stuff" interacting via Pomerons is distributed more or less as a gaussian in impact parameter space. This is all a support for the multiperipheral amplitude being a sensible starting point for a theory of diffraction.

Now for very long times, $y \rightarrow \infty$; that is $\log s \rightarrow \infty$. Only those Reggeons with the smallest Δ_0 will survive. All others will be damped by $e^{-\Delta_0 y}$ in the Green's function. Well, the smallest Δ_0 is for the Pomeron, $\Delta_0 = 1 - \alpha_0 = 0$. In the limit then where $\log s$ is large, only the Pomeron and its interactions need be considered. If one is discussing a process like charge exchange, then clearly at least one Reggeon carrying the appropriate quantum numbers need be exchanged, and accompanying it will be as many Pomerons as one likes. Actually the

argument just given shows that only one quantum number carrying Reggeon will survive in the limit (Abarbanel and Sugar, 1974; Gribov et al., 1971). For diffraction scattering, Pomerons alone are sufficient.

If we deal with only the Pomeron, then the neighborhood of $E=0$ is where we need concentrate our attention. Furthermore, since we wish to study $t \approx 0$, we will also be interested in $\vec{q} \approx 0$. From the point of view of the Reggeon field theory, then, we are concerned with the study of an infrared problem to learn about $s \rightarrow \infty$, t small, diffraction scattering.

Since we are focusing our attention only on E_i , $\vec{q}_i \approx 0$, we want to include in our field theory only the contributions which require the least phase space $dE_i d^2q_i$ when they operate. Those interactions are the ones with the fewest number of fields and no derivative couplings. All this points our concentration on

$$\mathcal{L}_I(\vec{x}, \tau) = -\frac{\lambda_0}{2} \phi^+(\vec{x}, \tau) \phi(\vec{x}, \tau) \left[\phi^+(\vec{x}, \tau) + \phi^-(\vec{x}, \tau) \right] \quad . \quad (111)$$

More rigorous arguments (Calucci and Jengo, 1975) can be made for the pre-dominance of this interaction, and its importance can be defended by detailed calculation (Abarbanel and Bronzan, 1974c; Bardeen et al., 1975). The results of these calculations show that terms involving $2 \rightarrow 2$ or $1 \rightarrow 3$ couplings as in Fig. 40 are the next most important. When all graphs are summed, this interaction modifies $\alpha(t)$ by factors of $t/(\log t)^5$, which is very mild, and makes contributions to the total cross section down by powers of $\log s$ relative to the ϕ^3 coupling of (111).

Before we can write down the final field theory one more important point must be noted. In the graph of Fig. 44 we have a relative minus sign compared to the single Pomeron exchange graph of Fig. 41. The pedestrian origin of this

sign is that each Pomeron carries a factor

$$\xi_\alpha = \frac{1 + e^{-i\pi\alpha(t)}}{\sin \pi\alpha(t)} = -i$$

near $t=0$ and each loop integration has a factor $-i$. So the pole term has a phase $-i$ while the Pomeron loop has a phase $(-i)^2 (-i) = i$. Physically the change in sign means that the amplitude of Fig. 44 subtracts from the pole exchange, which an absorptive Pomeron ought to do. In the field theory formulation we may arrange this automatically by letting the triple Pomeron coupling, λ_0 , be pure imaginary (Gribov, 1968): $\lambda_0 = ir_0$ (Fig. 44).

The full Lagrange density we now must study in the infrared limit is

$$\mathcal{L}(\vec{x}, \tau) = \frac{i}{2} \phi_0^+ \frac{\vec{\partial}}{\partial \tau} \phi_0 - \alpha'_0 \nabla \phi_0^+ \cdot \nabla \phi_0 - \Delta_0 \phi_0^+ \phi_0 - \frac{ir_0}{2} \phi_0^+ \phi_0 (\phi_0^+ + \phi_0) . \quad (112)$$

Furthermore we want to study this to all orders in r_0 , since a priori near $E, \vec{q}=0$ all graphs are of equal importance. The appropriate tool must be non-perturbative to be reliable. The renormalization group is the answer (Abarbanel, 1974a; Coleman, 1973; Wilson and Kogut, 1974).

When we have finished solving the field theory defined by (112), we will find it to depend on four numbers:

1. The scale of the renormalized Pomeron field which we can arrange to be equal to one. This is done by rescaling the unrenormalized field $\phi_0(\vec{x}, \tau)$ by a factor $Z_3^{1/2}$

$$\phi(\vec{x}, \tau) = Z_3^{-1/2} \phi_0(\vec{x}, \tau) . \quad (113)$$

Z_3 is yet to be determined.

2. A new "slope" parameter α' which is a function of the arbitrary point E_N, k_N in energy momentum space where we choose to define the field theory

α' is related by a scale change to α'_0 :

$$\alpha' = Z_2^{-1} \alpha'_0 . \quad (114)$$

3. A new gap or mass parameter Δ which is also a function of E_N and k_N .

It is given by

$$\Delta = Z_4^{-1} \Delta_0 . \quad (115)$$

4. A new coupling constant r . Again it is a function of the arbitrary normalization point of the theory. It is related to the bare value r_0 by

$$r = Z_3^{3/2} Z_1^{-1} r_0 . \quad (116)$$

Each of these scalings defines a new set of parameters. We will express the renormalized Green's functions of the theory in terms of these parameters and the E_i, \vec{q}_i of the Pomerons. These parameters depend on the normalization point of the theory. This normalization point is precisely like a subtraction in dispersion theory and is familiar from the study of quantum electrodynamics. Suppose we change the normalization point from E_N to $E_N + \delta E_N$. Clearly the physics of our problem doesn't change; that's all in the Lagrangian (112). The parametrization of Green's functions will change slightly. The parameters $1, \alpha', \Delta,$ and r must change so as to preserve the physics:

$$1 \rightarrow 1 + \left(E_N \frac{\partial}{\partial E_N} \log Z_3 \right) \frac{\delta E_N}{E_N} , \quad (117)$$

$$= 1 + \gamma \frac{\delta E_N}{E_N} \quad (118)$$

$$\alpha' \rightarrow \alpha' + \alpha' \left(E_N \frac{\partial}{\partial E_N} \log Z_2^{-1} \right) \frac{\delta E_N}{E_N} , \quad (119)$$

$$= \alpha' \left[1 + \tau \frac{\delta E_N}{E_N} \right] , \quad (120)$$

$$\Delta \rightarrow \Delta + \Delta \left(E_N \frac{\partial}{\partial E_N} \log Z_4^{-1} \right) \frac{\delta E_N}{E_N} , \quad (121)$$

$$= \Delta \left[1 + \eta \frac{\delta E_N}{E_N} \right] , \quad (122)$$

and

$$r \rightarrow r + r \left(E_N \frac{\partial}{\partial E_N} \log Z_3^{3/2} Z_1^{-1} \right) \frac{\delta E_N}{E_N} , \quad (123)$$

$$= r \left[1 + \hat{\beta} \frac{\delta E_N}{E_N} \right] . \quad (124)$$

In order to preserve the physics under this change of parametrization the parameters must enter the Green's functions in a prescribed fashion. Basically they must represent the same quantity as E_N is varied. Thus they are a non-linear, nontrivial representation of motions along the real line. This is the renormalization group.

To best express the content of the renormalization group constraints we consider the n Pomeron \rightarrow m Pomeron proper vertex function $\Gamma^{(n,m)}(E_1, \vec{q}_1)$ (Abarbanel and Bronzan, 1974a,b; Migdal et al., 1974), which is the $n \rightarrow m$ Green's function with external legs removed. $\Gamma^{(1,1)}(E, \vec{q}^2)$ is the inverse propagator and contains the spectrum of the theory. We are now dealing with Pomerons alone (the M_K functions from above) and will reintroduce particles shortly. The renormalized $\Gamma^{(n,m)}$ is a function of α' , Δ and the dimensionless coupling constant

$$g = \frac{r}{(\alpha')^{D/4}} E_N^{D/4 - 1} , \quad (125)$$

where D is the number of dimensions of impact parameter space.

The generalization to D transverse dimensions is solely a technical aid. It allows one to nicely regularize and then renormalize the Feynman integrals of the field theory. In establishing the dimension of quantities in our field theory, separate dimensions must be attributed to space, \vec{x} , and "time", τ . In (125) we see that D=4 is selected out as that dimension where g, the dimensionless coupling, does not depend on the normalization point E_N used in defining the field theory. At D=4 the theory possesses a scale invariance under \vec{x}, τ scalings. D=2 in our real four space-time dimensional world.

$\Gamma^{(n, m)}$ is related to the unrenormalized $\Gamma_U^{(n, m)}$ computed in terms of $\alpha'_0, \Delta_0,$ and r_0 from the Lagrangian by

$$\Gamma^{(n, m)}(E_i, \vec{q}_i, \alpha', g, \Delta, E_N) = Z_3^{\frac{n+m}{2}} \Gamma_U^{(n, m)}(E_i, \vec{q}_i, \alpha'_0, r_0, \Delta_0) . \quad (126)$$

Since $\Gamma_U^{(n, m)}$ doesn't know about E_N , the point where we choose to normalize $\Gamma^{(n, m)}$, we have

$$\left[E_N \frac{\partial}{\partial E_N} + \tau \alpha' \frac{\partial}{\partial \alpha'} + \eta \Delta \frac{\partial}{\partial \Delta} + \beta \frac{\partial}{\partial g} - \frac{(n+m)}{2} \gamma \right] \Gamma^{(n, m)} = 0 , \quad (127)$$

$$\beta = E_N \frac{\partial}{\partial E_N} g , \quad (128)$$

and the other functions have been defined a moment ago.

Now the normalization conditions on the theory must define 1, α' , Δ , and r. We want Δ , the renormalized energy gap or mass to be zero, since

$$\Delta = 1 - \alpha(0) = 0 \quad (129)$$

for the Pomeron. This leads us to require

$$\Gamma^{(1, 1)}(E, \vec{q}^2) \Big|_{E=0}^{\vec{q}^2=0} = 0 . \quad (130)$$

The other parameters are defined by

$$\left. \frac{\partial}{\partial E} i\Gamma_U^{(1,1)} \right|_{\substack{E=-E_N \\ \vec{q}^2=0}} = Z_3^{-1} , \quad (131)$$

$$\left. \frac{\partial}{\partial \vec{q}^2} i\Gamma_U^{(1,1)} \right|_{\substack{E=-E_N \\ \vec{q}^2=0}} = -\alpha'_0 Z_2^{-1} Z_3^{-1} , \quad (132)$$

and

$$Z_1^{-1} = \frac{(2\pi)^{(D+1)/2}}{r_0} \Gamma_U^{(1,2)} \Big|_{E_1=2E_2=2E_3=-E_N; \vec{q}_i=0} . \quad (133)$$

This allows us to determine the Z_i and thus our renormalized parameters. Any other definitions entail a finite renormalization.

The crucial information is in the function $\beta(g)$ which is determined in lowest order perturbation theory to be

$$\beta(g) = -\frac{(4-D)}{4}g + \mathcal{K}g^3 , \quad (134)$$

with $\mathcal{K} > 0$ (Fig. 45). This has a zero at $g=g_1 \alpha(4-D)^{1/2}$ and

$$\beta_1 = \left. \frac{d\beta}{dg} \right|_{g_1} > 0 . \quad (135)$$

This information is important because the solution (Abarbanel, 1974a; Coleman, 1973) to the renormalization group equation tells us

$$\begin{aligned} \Gamma^{(n,m)}(\xi E_i, \vec{q}_i, \alpha', g, E_N) &= \Gamma^{(n,m)}(E_i, \vec{q}_i, \tilde{\alpha}'(-t), \tilde{g}(-t), E_N) \\ &\times \exp \int_{-t}^0 dt' \left[1 - \frac{n+m}{2} \gamma(\tilde{g}(t')) \right] , \end{aligned} \quad (136)$$

where

$$t = \log \xi \quad , \quad (137)$$

$$\frac{d\tilde{g}(t)}{dt} = -\beta(\tilde{g}(t)) \quad , \quad (138)$$

and

$$\frac{1}{\tilde{\alpha}'(t)} \frac{d\tilde{\alpha}'(t)}{dt} = 1 - \tau(\tilde{g}(t)) \quad . \quad (139)$$

The study of $\Gamma^{(n, m)}$ for $\xi \rightarrow 0$; that is, $E_i \rightarrow 0$, is reduced to the study of $\tilde{g}(-t = -\log \xi)$ as its argument $\rightarrow +\infty$. With the $\beta(g)$ for our theory

$$\tilde{g}(t) = e^{(4-D)t/4} \left[\frac{1}{g} + \frac{4\mathcal{K}}{4-D} (e^{(4-D)t/2} - 1) \right]^{-1/2} \quad , \quad (140)$$

with the boundary condition $\tilde{g}(0)=g$. Now as $t \rightarrow +\infty$ $\tilde{g}(t) \rightarrow g_1$. [If β_1 were negative, $\tilde{g}(t)$ would recede from such a zero.] So we learn that in the infrared limit, the Pomeron Green's functions we seek are determined by a zero of the function $\beta(g)$. If D were four, then $g_1=0$ and on the right hand side of (136) we would be instructed to determine $\Gamma^{(n, m)}$ by an effective free theory. If $D \neq 4$, as in physics, g_1 may still be small enough.

Anyway for E_i small enough $g \rightarrow g_1$. Using ordinary dimensional analysis we find this restricts $\Gamma^{(n, m)}$ to be of the form (Abarbanel and Bronzan, 1974a,b; Migdal et al., 1974)

$$\Gamma^{(n, m)}(E_i, \vec{q}_i, \alpha', g_1, E_N) = E_N \left(\frac{E_N}{\alpha'} \right)^{(2-n-m)D/4} \left(\frac{-E}{E_N} \right)^{1 - \frac{n+m}{2} \gamma(g_1) + z(g_1)(2-n-m)D/4} \\ \times \phi_{n, m} \left(\frac{E_i}{E}, \left(\frac{-E}{E_N} \right)^{-z(g_1)} \frac{\vec{q}_i \cdot \vec{q}_j \alpha'}{E_N}, g_1 \right) \quad , \quad (141)$$

where $E = \sum_{i=1}^n E_i$, $\phi_{n,m}$ is a dimensionless function of its scaled variables, and

$$z(g_1) = 1 - \tau(g_1) \quad . \quad (142)$$

$\phi_{n,m}$ is not determined by what we have said so far. Clearly the limit in which (141) makes sense must be

$$\left. \begin{array}{l} E_i \rightarrow 0 \\ E_i/E \text{ fixed} \\ \vec{q}_i \cdot \vec{q}_j / (-E)^Z \text{ fixed} \end{array} \right\} \quad . \quad (143)$$

We can draw two immediate consequences from this solution to our infrared problem:

1. If there is a renormalized Pomeron, which would arise as a zero of $\Gamma(1, 1)$, it must have the energy momentum relation

$$E(\vec{q}) = -E_N \left(\frac{\vec{q}^2 \alpha'}{E_N} \right)^{1/z(g_1)} \quad , \quad (144)$$

or

$$\alpha(t) = 1 + E_N \left(\frac{\alpha' t}{E_N} \right)^{1/z(g_1)} \quad , \quad (145)$$

which is not substantially different from the original multiperipheral Pomeron as long as $z(g_1) \approx 1$.

2. The contribution to the total cross section coming from one renormalized Pomeron exchange (Fig. 46) factorizes, and behaves as

$$\sigma_T^{AB}(s) \sim g_A g_B (\log s)^{-\gamma(g_1)} \quad . \quad (146)$$

Various attempts have been made to estimate the size of γ and z . The first was in an expansion around $D=4$ dimensions where the theory is scale invariant.

Since the zero of $\beta(g) g_1$ is proportional to $(4-D)^{1/2}$, this expansion is sure to be accurate near $D=4$. Its accuracy at $D=2$ cannot be determined a priori. The other method of determining these exponents is to use the analogue of solid state physics' high temperature expansion. The best efforts place the values in the range (Abarbanel and Bronzan, 1974a,b; Baker, 1974; Bronzan and Dash, 1974; Dash and Harrington, 1975; Ellis and Savit, 1975; Migdal et al., 1974)

$$+\frac{1}{4} \lesssim -\gamma \lesssim +\frac{1}{2} \quad , \quad (147)$$

and

$$\frac{9}{8} \lesssim z \approx \frac{5}{4} \quad . \quad (148)$$

It is important to note that higher order Pomeron exchanges involving $\Gamma^{(1,2)}$ and so on, give rise to lower and lower contributions to σ_{total} . The hierarchy of contributions is shown in Fig. 47. This means that the asymptotic total cross section will factorize and rise as $(\log s)^{-\gamma}$ according to Reggeon field theory.

IX. DEVELOPMENTS IN REGGEON FIELD THEORY

A. Early Work

The discussion so far has emphasized the summation of all graphs of the Reggeon Field Theory by use of the renormalization group. Earlier techniques emphasized instead the Schwinger-Dyson equations of the field theory which contain the full nonlinear information via coupled integral equations. For example, $\Gamma^{(1,1)}$, the inverse propagator satisfies (Fig. 48)

$$\begin{aligned}
 i\Gamma^{(1,1)}(E, \vec{q}^2) &= E - \alpha'_0 \vec{q}^2 - \Delta_0 \\
 &- \frac{i r_0}{2} \int \frac{d^2 q' dE'}{(2\pi)^{3/2}} \left\{ \Gamma^{(1,1)}(E', \vec{q}'^2) \Gamma^{(1,1)}(E-E', (\vec{q}-\vec{q}')^2) \right\}^{-1} \\
 &\times \Gamma^{(1,2)}(E', E-E', \vec{q}', \vec{q}-\vec{q}') \quad (149)
 \end{aligned}$$

The early Soviet work (Gribov and Migdal, 1969a, b, c) emphasized two possible solutions to this and related nonlinear equations:

1. A weak coupling solution where the integral in (149) remains negligible and the Pomeron remains a simple pole. As we have emphasized before, there is such theoretical disaster associated with a pure Pomeron pole that we need not further discuss it.

2. A strong coupling solution. Here the inverse propagator becomes

$$i\Gamma^{(1,1)} = (-E)^{1-\gamma} \phi_{1,1}(\vec{q}^2/(-E)^2) \quad , \quad (150)$$

just as in the renormalization group solution. This solution was arrived at in a manner quite different from the latter day renormalization group method. It was argued then that it led to a negative total cross section. Needless to say, it was rejected. In retrospect one can see that the scaling forms do formally satisfy the nonlinear integral equations of the theory yielding integral equations among

the scaling functions $\phi_{n,m}$. The argument that led to negative cross sections, however, went outside the field theory and was incorrect.

B. Secondary Trajectories

It is natural to ask how the theory of the Pomeron developed above affects Reggeons with quantum number exchange (ρ, ω, A_2, \dots) or $\alpha(1) < 1$ (f, \dots) (Abarbanel and Sugar, 1974; Gribov et al., 1971). Since it is the exchange of the ρ Reggeon with

$$\alpha_{\rho}(t) \approx \frac{1}{2} + t / \left(\frac{\text{GeV}}{c} \right)^2 \quad (151)$$

that is so accurately measured in the pion-nucleon charge exchange experiments mentioned above, the matter has direct experimental importance.

The theoretical issue involves the summation of the graphs in Fig. 49. Again this may be done using the renormalization group. In the theory of secondary trajectories one has two β functions. One for the triple Pomeron coupling and one for the Reggeon-Pomeron-Pomeron coupling shown in Fig. 49. One searches the effective coupling constant space for stable points in the infrared limit. The result is that the amplitude for charge exchange is modified from

$$T_{\text{CEX}}(s, t) = g_A g_B s^{\alpha_{\rho}(t)} \left(\tau_{\rho} + e^{-i\pi\alpha_{\rho}(t)} \right) \quad (152)$$

which it was for a pure pole ($\tau_{\rho} = -1$) by multiplication with $(\log s)^{-\gamma_{\rho}}$. The function $\alpha_{\rho}(t)$ remains linear for small t . Estimates of γ_{ρ} using an expansion about $D=4$ indicate it is very small: $-\gamma_{\rho} \approx 1/10$. So the t -channel Reggeon field theory for boson trajectories is in very attractive shape.

Fermion trajectories are quite a bit more complicated (Bartels and Savit, 1975; Gribov et al., 1970). The results of summing the same set of graphs as in Fig. 49 yields a Fermion $\alpha_F(u)$, measured in backward scattering, which is

almost linear in u , as indicated experimentally, Also for $u < 0$, one has both positive and negative parity poles in the J -plane. For $u > 0$ where fermion states would be observed, only positive parity states or only negative parity states are produced. This also is borne out by the observed Fermion states; no parity doublet of states has yet been found.

C. The Issue of s -Channel Unitarity

Reggeon field theories are constructed to satisfy t -channel unitarity as expressed via the Reggeon unitarity relations. It is not in the least obvious that the theory respects unitarity in the s -channel as well. Actually it is very difficult to formulate completely the consequences of s -channel unitarity since there are detailed relations that must hold for $T_{N \rightarrow M}$ that are hard to investigate. Nevertheless, some features can be studied.

An important aspect of unitarity in the s -channel is the Froissart bound which requires

$$\alpha(0) \leq 1 \quad , \quad (153)$$

and

$$-\gamma \leq 2 \quad . \quad (154)$$

Also fairly straightforward is the requirement that $\sigma_{\text{elastic}} \leq \sigma_{\text{total}}$ which requires

$$-\gamma \leq z \leq 2 \quad . \quad (155)$$

Now this second restriction is true in all numerical calculations of the indices γ and z . Furthermore by studying the lattice formulation of Reggeon field theory (Brower et al., 1975; Cardy and Sugar, 1975) it has been possible to show that the existence of a zero of $\beta(g)$ like g_1 where $\beta_1 > 0$ implies (155).

The question of whether $\alpha(0) \leq 1$ is more subtle, but is also tractable. The key observation is that the term $\Delta_0 \phi^+ \phi$ in the Reggeon Lagrangian (112) acts like

a mass term in more conventional field theory (Abarbanel, 1974b). When $\Delta = 1 - \alpha(0) = 0$, there must be a very special value of Δ_0 , call it Δ_{0C} (for critical), which is a complicated function of α'_0 and r_0 . This value is obtained by formally integrating Eq. (131) for $i\Gamma^{(1,1)}$ (Sugar and White, 1974a, b)

$$i\Gamma_U^{(1,1)}(E, 0) = - \left[\frac{r_0}{(\alpha'_0)^{D/4}} \right]^{4/4-D} \int_{\frac{yE_N}{-E}}^{\infty} dy \frac{1}{y^2} \frac{1}{Z_3(y)}, \quad (156)$$

where

$$y = \left[\frac{r_0}{(\alpha'_0)^{D/4}} \right]^{4/4-D} \frac{1}{E_N}. \quad (157)$$

Comparing this with perturbation theory tells us that

$$\Delta_{0C} = 1 - \alpha_{0C} = - \left[\frac{r_0}{(\alpha'_0)^{D/4}} \right]^{4/4-D} \int_0^{\infty} \frac{dy}{y^2} \left[1 - \frac{1}{Z_3(y)} \right], \quad (158)$$

which is negative. The value of the bare Pomeron intercept which produces $\alpha(0)=1$ is greater than one

$$\alpha_{0C} > 1. \quad (159)$$

In the theory which we have studied above we assumed $\alpha_0 = \alpha_{0C}$, so $\Delta = 0$. What happens when $\alpha_0 \neq \alpha_{0C}$? When $\alpha_0 < \alpha_{0C}$, one has $\Delta > 0$ or $\alpha(0) < 1$, and the familiar pattern of separated poles and branch cuts in E emerges. When $\alpha_0 > \alpha_{0C}$, the theory becomes unstable in expansion about $\phi = \phi^+ = 0$, and one must find new values to expand around. The fields develop expectation values in the ground state and in the end $\Delta > 0$ again (Abarbanel et al., 1975d, e). For all values of α_0 the question of $\alpha_0 > \alpha_{0C}$ is examined by looking at the effective action (Coleman, 1973) of the Reggeon field theory. The extrema of this quantity determine the points around which one expands the quantum field. For $\alpha_0 < \alpha_{0C}$, these

are at $\phi = \phi^+ = 0$. When α_0 passes through α_{0C} , one moves to a different branch of the solutions and the fields develop expectation values. In conventional field theory this has the name spontaneous symmetry breaking. In statistical physics (Fischer, 1974; Wilson and Kogut, 1974) this corresponds to a phase transition where the expectation value, in the theory of magnets say, is the spontaneous magnetization. For all values of the input Pomeron intercept, α_0 , the output intercept $\alpha(0) \leq 1$. It is absolutely crucial in this that there be Pomeron interactions. Without them the Pomeron intercept would blithely go on up through one and never stop. This is precisely the situation which prevails in the multi-peripheral model. Reggeon Field Theory has been arranged to reduce to this when there are no Reggeon interactions.

There are several other requirements of s-channel unitarity which come in the form of inequalities like (155). They are met in the strong coupling solution of Reggeon field theories we have presented above (Cardy, 1975).

An heuristic argument can be made why Reggeon field theories satisfy the simple inequality constraints of s-channel unitarity. It is known by construction that eikonal models as discussed above do satisfy these requirements. Among the additions of Reggeon field theory to the eikonal models is more absorption through Pomeron interactions. This is going to decrease the eikonal amplitudes and presumably satisfy the same inequalities. Whether the detailed s-channel unitarity requirements are satisfied is not known. As a bold conjecture let me state that Reggeon field theories, built to meet t-channel unitarity, also satisfy s-channel unitarity.

There have been developed methods to study the s-channel content of Reggeon field theories. The two prime techniques are as follows:

1. Processes in the s-channel, as in the multiperipheral model, build up

the basic or bare Reggeons which go into the Reggeon graphs of Reggeon field theory. We have seen many examples of this. If we have a rule (Abramovskii et al., 1974; Caneschi and Jengo, 1975; Cardy and Suranyi, 1975; Koplik and Mueller, 1975; McLerran and Weis, 1975; Suranyi, 1975) for opening up a Reggeon and exposing its s-channel particle content, then we can take Reggeon graphs and enumerate their contribution to any given physical process in the s-channel.

The simplest graph is just one Reggeon exchange (Fig. 50) which we open up by taking the absorptive part. Taking this to reproduce the results of the multiperipheral model (flat spectrum in rapidity for inclusive processes, etc.) we may take more complicated graphs, such as Fig. 51, to study corrections to the multiperipheral model.

This procedure commits one to a specific mechanism for the building up of a Reggeon. Using the multiperipheral model as that choice makes excellent sense. However, the utility of the technique of cutting open Reggeons must break down as one arrives at energies where the scaling solutions discussed above become important. The reason is just that the number of graphs becomes infinite, and resumming cut graphs requires a new field theory of cut and uncut Reggeons. Such field theories have been developed and explored (Caneschi and Jengo, 1975; Cardy and Suranyi, 1975; Suranyi, 1975). For simple aspects of multiparticle production such as the average multiplicity one finds

$$\langle n \rangle (s) \sim (\log s)^{1-\gamma} \quad , \quad (160)$$

which rises faster than the logs of the multiperipheral model. Also the higher moments behave as

$$\langle n^k \rangle (s) \sim (\log s)^{k(1-\gamma)} \quad k=1, 2, \dots \quad . \quad (161)$$

2. The other approach has been to study specific s-channel processes and develop a calculus of Reggeons appropriate to it. Then one uses a field theory and, of course, the renormalization group to sum up all contributions to these processes in the $E_1, \vec{q}_1 \rightarrow 0$ limit. This has been used in the study of production amplitudes $T_{2 \rightarrow N}$ (Bartels, 1975a,b) and inclusive cross sections in the triple Regge region (Fig. 52) (Abarbanel et al., 1975a; Cardy et al., 1975).

The formulation of a field theory for either $T_{2 \rightarrow N}$ amplitudes or the triple Regge amplitudes, involves amusing complications coming from the presence of many partial wave amplitudes or the possibility of nonconservation of Reggeon energy.

In the case of $T_{2 \rightarrow N}$ one must sum the Reggeon graphs in Fig. 53 to evaluate the partial cross section for N particles $\sigma_N(s)$. Each of the solid dots represents a particle being produced. Here one must evaluate the renormalization of the additional vertex for Pomeron-Pomeron-particle which is not encountered in the elastic scattering problem. One finds (Anselm and Dyatlov, 1968; Bartels and Rabinovici, 1975) that each $\sigma_N(s)$ behaves

$$\sigma_N(s) \sim (\log s)^{-5/6} \quad . \quad (162)$$

The exponent is again determined in expansion around $D=4$. This calculation serves to demonstrate that the shielding effect of absorptive Pomeron corrections does fix up the old Finkelstein-Kajantie disease of the multiperipheral model (Zachariasen, 1971). Without Pomeron corrections $\sigma_N(s)$ grew faster than $(\log s)^2$ for N large enough and violated the elementary relation $\sigma_N < \sigma_{\text{total}} < (\log s)^2$.

The same calculation shows that Pomerons alone are not sufficient to build up a $\sigma_N(s)$ which when summed on N yields the σ_{total} of the full ϕ^3 Reggeon field theory. Instead $\sum_N \sigma_N \sim \sigma_{\text{elastic}} < \sigma_{\text{total}}$. Since the contributions to $\sigma_N(s)$

involve looking into the bare Pomeron couplings to discover how they are built from more fundamental processes, it is perhaps not surprising that Pomerons alone do not build Pomerons. Additional contributions from secondary objects will be needed. This is in striking contrast to the attempts from the s -channel point of view to make $\sigma_N(s)$ and $\sigma_{\text{total}}(s)$ from a self-consistent Pomeron.

The study of the triple Pomeron region of inclusive processes is important for in the multiperipheral model where $\alpha(t) = 1 + \alpha't$, the study of the graph in Fig. 52 showed that the triple Pomeron coupling had to vanish when $t=0$. (Abarbanel et al., 1971b). Looking into this coupling one found further and further restrictions on zero momentum transfer Pomeron couplings until it was shown that the Particle-Particle-Pomeron coupling which governs total cross sections had to vanish as well (Brower and Weis, 1972).

A Reggeon field theory for this process involves the energy nonconserving triple Pomeron vertex $\tilde{\Gamma}^{(1,2)}(E_1, \vec{q}_1)$ which reduces to our usual $\Gamma^{(1,2)}$ when $E_1 = E_2 + E_3$ (Fig. 52). The energy nonconservation arises because the process involves an intermediate "time", $\tau = \log M^2$, M^2 = the missing mass, in the progression of Reggeons from zero time up to $\log s$. One must sum up Reggeon diagrams as in Fig. 54 and more tricky as in Fig. 55, using the renormalization group (Abarbanel et al., 1975b; Frazer and Moshe, 1975).

The result of operating this machinery is that the total cross section from the triple Regge region behaves as $(\log s)^{-\gamma}$ and not greater than $\sigma_T(s)$ as in the multiperipheral model. So the interacting Pomeron restores the consistency with the elementary requirement $\sigma_{\text{triple Regge}} \leq \sigma_{\text{total}}$. The triple Pomeron vertex need not vanish analytically at $t=0$, and none of the Pomeron decoupling theorems need be addressed. The differential cross section in the triple Pomeron region has

more or less the form

$$\frac{d\sigma}{dt d \log M^2} \sim (\log M^2)^{-\gamma} / (\log s/M^2)^{-2\gamma} e^{-t(\log s)^2}, \quad (163)$$

for $\log M^2 \gg \log s/M^2$. This has no tendency to vanish at $t=0$ and gives the integrated cross section $(\log s)^{-\gamma}$ mentioned above. This closes the circle on the mysterious Pomeron decoupling theorems and provides substantial support for the consistency of Reggeon field theories with s -channel unitarity.

D. Other Matters

There are two other interesting results within the framework of Reggeon field theory which bear reporting. The first has to do with scattering on nuclei (Kancheli, 1973; Lehman and Winbow, 1974; Schwimmer, 1975). In the single pole approximation (Fig. 56) when the nuclear radius $R_0 A^{1/3}$ is large compared to the impact parameter fluctuation distance $\sqrt{\alpha' \log s}$ given by the Green's function (110)

$$\sqrt{\alpha' \log s} \ll R_0 A^{1/3}, \quad (164)$$

the total cross section should behave as

$$\sigma_{\text{total}}(s) \approx 2\pi R_0^2 A^{2/3}, \quad (165)$$

and the multiplicity of produced particles as

$$\langle n \rangle_A(s) \sim A^{1/3} \log s. \quad (166)$$

Now experiment (Busza et al., 1974) shows that the cross section does behave more or less as $A^{2/3}$, but the multiplicity is essentially independent of A . What is missing is interaction among the Pomerons. Figure 57 gives the leading term. Now the multiplicity grows as $\log s$ essentially independent of A . One may heuristically understand this by thinking of the Pomeron interactions with the A

nucleons as just producing a new Pomeron-Nucleus-Nucleus vertex function as in the right hand part of Fig. 57. Now a constant cross section and $\langle n \rangle \sim \log s$ are quite natural. Pomeron radiative corrections as in Fig. 58 have not yet been accounted for, but the whole apparatus described above is ready for that.

Finally there has been an interesting technical achievement in determining not only the scaling indices γ and z but also the scaling functions like $\phi_{1,1}$ in Eq. (141) (Abarbanel et al., 1975b; Frazer and Moshe, 1975). In particular for $\Gamma^{(1,1)}$ the functional dependence on the scaling variable is determined by the two equations

$$i\Gamma_U^{(1,1)}(E, \vec{q}^2, \alpha'_0, r_0) = - \frac{(-E)^{1-\gamma}}{1-\gamma} [1 + \eta(1+\tau)] \left[1 + \frac{\eta}{2}\right]^{2\tau} \quad (167)$$

and the scaling variable η is given through

$$\frac{\alpha'_0 \vec{q}^2}{(-E)^{1+\tau}} = \eta(1 + \eta/2)^\tau \quad (168)$$

These are valid in the expansion in $\epsilon=4-D$ described before and to the appropriate order $-\gamma=\epsilon/12$ and $\tau=\epsilon/24$.

The technique is essentially to express $\Gamma^{(1,1)}$ in terms of integrals over the Z_i as done in (156). Then determine the Z_i using the renormalization group equations for them and the expansion about $D=4$ to establish the coefficients in these differential equations. Using a general normalization point E_N, \vec{q}_N^2 to define the theory one is able to determine the dependence of the Z_i on the dimensionless variables g (Eq. 125) and $\eta = \alpha'_0 \vec{q}_N^2 / E_N$. This yields up (167) and (168) by means of an expansion in ϵ . This result shows that there are no fixed singularities at $E=0$ for \vec{q}^2 fixed. Further it allows one to arrive at an explicit formula for the elastic differential cross section which exhibits the usual sharp fall off in t for small t and then "bounces", that is has a zero and a secondary maximum which

lies about six orders of magnitude below the diffraction peak at $t=0$. This, crude as it is, appears to be in rough accord with the data at the CERN-ISR (Giacomelli, 1974).

X. ASSESSMENT OF THE t -CHANNEL APPROACH

As I have indicated several times in this article, I very much favor the view from the t -channel. It presents a consistent, attractive way to deal with the interplay between Regge poles (or the multiperipheral model, if you will) and the branch points demanded by unitarity. Indeed, it does it in a formal structure that is an abstraction of unitarity itself. With Reggeon field theories we are able to focus our attention on two critical indices γ and z for the elastic amplitude

$$T(s, t) = s \int \frac{dE}{2\pi i} s^E \xi_E \frac{1}{(-E)^{1-\gamma} \phi_{1,1}(\vec{q}^2/(-E)^z)} \quad , \quad (169)$$

which characterize the total cross section

$$\sigma_T(s) \sim (\log s)^{-\gamma} \quad , \quad (170)$$

and the shrinkage of the diffraction peak. The leading asymptotic amplitude factorizes, despite the presence of branch cuts. s -channel unitarity is at least enforced at the level of crucial inequalities; such as, $\alpha(0) \leq 1$, $-\gamma < 2$ and so forth. The problems of a ρ trajectory with $\alpha_\rho(t)$ remaining almost linear and of Fermion Regge behavior are very neatly answered. The possibility of using the field theory formalism in the study of specific interesting s -channel processes has proven real and has allowed one to further delve into the key question of s -channel unitarity.

The matter of the full behavior of diffraction amplitudes has hardly been set to rest, however. Looking back at our list of properties of diffraction, one will note that we have not even begun to deal with the question of the vertices

Pomeron-Particle-Particle and any selection rules for it (Leith, 1974). We have not faced up to the question why $\alpha(0)=1$, but only have been able to demonstrate that it cannot be greater (Abarbanel et al., 1975d). Frankly, these questions are, I believe, not amenable to answer within the framework discussed in this paper. More about it later.

An important issue we have postponed is when we ought to expect the scaling behavior to set in. The dimensionless expansion parameter of the Reggeon field theory is

$$\frac{r_0^2}{\alpha_0'} \log s \quad . \quad (171)$$

Certainly as long as this is much less than one, we need not look for the scaling solution since the only graph of any importance will be the old one Pomeron exchange. Since it has $\alpha_0 > 1$, it will give a rising total cross section. From data on the triple Regge regime of $pp \rightarrow p+X$ and $pd \rightarrow d+X$ one learns that

$$\frac{r_0^2}{\alpha_0'} \sim \frac{1}{50} \quad , \quad (172)$$

so when

$$\log s \gtrsim 25 \quad , \quad (173)$$

the Moscow-Batavia scaling solution will certainly be necessary. A more precise estimate examines how far away from Reggeon energy $E=0$ we can trust our scaling formula at $D=2$

$$i\Gamma(1, 1)(E, 0) = - \int_0^{-E} dx \left[1 + \frac{3r_0^2}{8\pi\alpha_0'x} \right]^{-1/6} \quad . \quad (174)$$

This deviates from the scaling formula noted in Eq. (167) and (168) by the time (Abarbanel et al., 1975b)

$$E \approx \frac{3r_0^2}{8\pi\alpha'_0} , \quad (175)$$

or when

$$\log s \gtrsim 5 . \quad (176)$$

Other estimates (Amati and Jengo, 1975) of the same "transition" energy lie at $\log s \approx 9$ or 10 . Since at the maximum energy the CERN-ISR has $\log s \approx 8$ and a 1000 GeV/c on 1000 GeV/c colliding beam would have $\log s \approx 14$, one may (let optimism prevail!) be in or about to go through the transition region.

Further optimism would suggest that phenomenology done with the scaling formulae even at the present highest energies might be significant.

If we have not yet entered the scaling regime, then it is difficult to give an a priori estimation of what would comprise a useful phenomenology in the context of Reggeon field theory. Certainly one will be involved in the evaluation of at first a few and, then as s increases, of more and more terms of perturbation theory for whatever field theory one chooses. Since terms with many derivative couplings and high powers of the Pomeron field are suppressed quite rapidly, one might imagine adding just

$$-\frac{\lambda_0}{4} (\phi^+ \phi)^2 - \frac{\lambda_1}{6} (\phi^+ \phi^3 + \phi^{+3} \phi) + \text{a few derivatives} , \quad (177)$$

to begin a finite phenomenology. The territory is basically unexplored.

There is another suggestion due to Gribov (Gribov, 1975) for finding a diffraction theory useful at "intermediate" energies. He notes that the Pomeron slope α'_0 is like an effective mass

$$E = \vec{q}^2 / 2m_{\text{eff}} + \Delta , \quad (178)$$

$$m_{\text{eff}} = \frac{1}{2\alpha'_0} \quad , \quad (179)$$

so that the Pomeron, with $\alpha'_0 \approx 0.3$ (GeV/c)⁻² is much less mobile in \vec{x}, τ space than, say, a ρ meson with $\alpha'_0 \approx 1$. Until the times ($\log s$) become very large, the rapidly moving lower lying trajectories and even particles will dominate the t-channel dynamics. He has formulated a diffraction theory as an expansion around $m_{\text{eff}} = \infty$ or $\alpha'_0 = 0$. It goes into the Moscow-Batavia scaling solution. It, too, is basically unexplored territory.

The t-channel view of Reggeon field theory teaches us a lesson which is attractive while disappointing. We learn that a few basic bare Pomeron parameters (α'_0 , r_0 , and maybe others) are sufficient to yield the asymptotic behavior of diffraction amplitudes. We are rewarded by a simple, universal behavior whose detailed features lie in a small number of critical indices like γ and z . This is the attractive part. The disappointing part is that in large s , small t physics we learn nothing about the underlying structure of the hadrons themselves. We have averaged over hadron coordinates in forming the Reggeon field $\phi(\vec{x}, \tau)$ in the first place. Then we took a limit which emphasized an infinite correlation length in rapidity space ($\propto 1/\Delta$) and thus washed out the details of the production processes which occur at finite rapidity gaps.

The analogy with systems like a magnet near a critical temperature is persuasive. One is able to characterize the interesting quantities such as the susceptibility and spontaneous magnetization by a few universal critical indices. However, in the neighborhood of the critical temperature the correlation length among spins goes to infinity and one does a grand averaging over the detailed coordinates of the original magnetic system. It eventually doesn't matter if the

spin lattice is body centered cubic or face centered cubic or if the spin-spin interactions are nearest neighbor or fifth nearest neighbor; all that gets washed out.

XI. OUTLOOK: THE BARE POMERON AND $\alpha(0)=1$

We have come close to the conclusion of our overview of theories of hadron diffraction. We have looked at diffractive processes from the direct channel by examining the production amplitudes which build up diffraction through unitarity. We have peered down the t-channel to satisfy unitarity in that direction through the medium of Reggeon field theories.

I would like to end this extended discussion not by reviewing the review but by pointing to the crucial problem raised by the last several years' hard effort in the theory of high energy hadron scattering. This is the question of the bare Pomeron and bare (or noninteracting) Reggeons in general. In the Reggeon field theories we found that having been given a set of parameters $\alpha_0, \alpha'_0, r_0, \dots$ for the Lagrangian, we could calculate, using the renormalization group or whatever technique, a universal asymptotic behavior for any s-channel process we like. Two very important matters remained unaddressed: (1) Where do the bare Reggeon parameters come from? Are they "fundamental" quantities in theories of diffraction to be determined by experiment? Or are they calculable from some underlying field theory or S-matrix principles? (2) If we adopt the view that, indeed, the Pomeron intercept $\alpha(0)=1$, then a special relation among the bare parameters (like Eq. (158)) must be met (Abarbanel et al., 1975d). I haven't the answers to these questions. There has been some work on the former; the latter is wide open.

We have identified the bare Pomeron or bare Reggeon with the multiperipheral model. The reader will have noticed that the key element in Pomeron making was the presence of bound states in the t -channel whose total spin J varied with t : $J=\alpha(t)$. Making the Pomeron or other Reggeon then becomes a question of finding the bound states from some underlying field theory, say, and studying their variation in the (J, t) plane. Clearly then we are adopting the point of view that the bare Pomeron parameters come from an underlying theory. In Fig. 59 is a schematic flow chart of the hierarchy of hadron physics suggested by this outlook. The bulk of this article has concentrated on the bottom or middle box. The questions we are raising here probably find their answers in the top box. "Fundamentality" decreases as one goes down the page.

There are at least two major views on the study of the bare Pomeron. One is to concentrate on good old quantum field theory and try to find the spectrum in the (J, t) plane. Attention has focused (properly I suspect) on theories which have "asymptotic freedom"; namely, ultraviolet behavior which is almost that of free field theory (Coleman, 1973). The most realistic example of this is non-Abelian gauge theories, although, because of its simpler structure, ϕ^3 theory in six space-time dimensions has been studied in this category (Cardy, 1974; Lovelace, 1975). These theories have very complex infrared behavior and, since bound states grow on infrared or soft quantum exchange (hard quanta destroy binding), the problem remains. Indications are encouraging, however, since ϕ^3 in six dimensions shows Regge pole behavior while similar field theories: ϕ^4 in four dimensions and electrodynamics do not. The latter two are not free in the ultraviolet region, and that makes all the difference.

The second approach is complementary to this field theory and in a sense resides in the middle box of Fig. 59. Without specifying what field theory one

makes hadrons from, it is proposed to classify the Feynman graphs of the theory according to the "planarity". (There is a more precise topological definition (Chan et al., 1975; Chew and Rosenzweig, 1975; Ciafaloni et al., 1975; Schmid and Sorensen, 1975).) One can do this by hand or by introducing a $U(N)$ internal symmetry group and considering N to be large. ($N=3$ may be large enough.) The leading graphs in powers of N are planar. They, in a multiperipheral sense, are identified with Reggeons involving quantum number exchange, certainly with $\alpha(0) < 1$. Next in orders of N are a set of nonplanar graphs which are identified with the bare Pomeron. Again it is a pole in the J plane whose α_0 is bigger than the quantum numbered Reggeon since there are more graphs. In this scheme the triple Pomeron vertex comes out $O(1/N)$ giving some rationale for the smallness of the observed number (Eq. (172)). Although at the time of this writing it is too early to assess the quantitative value of the "topological Pomeron" or the fundamental field theory approach they do promise to be valuable tools in the search for the bare Pomeron.

Acknowledgements

I am greatly indebted to colleagues in the U. S. and USSR far too numerous to name individually for years of conversation and discussion on diffraction scattering. A special acknowledgement to J. B. Bronzan and L. M. Saunders will, however, express my deeper debt to them.

REFERENCES

- Abarbanel, H.D.I., 1972a, in Lectures in Theoretical Physics, eds. A. Barut and W. E. Britten (Colorado Associated University Press, Boulder, Colorado), p. 3.
- _____ 1972b, Phys. Rev. D 10, 2788.
- _____ 1974a, Proceedings of the Summer Institute on Particle Physics, Stanford Linear Accelerator Center, SLAC-179, Vol. I, p. 399.
- _____ 1974b, Phys. Letters 49B, 61.
- Abarbanel, H.D.I. and J. B. Bronzan, 1974a, Phys. Letters 48B, 345.
- _____ 1974b, Phys. Rev. D 9, 2397.
- _____ 1974c, Phys. Rev. D 9, 3304.
- Abarbanel, H.D.I. and C. Itzykson, 1969, Phys. Rev. Letters 23, 53.
- Abarbanel, H.D.I. and R. L. Sugar, 1974, Phys. Rev. D 10, 721.
- Abarbanel, H.D.I., J. Bartels, J. B. Bronzan, and D. Sidhu, 1975a, Fermilab preprint 75/29-THY.
- _____ 1975b, Fermilab preprint 75/49-THY.
- Abarbanel, H.D.I., J. B. Bronzan, R. L. Sugar, and A. R. White, 1975c, Fermilab preprint 75/36-THY, Physics Reports, to be published.
- Abarbanel, H.D.I., J. B. Bronzan, A. Schwimmer, and R. L. Sugar, 1975d, Stanford Linear Accelerator Center, SLAC-PUB-1619.
- _____ 1975e, to be published.
- Abarbanel, H.D.I., G. F. Chew, M. L. Goldberger, and L. M. Saunders, 1971a, Ann. Phys. (N.Y.) 73, 156.
- _____ 1971b, Phys. Rev. Letters 26, 937.
- Abramovskii, V. A., V. N. Gribov, and O. V. Kancheli, 1974, Sov. J. Nucl. Phys. 18, 308.

- Amati, D. and R. Jengo, 1975, CERN preprint TH.2000.
- Amati, D., A. Stanghellini, and S. Fubini, 1962, *Nuovo Cimento* 26, 896.
- Amati, D., L. L. Foldy, A. Stanghellini, and L. Van Hove, 1964, *Nuovo Cimento* 32, 1685.
- Anselm, A. A., and I. T. Dyatlov, 1968, *Sov. Phys. JETP* 27, 533.
- Arbab, F. and J. D. Jackson, 1968, *Phys. Rev.* 176, 1796.
- Auerbach, S., R. Aviv, R. L. Sugar, and R. Blankenbecler, 1972, *Phys. Rev. D* 6, 2216.
- Aviv, R., R. L. Sugar, and R. Blankenbecler, 1972, *Phys. Rev. D* 5, 3253.
- Baker, M., 1974, *Nucl. Phys.* 80B, 62.
- Baker, M. and R. Blankenbecler, 1962, *Phys. Rev.* 128, 415.
- Ball, J. and F. Zachariasen, 1974, *Nucl. Phys.* B72, 149.
- Barnes, A. V., D. J. Mellema, A. V. Tollestrup, R. L. Walker, O. L. Dahl, R. A. Johnson, R. W. Kenney, and M. Pripstein, 1974, *Proceedings of the Summer Institute on Particle Physics, Stanford Linear Accelerator Center, SLAC-179, Vol. II, p. 1.*
- Bartels, J., 1975a, *Phys. Rev. D* 11, 2977.
- _____, 1975b, *Phys. Rev. D* 11, 2989.
- Bartels, J. and E. Rabinovici, 1975, Fermilab preprint 75/43-THY.
- Bartels, J. and R. Savit, 1975, *Phys. Rev. D* 11, 2300.
- Bertocchi, L., S. Fubini, and M. Tonin, 1962, *Nuovo Cimento* 25, 626.
- Bjorken, J. D. and S. D. Drell, 1964, *Relativistic Quantum Fields* (McGraw Hill, New York).
- Blankenbecler, R. and M. L. Goldberger, 1962, *Phys. Rev.* 126, 766.
- Blankenbecler, R. and C. T. Sachrajda, 1975, *Stanford Linear Accelerator Center, SLAC-PUB-1577, to be published in Phys. Rev. D.*
- Blankenbecler, R. and R. L. Sugar, 1969, *Phys. Rev.* 183, 1387.

- Blankenbecler, R., J. R. Fulco, and R. L. Sugar, 1974, Phys. Rev. D 9, 736.
- Bronzan, J. B. and J. W. Dash, 1974, Phys. Rev. D 10, 4208.
- Brower, R. C. and J. H. Weis, 1972, Phys. Letters 41B, 631.
- Brower, R. C., C. E. De Tar, and J. H. Weis, 1974, Phys. Reports 14C, 257.
- Brower, R. C., J. Ellis, R. Savit, and W. J. Zakrzewski, 1975, CERN preprint TH.1973.
- Bøggild, H. and T. Ferbel, 1974, "Inclusive Reactions" in Ann. Rev. Nucl. Sci. 24, 451.
- Busza, W., J. Elias, D. Jacobs, M. Sogard, P. Swartz, and C. Young, 1974, MIT preprint, Report at the Topical Meeting on High Energy Collisions Involving Nuclei, Trieste, September, 1974.
- Calucci, G., and R. Jengo, 1975, Nucl. Phys. B84, 413.
- Caneschi, L. and R. Jengo, 1975, Nucl. Phys. B89, 19.
- Caneschi, L. and A. Schwimmer, 1972, Nucl. Phys. B48, 519.
- Cardy, J. L., 1974, UC Santa Barbara preprint.
- _____ 1975, UC Santa Barbara preprint.
- Cardy, J. L. and R. L. Sugar, 1975, UC Santa Barbara preprint.
- Cardy, J. L. and P. Suranyi, 1975, UC Santa Barbara preprint.
- Cardy, J. L., R. L. Sugar, and A. R. White, 1975d, Phys. Letters 55B, 384.
- Chan, H.-M., J. E. Paton, and T. S. Tsau, 1975, Nucl. Phys. B86, 479.
- Chang, S. J., and S. K. Ma, 1969, Phys. Rev. Letters 22, 1334.
- Cheng, H. and T. T. Wu, 1969, Phys. Rev. Letters 22, 666.
- Chew, G. F., 1961, S-Matrix Theory of Strong Interactions (Benjamin, New York).

- Chew, G. F. and S. C. Frautschi, 1961, Phys. Rev. Letters 7, 394.
- Chew, G. F. and C. Rosenzweig, 1975, LBL preprint 3834.
- Chiu, C. B., 1972, Ann. Rev. Nucl. Sci. 22, 255.
- Chou, T. T. and C. N. Yang, 1968, Phys. Rev. 170, 1591.
- Ciafaloni, M. and G. Marchesini, 1975, Nucl. Phys. B88, 109.
- Ciafaloni, M., G. Marchesini, and G. Veneziano, 1975, Weizmann Institute preprints WIS-75-22.
- Coleman, S., 1973, "Secret Symmetry," Lectures at the International Summer School of Physics, Ettore Majorana.
- Collins, P.D.B., 1971, Phys. Reports 1C, 103.
- Dash, J. W. and S. Harrington, 1975, University of Oregon preprint OITS-75-2.
- Dash, J. W. and A. Pignotti, 1970, Phys. Rev. D 2, 2389.
- Dash, J. W., J. R. Fulco, and A. Pignotti, 1970, Phys. Rev. D 1, 3164.
- De Tar, C. E., 1971, Phys. Rev. D 3, 128.
- Drell, S. D. and A. C. Hearn, 1966, High Energy Physics (Academic Press, New York), Chapter 9.
- Durand, L. and R. Lipes, 1968, Phys. Rev. Letters 20, 637.
- Eden, R. J., 1967, High Energy Collisions of Elementary Particles (Cambridge University Press).
- Ellis, J. and R. Savit, 1975, CERN preprint TH.1974.
- Fermilab Single Arm Spectrometer Group, 1975, Fermilab preprint 75/48-EXP.
- Finkelstein, J. and F. Zachariasen, 1971, Phys. Letters 34B, 431.
- Fisher, M. E., 1974, Rev. Mod. Phys. 46, 597.
- Frautschi, S. C., 1963, Regge Poles and S-Matrix Theory (Benjamin, New York).
- Frautschi, S. C. and B. Margolis, 1968, Nuovo Cimento 56A, 1155.

- Frazer, W. R. and M. Moshe, 1975, UC San Diego preprint, 10P10-154.
- Froissart, M., 1961a, Phys. Rev. 123, 1053.
- _____ 1961b, Proceedings of the La Jolla Conference (unpublished).
- Fubini, S., 1963, in Strong Interactions and High Energy Physics, ed. R. G. Moorehouse (Oliver and Boyd, Edinburgh, Scotland).
- Giacomelli, G., 1974, Proceedings of the Summer Institute on Particle Physics, Stanford Linear Accelerator Center, SLAC-179, Vol. II, p. 299.
- Glauber, R. J., 1959, in Lectures in Theoretical Physics, eds. W. B. Brittin and L. G. Dunham (Interscience Publishers, Inc., New York), Vol. I., p. 315.
- Goldberger, M. L. and K. M. Watson, 1964, Collision Theory (John Wiley, New York), Chapter 6 and Appendix E.
- Gottfried, K. and J. D. Jackson, 1964, Nuovo Cimento 34, 735.
- Gribov, V. N., 1962, Sov. Phys. JETP 15, 873.
- _____ 1968, Sov. Phys. JETP 26, 414.
- _____ 1975, "A Theory of the Heavy Pomeron," Leningrad preprint 148.
- Gribov, V. N. and A. A. Migdal, 1969a, Sov. J. Nucl. Phys. 8, 583.
- _____ 1969b, Sov. J. Nucl. Phys. 8, 703.
- _____ 1969c, Sov. Phys. JETP 28, 784.
- Gribov, V. N., E. M. Levin, and A. A. Migdal, 1970, Sov. J. Nucl. Phys. 11, 378.
- _____ 1971, Sov. J. Nucl. Phys. 12, 93.
- Gribov, V. N., I. Ya. Pomeranchuk, and K. A. Ter-Martirsoyan, 1965, Phys. Rev. 139, B184.
- Jones, C. E., F. E. Low, S. H. Tye, G. Veneziano, and J. E. Young, 1972, Phys. Rev. D 6, 1033.

- Kancheli, O. V., 1973, Sov. Phys. JETP Letters 18, 273.
- Koplik, J. and A. H. Mueller, 1975, Columbia University preprint
CO-2271-57.
- Kycia, T. F., 1974, Proceedings of the Summer Institute on Particle Physics,
Stanford Linear Accelerator Center, SLAC-179, Vol. II, p. 23.
- Lehman, E. S. and G. A. Winbow, 1974, Phys. Rev. D 10, 2962.
- Leith, D.W.G.S., 1974, Proceedings of the Summer Institute on Particle
Physics, Stanford Linear Accelerator Center, SLAC-179, Vol. I, p. 1.
- Levy, M. and J. Sucher, 1969, Phys. Rev. 186, 1656.
- Lovelace, C., 1971, Phys. Letters 34B, 500.
- Lovelace, C., 1975, Rutgers University preprint.
- Mandelstam, S., 1963, Nuovo Cimento 30, 1113, 1127, 1148.
- Martin, A., 1963, Phys. Rev. 129, 1432.
- Martin, A. and F. Cheung, 1970, Analyticity Properties and Bounds of the
Scattering Amplitudes (Gordon and Breach, New York).
- McLerran, L. D. and J. H. Weis, 1975, University of Washington preprint
RLO-1388-673.
- Migdal, A. A., A. M. Polyakov, and K. A. Ter-Martirosyan, 1974, Phys.
Letters 48B, 239; Zh. Eksp. Teor. Fiz. 67, 84.
- de Montaigne, M., 1585-1588, "Du repentir."
- Pomeranchuk, I. Ya., 1958, Sov. Phys. JETP 7, 499.
- Pomeranchuk, I. Ya. and L. B. Okun, 1956, Sov. Phys. JETP 3, 307.
- Regge, T., 1960, Nuovo Cimento 18, 947.
- Schmid, C. and S. Sorensen, 1975, ETH, Zurich, preprint.
- Schwimmer, A., 1974, Nucl. Phys. B75, 446.
- _____ 1975, Caltech preprint 68-487.

Stanley, H. E., 1971, Introduction to Phase Transitions and Critical Phenomena
(Clarendon, Oxford).

Sugar, R. L., 1972, in Lectures in Theoretical Physics, eds. A. Barut and
W. E. Brittin (Colorado Associated University Press, Boulder, Colorado),
p. 47.

Sugar, R. L. and A. R. White, 1974a, Phys. Rev. D 10, 4063.

_____ 1974b, Phys. Rev. D 10, 4074.

Suranyi, P., 1975, Phys. Rev., to be published.

White, A. R., 1972, Nucl. Phys. B50, 93, 130.

Wick, G. C. and R. Cutkosky, 1954, Phys. Rev. 96, 1124, 1135.

Wilson, K. G. and J. Kogut, 1974, Phys. Reports 12C, 75.

Zachariassen, F., 1971, Phys. Reports 2C, 1.

_____ 1974, "Self Consistent Models of the Pomeron," Invited Talk at the
September, 1974 meeting of the Division of Particles and Fields of the
American Physical Society, Williamsburg, Virginia; Caltech preprint
68-464.

FIGURE CAPTIONS

1. The measured total cross sections for π^\pm , K^\pm , \bar{p} and p incident on protons. The references on the figure may be found in Kycia (Kycia, 1974) from whom the graph has been taken. $s \propto p_{\text{lab}}$.
2. The measured cross section for $\pi^- p \rightarrow \pi^0 n$ (called σ_{CEX}). The references on the figure may be found in Barnes et al. (Barnes et al., 1974) from whom the graph has been taken. $s \propto p_{\text{lab}}$. Compare the rapid fall off of this cross section with the slow variation of the total cross sections.
3. The two body \rightarrow two body collision $AB \rightarrow A'B'$. When the quantum numbers of the vacuum ($I=0$, $P=G=C=+1, \dots$) are allowed in the t direction, then we have cross sections which are almost constant in s for fixed, small t as $s \rightarrow \infty$. This is a key signal of diffractive processes.
4. (a) The s -channel point of view in looking at the diffraction amplitude of Fig. 3. One examines each N particle intermediate state.
(b) The t -channel point of view in looking at the diffraction amplitude of Fig. 3. One characterizes the s dependence by the allowed exchange mechanisms. Diffraction requires the effective spin of the exchange to be one.
5. The unitarity relation in the s -channel. It relates the imaginary part of the two body amplitude to the production amplitudes $T_{AB \rightarrow N}$.
6. Double exchange of the wiggly line of Fig. 4b with effective spin ≈ 1 . Each exchange contributes a power of s^1 while the integral around the loop contributes a power s^{-1} . The net amplitude behaves as s^1 which is the same order as the single exchange in Fig. 4b.
7. Some measured elastic total cross sections. The points at 50, 100, and 175 GeV/c for $\pi^- p$, $K^- p$, and $\bar{p}p$ are taken from recent Fermilab experiments

(Fermilab, 1975). All other points are from references in Leith (Leith, 1974) from whom the graph has been borrowed.

8. The inclusive cross sections for $pp \rightarrow A + \text{anything}$ where $A = \pi^\pm, K^\pm, p$ and \bar{p} . This graph shows $d\sigma/d^2p_T dy$ for a fixed value of the produced particles' transverse momentum ($p_T = 0.4 \text{ GeV}/c$) as a function of the incident energy (s) and the rapidity of the produced particle. The independence of s is striking. References on the graph may be found in Giacomelli (Giacomelli, 1974) from whom the figure is borrowed.
9. Plots of $\rho(E) = \text{Re } T(E, t=0)/\text{Im } T(E, t=0)$ for elastic proton proton scattering. $s \propto E$. The curves on the graphs should be ignored. References on the graph may be found in Leith (Leith, 1974) from whom the figure is borrowed.
10. The ratio of the differential cross sections $Ap \rightarrow AN^*(1688)/Ap \rightarrow Ap$ for $A = \pi^-, K^-$ and \bar{p} as a function of t . The equality of these ratios is a test of factorization.
11. On the left is the amplitude for $\pi^-(K^-) + p \rightarrow \text{anything} + p$. When this amplitude is squared the picture on the right emerges. The ratio of $\pi^- p \rightarrow X+p$ and $K^- p \rightarrow X+p$ cancels out the little dragonfly of Pomeron and four protons and leaves a number equal to $\sigma_{\text{total}}(\pi^- p)/\sigma_{\text{total}}(K^- p)$, independent of s , t , and x .
12. The reactions $\pi^- p \rightarrow X+p$ and $K^- p \rightarrow X+p$ plotted as a function of x the fraction of beam momentum carried by the recoil proton. The ratio of these cross sections should be independent of x , beam energy and t , the momentum transferred between the protons. References to the data may be found in Leith (Leith, 1974) from whom the figure is borrowed.
13. The slope parameter $b(s)$ in elastic scattering. The elastic cross section is parametrized as $d\sigma/dt = (\text{constant}) \exp - 2b(s)t$ and the data shown is for $t = 0.2 \text{ (GeV}/c)^{-2}$.

14. Mass spectrum for $N\pi\pi$ in the reaction $\bar{K}N \rightarrow \bar{K}(N\pi\pi)$ at beam momentum of 10 GeV/c. References to the data will be found in Leith (Leith, 1974) from whom the figure is borrowed.
15. An exchange of quantum numbers along the wiggly line connecting particles rapidly moving by each other requires radiation as the wiggly line rapidly changes its momentum. This decreases the cross section into the channel shown. When vacuum quantum numbers are exchanged, no radiation need occur.
16. Total cross sections plotted versus $(p_{\text{lab}})^{-1/2}$ showing how particle and antiparticle cross sections approach each other as $s \propto p_{\text{lab}} \rightarrow \infty$. Data is referred to by Leith (Leith, 1974) from whom the graph is borrowed.
17. The exchange of a spin J_R , mass m_R resonance in the s-channel.
18. The exchange of a spin J_R , mass m_R resonance in the t-channel.
19. The simplest peripheral amplitude approximation to elastic scattering: exchange of a spin 0 particle in the t-channel.
20. The most elementary multiperipheral approximation to the $2 \rightarrow N$ production amplitude: single particles are produced by the repeated exchange of a spinless particle in the $t_i = Q_i^2$ channel. More complicated multiperipheral models have clusters of particles produced with total momenta p_i and/or more elaborate exchanges in the t_i channels. When such augmentation does not change the "smoothness" of the potential K (Eq. (33)), much the same consequences follow.
21. The multiperipheral integral equation.
22. The partially diagonalized multiperipheral integral equation. l and t are parameters in the equation (i.e., they have been diagonalized), and the dynamics resides in the two dimensional \vec{p} space.

23. Two body scattering taking place via the double exchange of potential V_1 and potential V_2 . Going over to impact parameter space makes the T matrix a product of V_1 and V_2 . The impact parameter is thus like a generalized s-channel angular momentum.
24. The multiperipheral approximation to the $2 \rightarrow N$ production amplitude. Each T is a two body amplitude. The whole process is expressed in rapidity, impact parameter space.
25. Elastic rescattering correction to the y, \vec{b} form of the multiperipheral amplitude. One introduces rescattering between pairs of particles by multiplying with $\sqrt{s} = \exp i\delta(\Delta y, \Delta \vec{b})$ for each pair. Corrections are multiplicative in y, \vec{b} space.
26. Many particle interactions missing in the elastic rescattering approximation.
27. The iterative approach to rescattering corrections in the s-channel. Pomeron interactions produce the many particle interactions absent from Fig. 25.
28. The many Pomeron [eikonal phase χ] exchange graphs summed by the eikonal approximation. The factor $N!$ and the relation $g_N = (g_1)^N$ are crucial to the exponentiation of the eikonal formula. They are not expected in general.
29. Pomeron interactions missing from the eikonal formula. They will crucially alter the couplings and combinatorial factors needed to exponentiate the eikonal phase or Born term.
30. The kernel for the multiperipheral bootstrap model: elastic unitarity involving $T(s, t)$ itself.
31. The dominant double exchange graph in the high energy limit. The colliding particles break up to exchange the Reggeons at the same time. Figure 30 requires Reggeon emission at different times, but as $s \rightarrow \infty$ the colliding particles spend less and less time in each other's vicinity.

32. The contribution to elastic unitarity from Fig. 30.
33. Kinematics of the two Reggeon exchange contribution to the t-channel partial wave amplitude $F(J, t)$. N_2 is the amplitude for two particles \rightarrow two Reggeons.
34. The approximation to N_2 coming from the double cross graph of Fig. 31.
35. The contribution of two Reggeons to an absorptive part (discontinuity in J) of $F(J, t)$. This is the simplest Reggeon unitarity relation. It can be "rigorously" derived from analytically continued four particle unitarity for t-channel partial waves. It is also true in all models.
36. The simplest graph that contributes Reggeon branch points to N_2 , the particle-Reggeon transition amplitude.
37. The pole and branch points in the Reggeon energy ($E=1-J$) plane. If the on-shell Reggeon energy satisfies $\epsilon(\vec{q}=0)=0$ ($\alpha(0)=1$), then all the cuts collapse on the pole at $E=0$ when $\vec{q}=0$.
38. Reggeon unitarity for the particle-Reggeon amplitude N_2 showing the two Reggeon cut. The four Reggeon amplitude M_4 enters here.
39. Reggeon unitarity for the Reggeon amplitude M_4 showing the two Reggeon cut.
40. Examples of Reggeon interactions showing $1\rightarrow 2$, $2\rightarrow 2$, and $3\rightarrow 3$. When quantum numbers allow, any number of Reggeons may go into any other number. Both heuristic and firmer arguments show that only the triple coupling is important for the eventual asymptotic behavior of cross sections.
41. Space-time picture of a Reggeon. It diffuses with the Green's function Eq. (110) from a hadron at zero rapidity, zero impact parameter to another hadron at (y, \vec{b}) .
42. Double Reggeon exchange from hadron to hadron.

43. Reggeons interacting on their way from one hadron to another. Between interactions they propagate with the Green's function (110). Eventually all Reggeons except the Pomeron with $\Delta=0$ are killed by this propagator.
44. The minus sign associated with absorption. It is taken to each triple Pomeron vertex as $\sqrt{-1}$.
45. The function $\beta(g)$ for Reggeon field theory. In the infrared limit ($E, \vec{q} \rightarrow 0$) governing diffraction scattering the effective coupling constant of the theory becomes g_1 where $\beta(g_1)=0$. In Reggeon field theory $g_1 \propto \sqrt{4-D}$ where D is the number of dimensions of impact parameter space. This suggests a fruitful expansion in $\epsilon=4-D$ for $D \leq 4$. Physics takes place at $D=2$.
46. The dominant asymptotic contribution to the elastic cross section and total cross section. $\sigma_T^{AB}(s)$ factorizes and rises as $(\log s)^{-\gamma}$. $-\gamma$ is a positive number which is one of the critical exponents in the scaling form of the Moscow-Batavia Pomeron. Numerical estimates indicate $1/4 \lesssim -\gamma \lesssim 1/2$.
47. The hierarchy of contributions to the total cross section in Reggeon field theory. The leading term factorizes; the others need not.
48. The Schwinger-Dyson equation of Reggeon field theory. Early Soviet work attempted to find self consistent solutions to this kind of nonlinear equation.
49. Reggeon graphs summed to study the Pomeron or absorptive corrections to secondary Reggeons (ρ, A_2, \dots) or Fermions. The Pomeron is shown with a wiggly line; it enters to all orders. The other Reggeon, which has $\alpha(0) < 1$, enters only once.
50. The model for cutting open a Reggeon to study its s-channel particle content. It's the multiperipheral amplitude, of course.
51. Processes one may learn about by cutting open the simplest triple Pomeron graph.

52. The triple Reggeon region for inclusive reactions. Reggeon energy is not conserved here because an intermediate fixed "time" = $\log M^2$ is exposed.
53. Reggeon graphs to be summed in the study of $2 \rightarrow N$ production cross sections. Each heavy dot is a particle produced.
54. One of the Reggeon graphs to be summed in the study of the asymptotic behavior of the triple Regge region of inclusive reactions. Reggeon rules do not allow Reggeons to traverse between the t_1 and t_2 channels.
55. A pleasant complication in the Reggeon graphology for the triple Reggeon region of inclusive processes.
56. The simple Pomeron exchange for particle scattering on nuclei. It gives a multiplicity of produced particles $\propto A^{1/3} \log s$ for a nucleus of A nucleons. Experiment gives only $\log s$.
57. The dominant graph for particle-nucleus scattering. It gives a multiplicity $\propto \log s$.
58. Pomeron radiative corrections to particle-nucleus scattering.
59. The hierarchy of hadron physics. This review dwells primarily in the middle and lower boxes. The upper box contains the secret of the bare Pomeron.

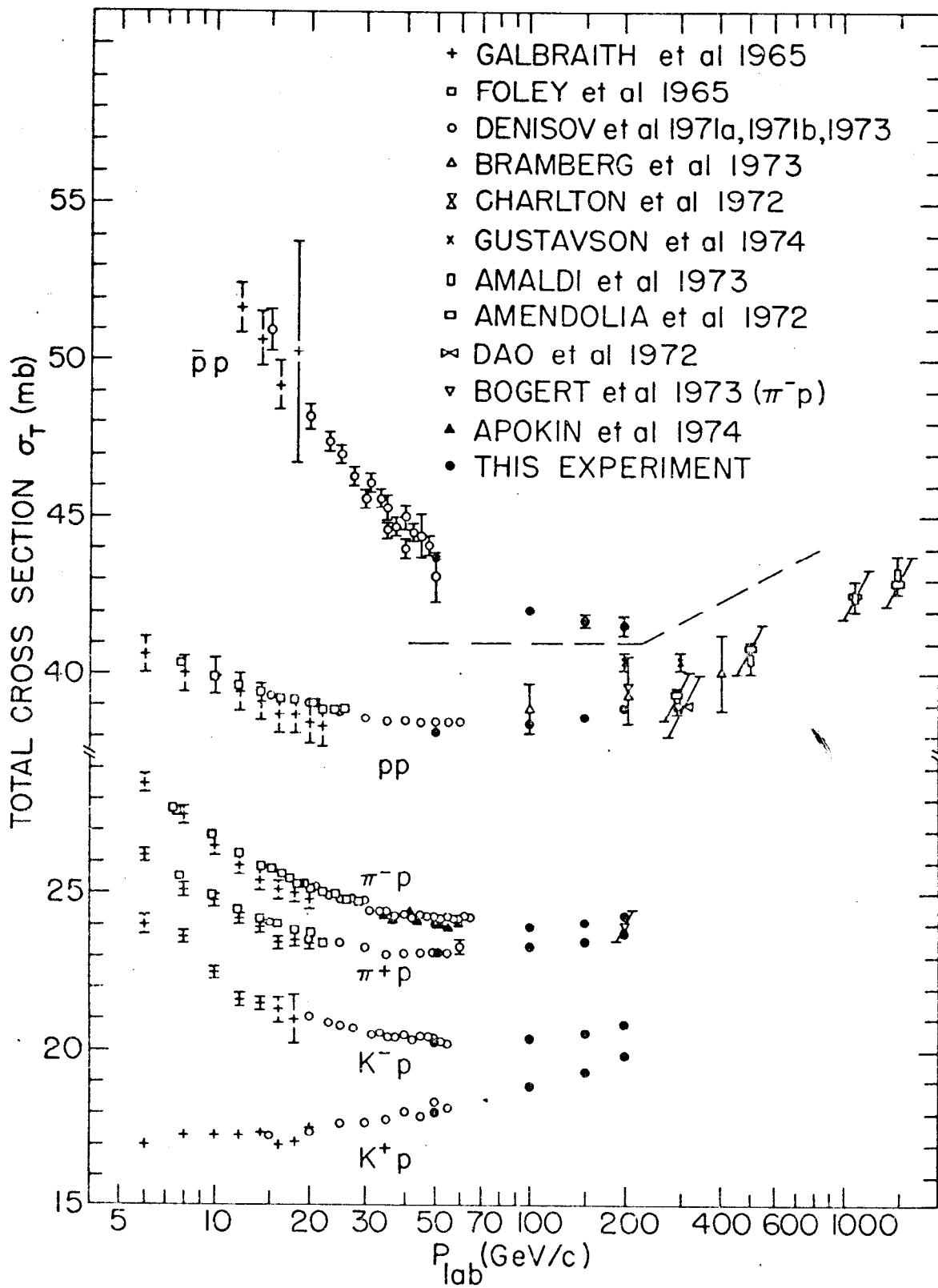


Fig. 1

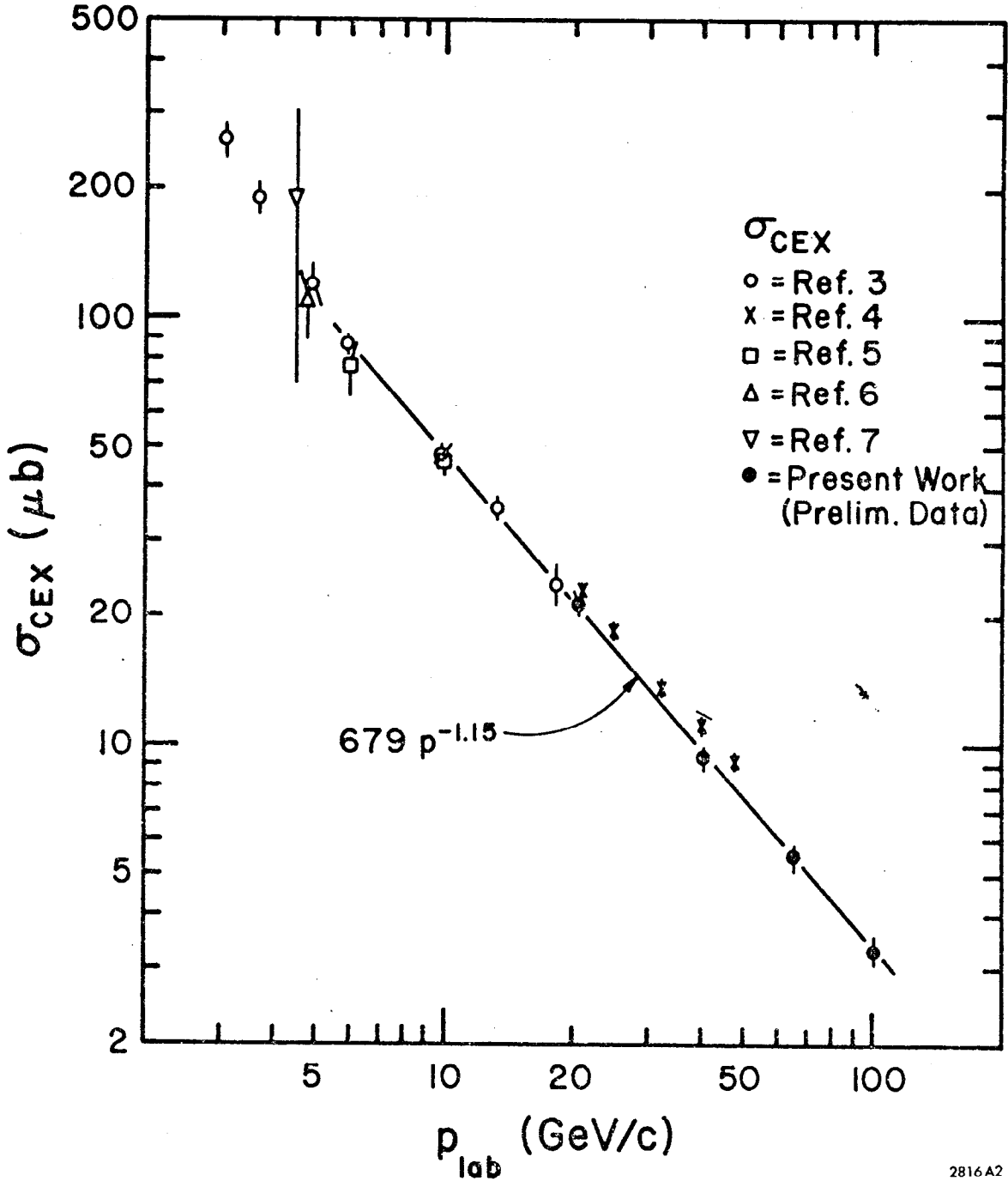


Fig. 2

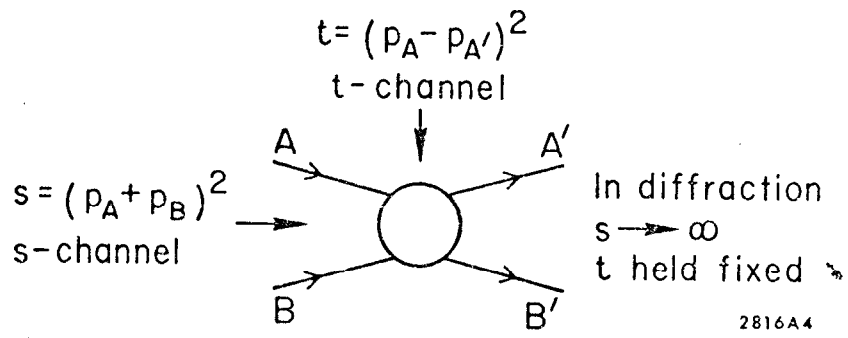


Fig. 3

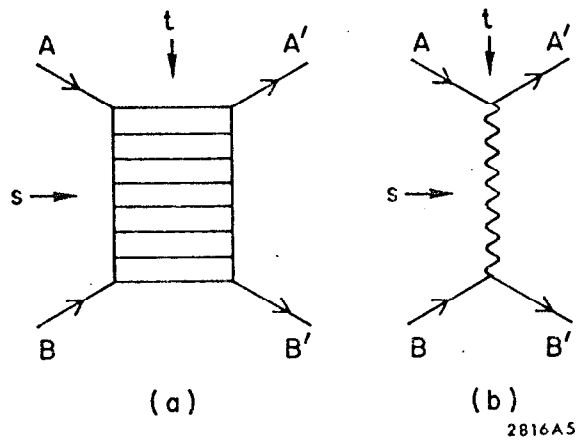


Fig. 4

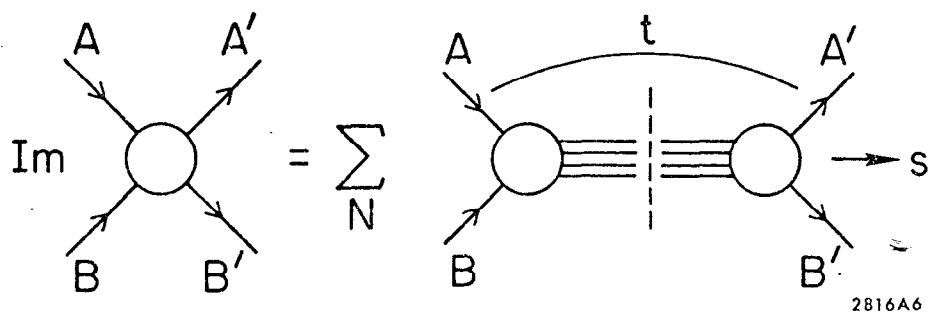


Fig. 5

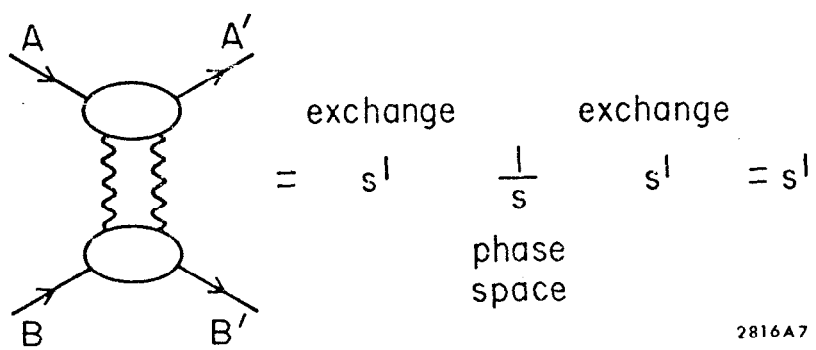


Fig. 6

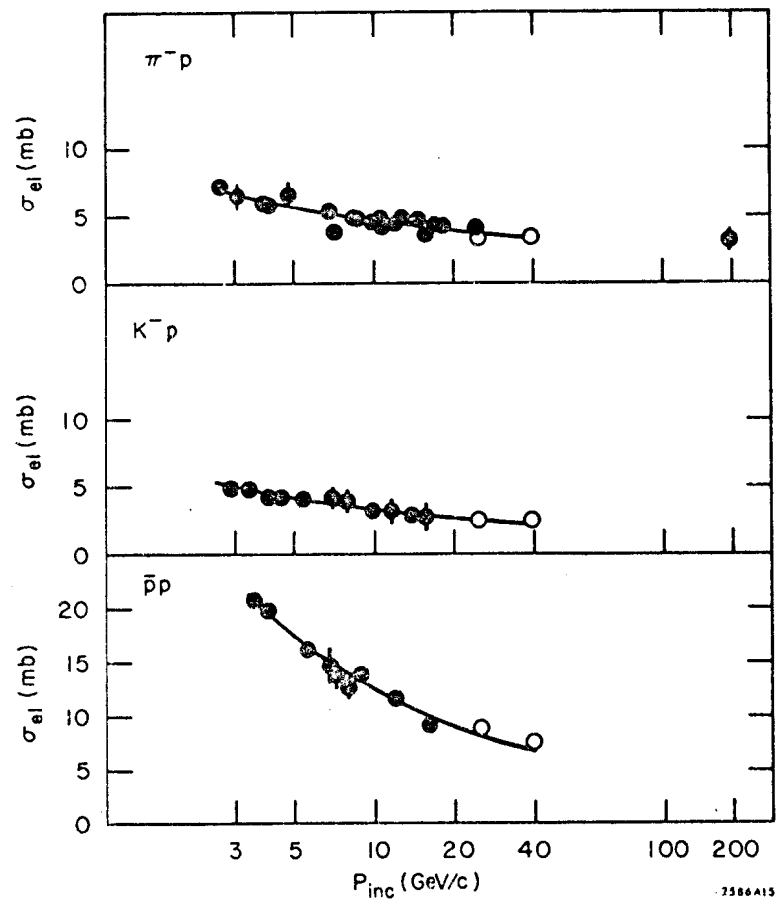
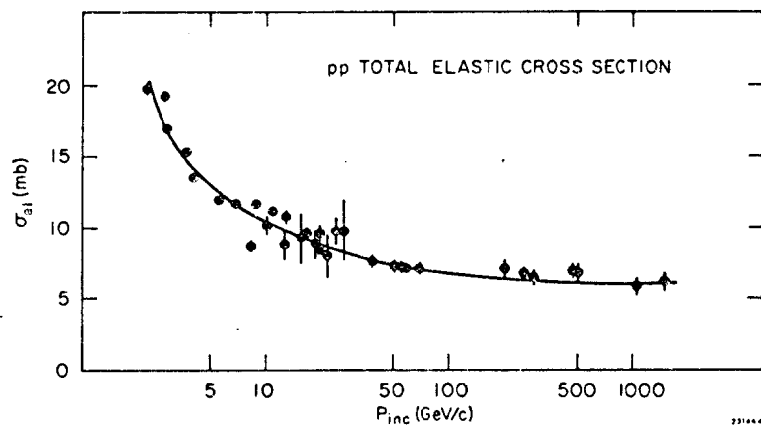
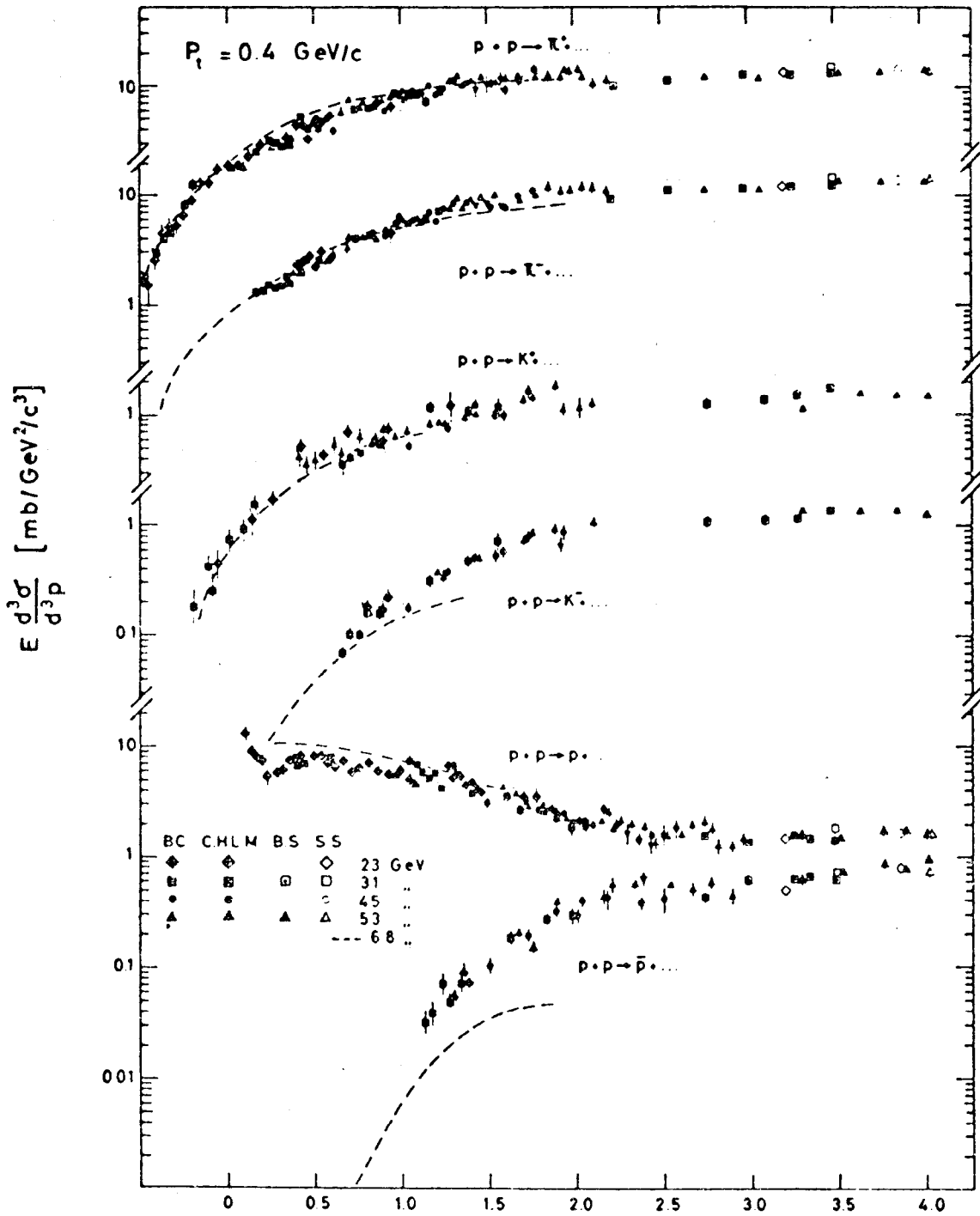


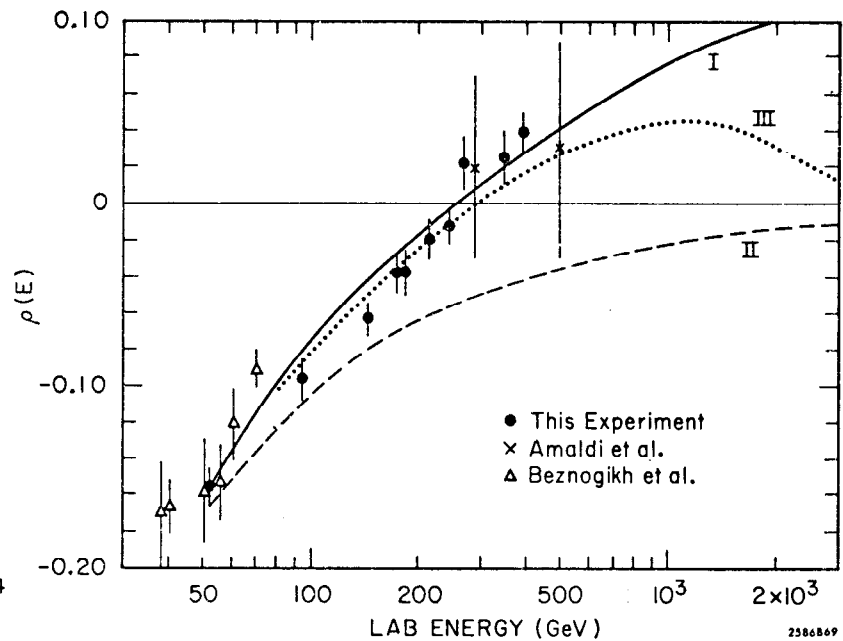
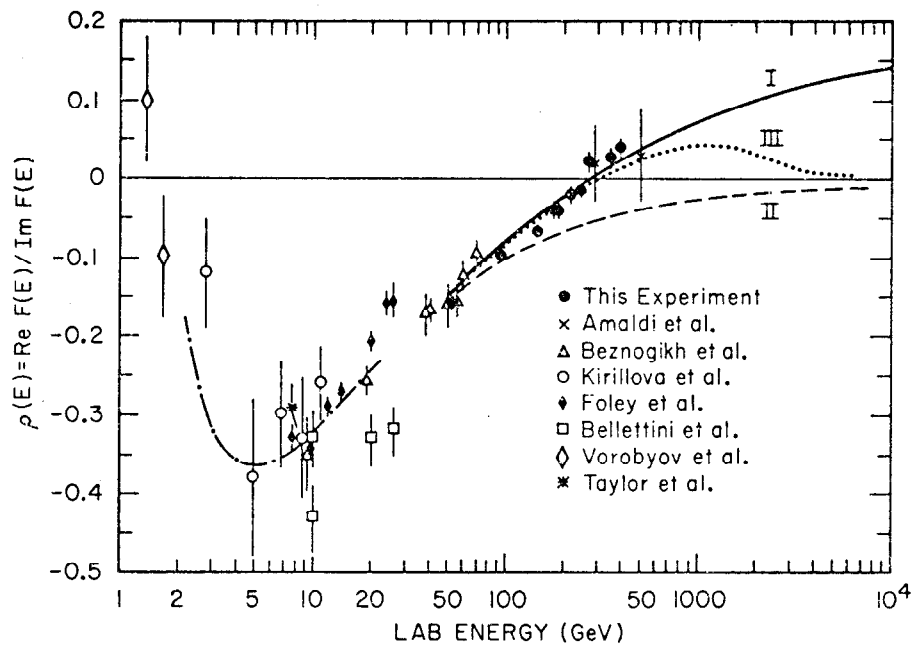
Fig. 7



61710

2316A3

Fig. 8



2586869

Fig. 9

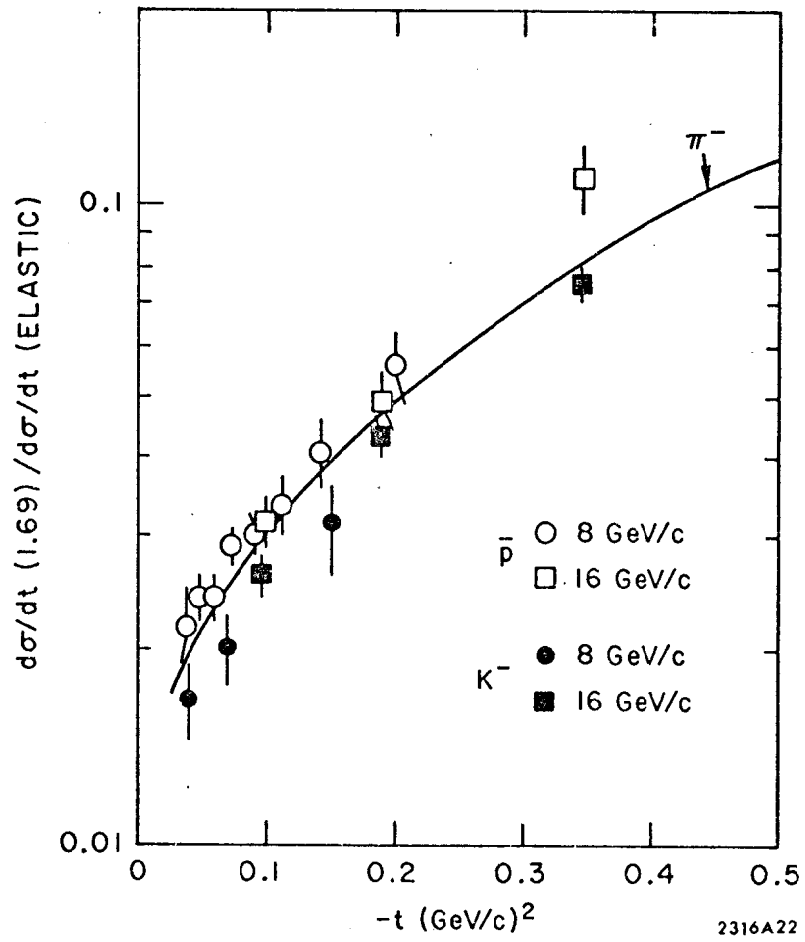


Fig. 10

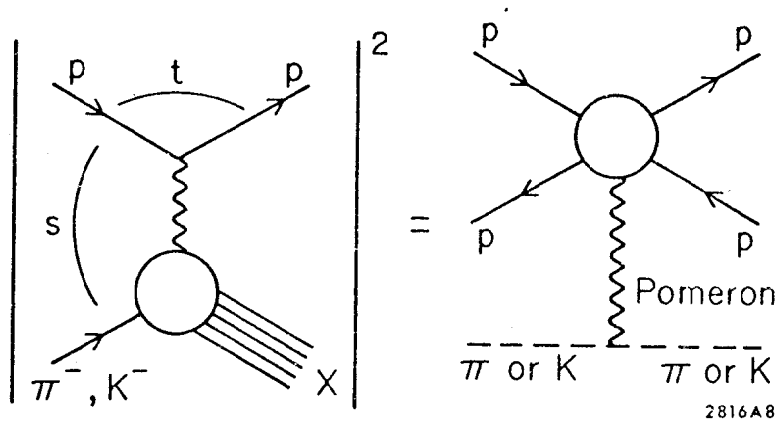


Fig. 11

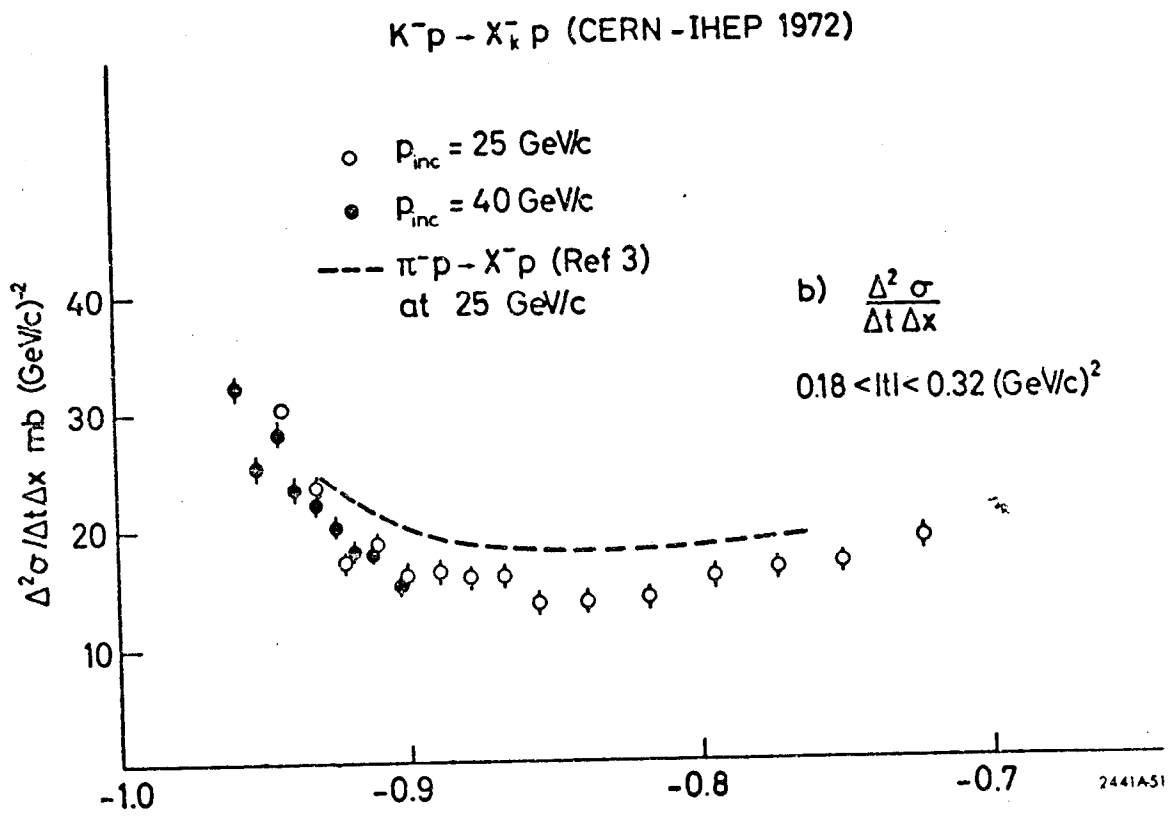


Fig. 12

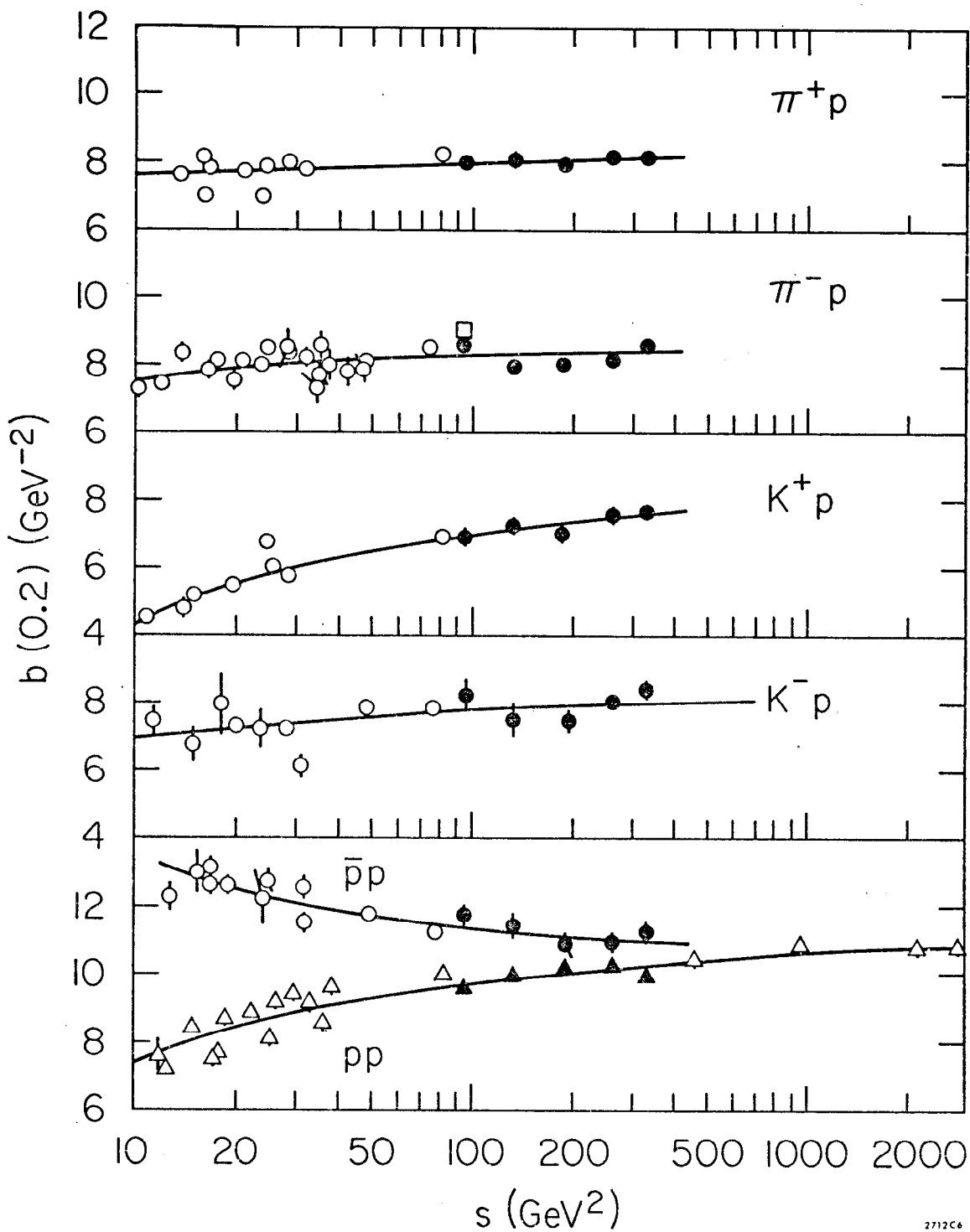


Fig. 13

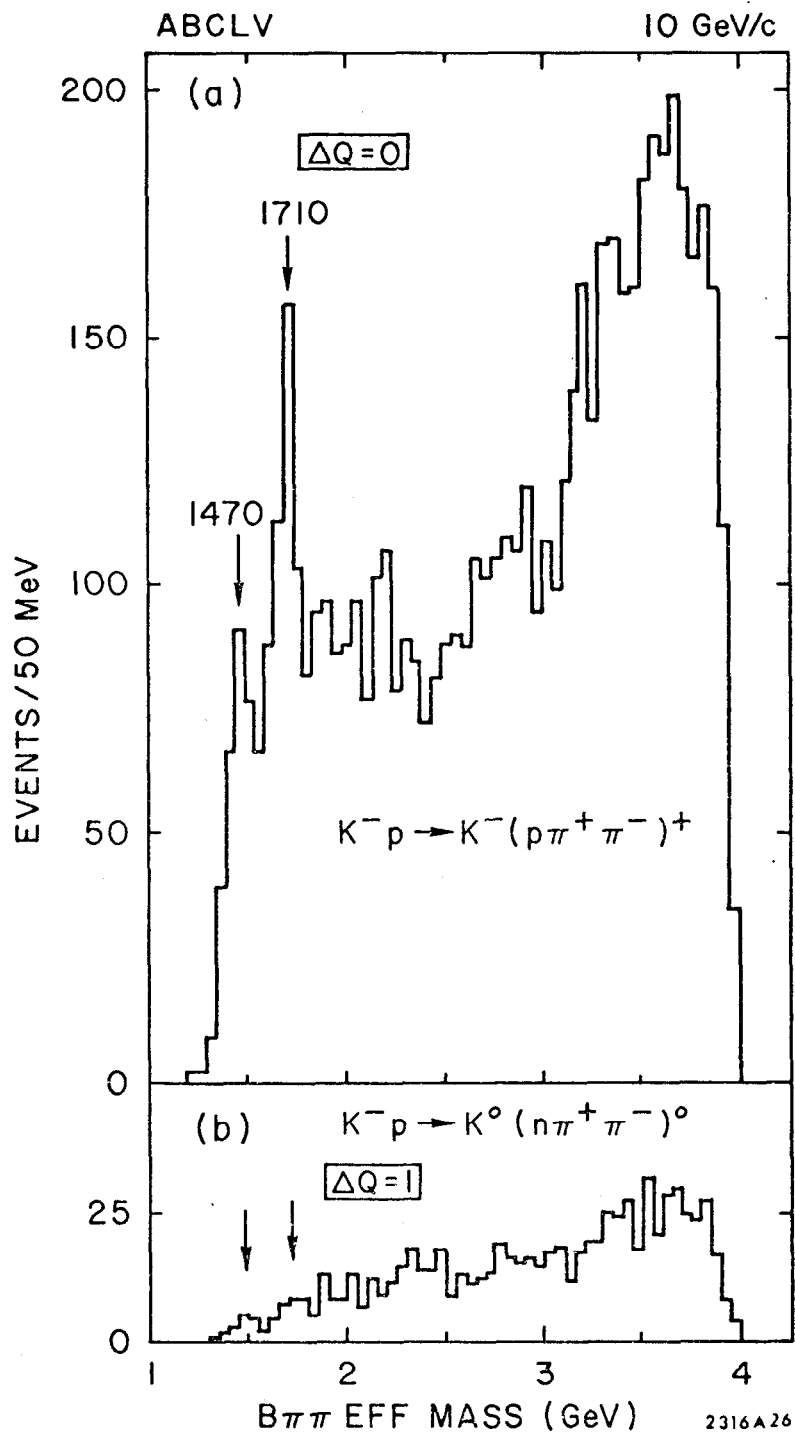


Fig. 14

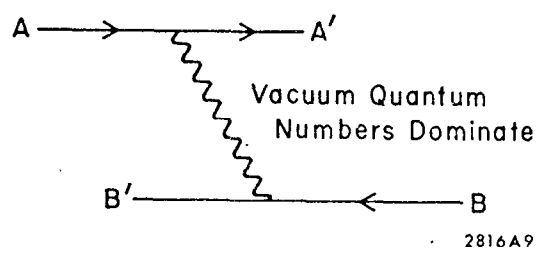


Fig. 15

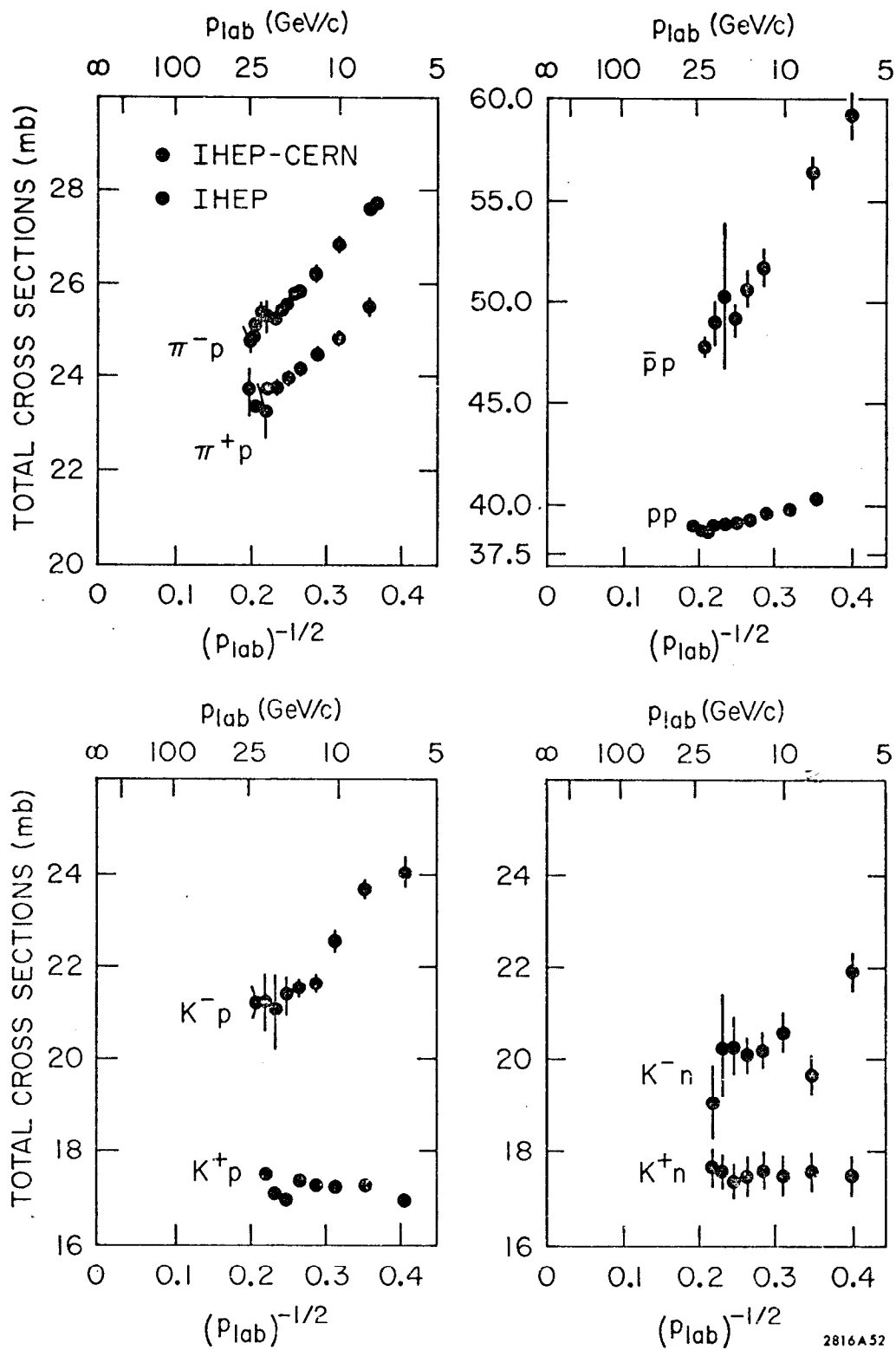


Fig. 16

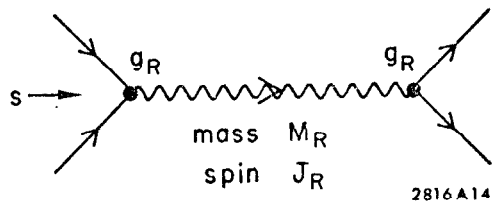


Fig. 17

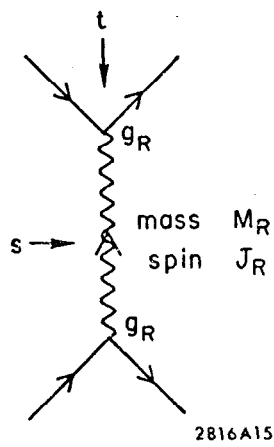


Fig. 18

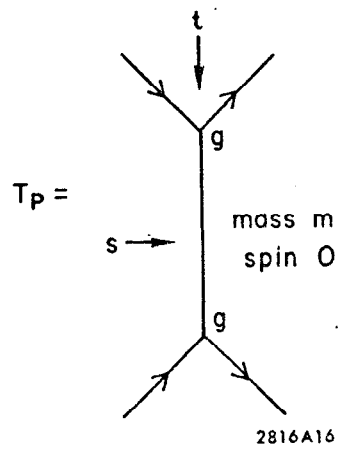


Fig 19

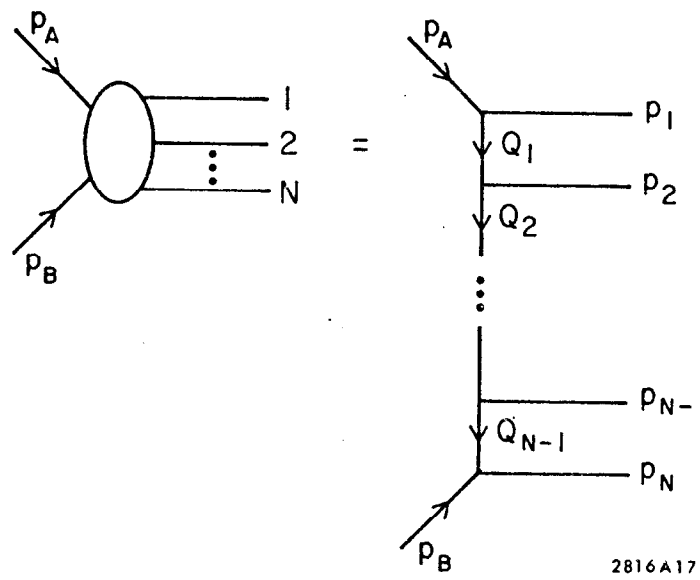


Fig. 20

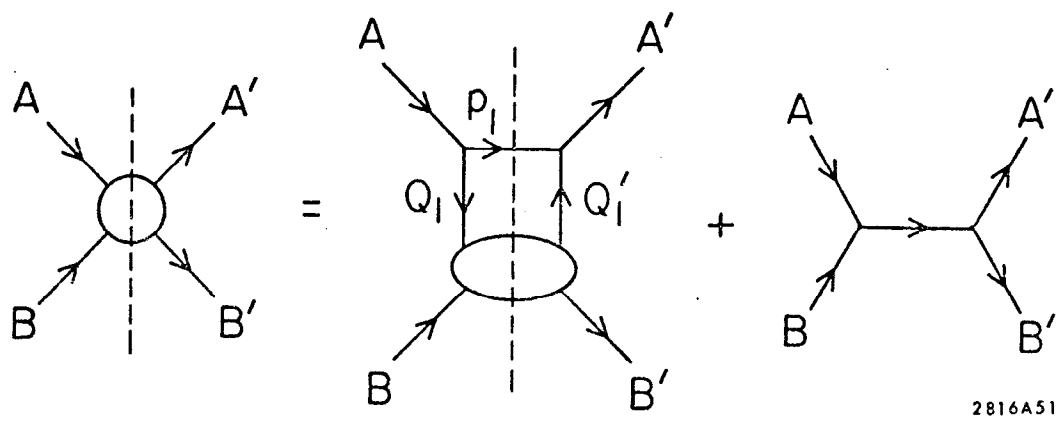
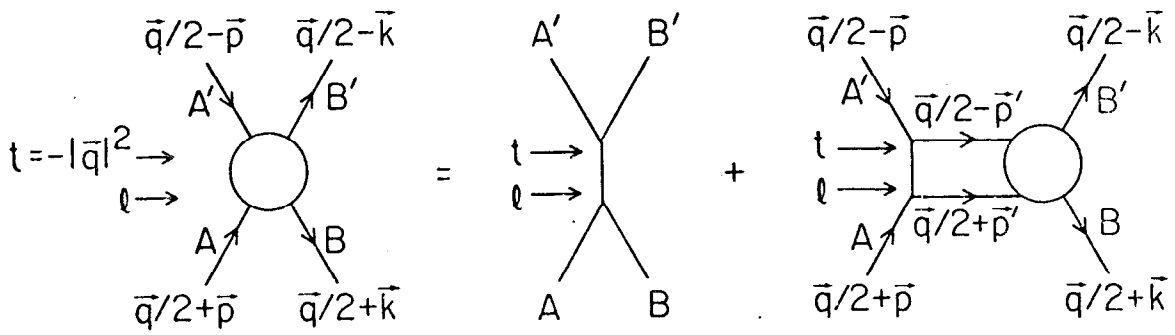
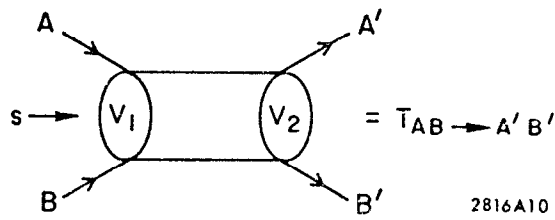


Fig. 21



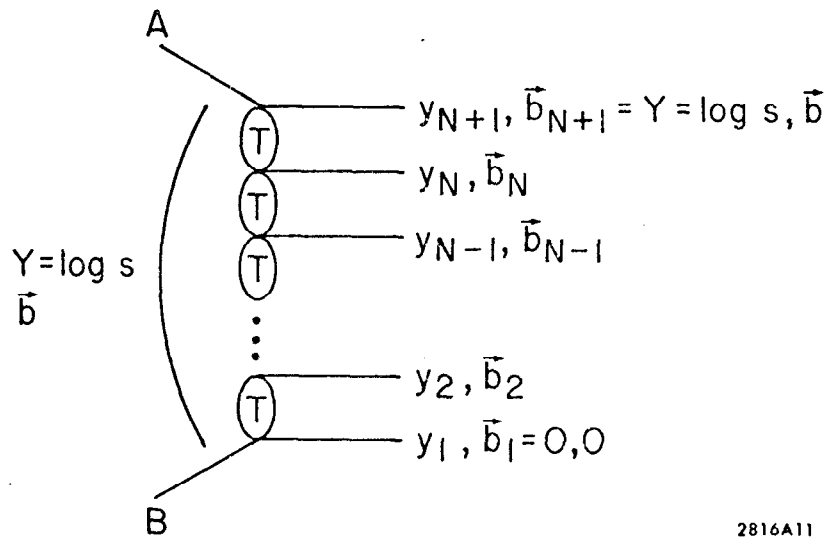
2816A13

Fig. 22



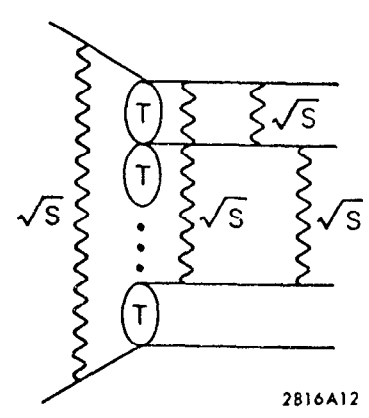
2816A10

Fig. 23



2816A11

Fig. 24



2816A12

Fig. 25

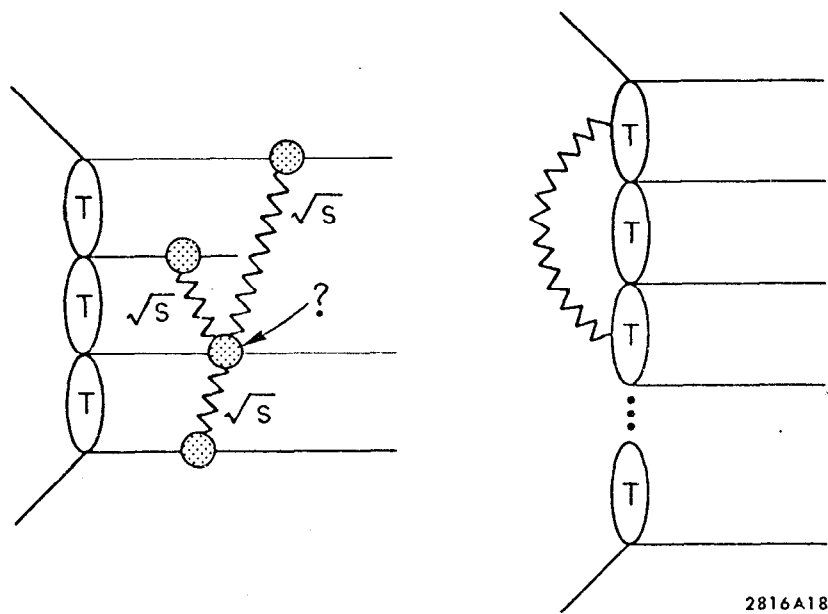


Fig. 26

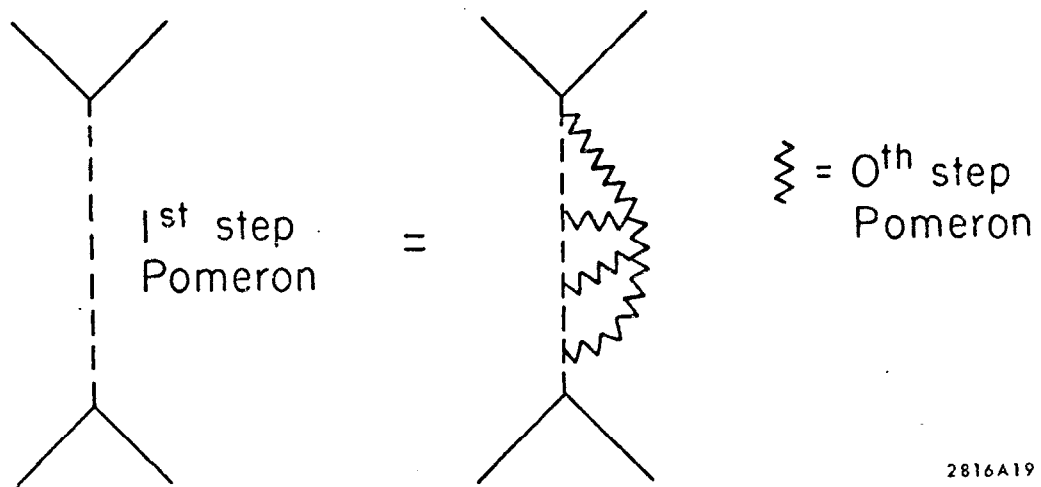
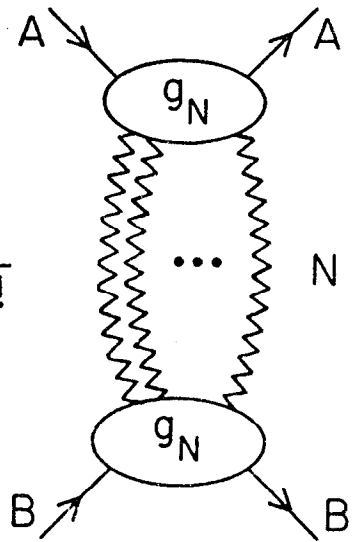


Fig. 27

$$T_{\text{eikonal}}(s, t) = \sum_{N=1}^{\infty} \frac{1}{N!}$$


2816A20

Fig. 28

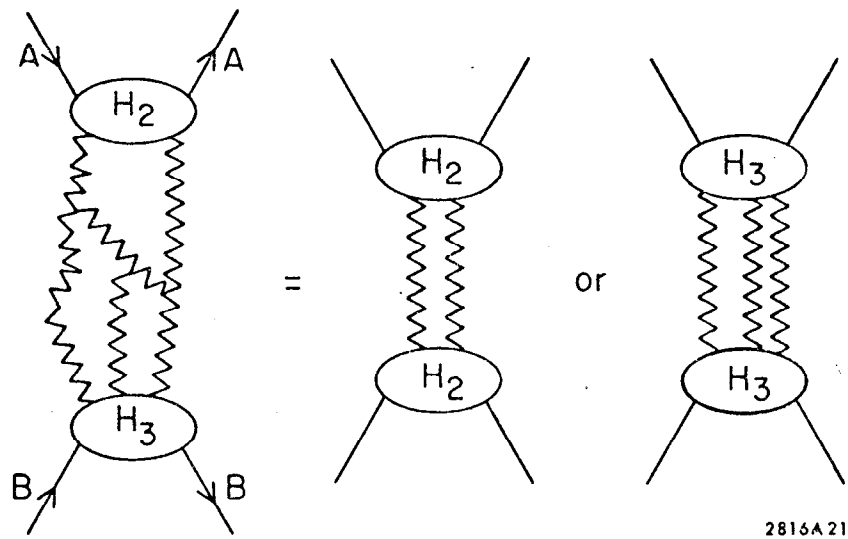


Fig. 29

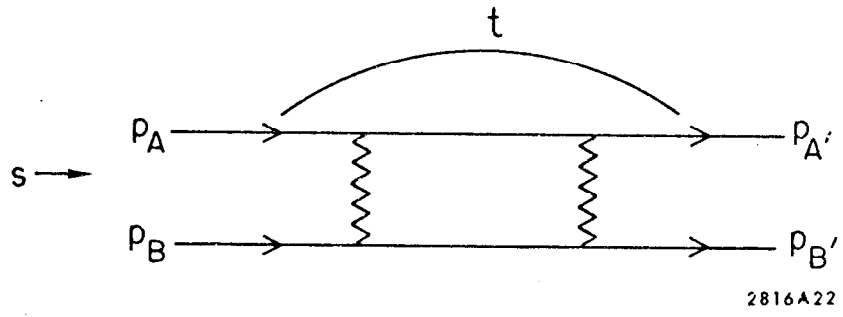


Fig. 30

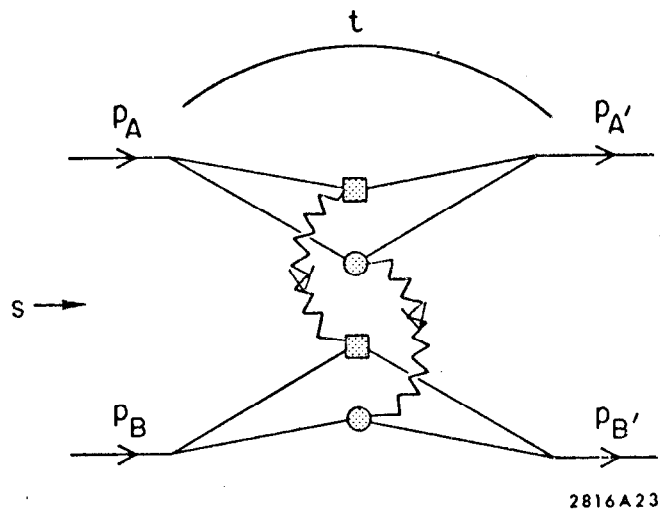


Fig. 31

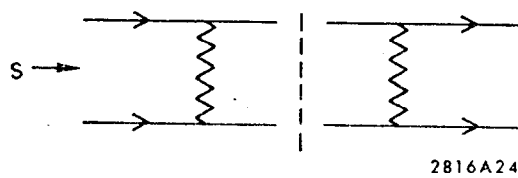


Fig. 32

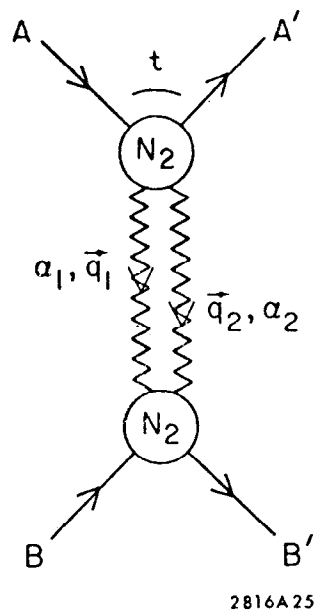


Fig. 33

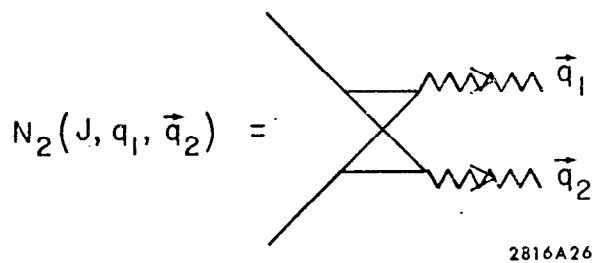


Fig. 34

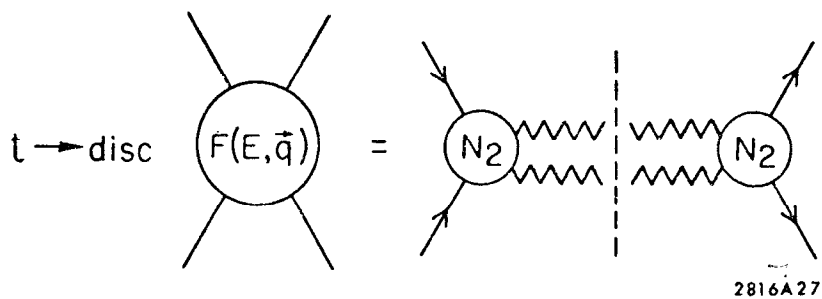


Fig. 35

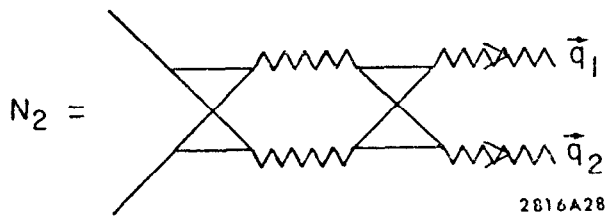


Fig. 36

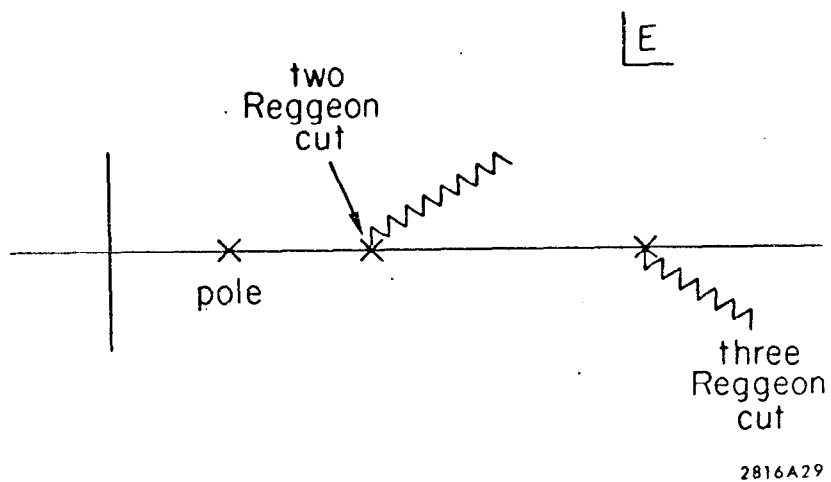


Fig. 37

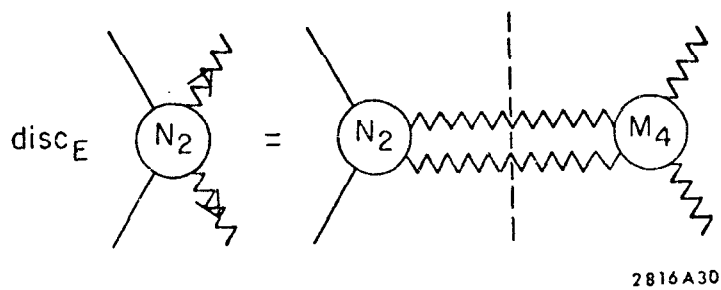
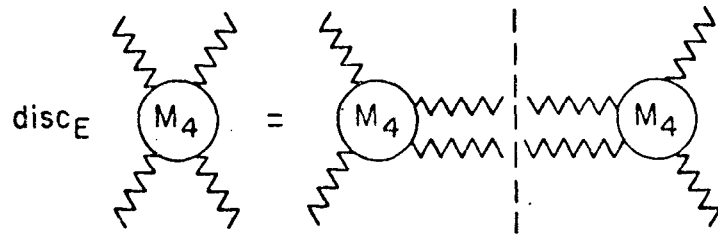
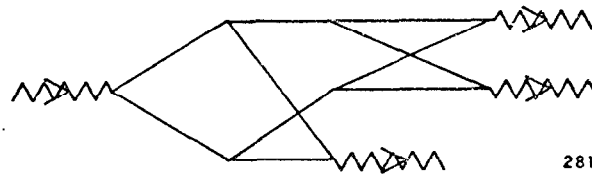
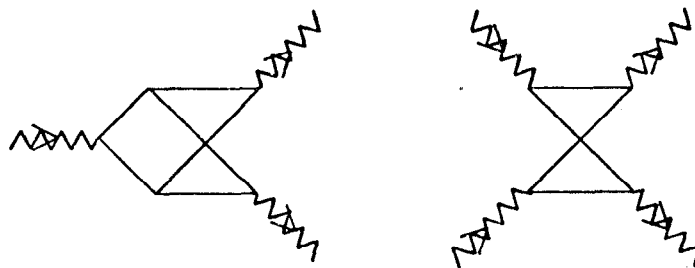


Fig. 38



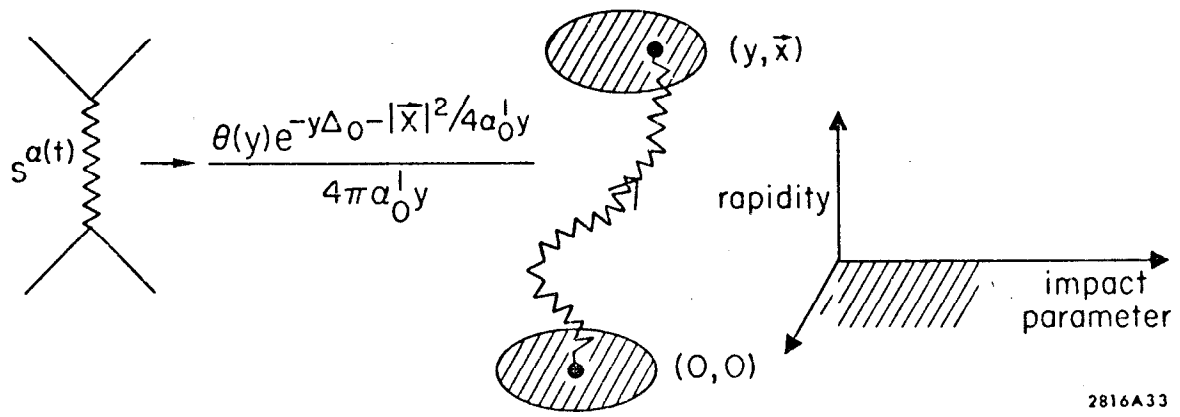
2816A31

Fig. 39



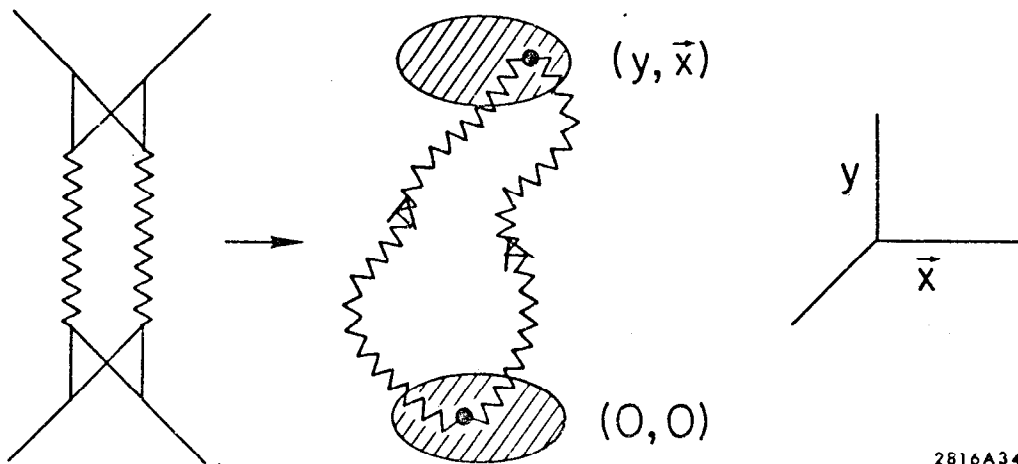
2816A32

Fig. 40



2816A33

Fig. 41



2816A34

Fig. 42

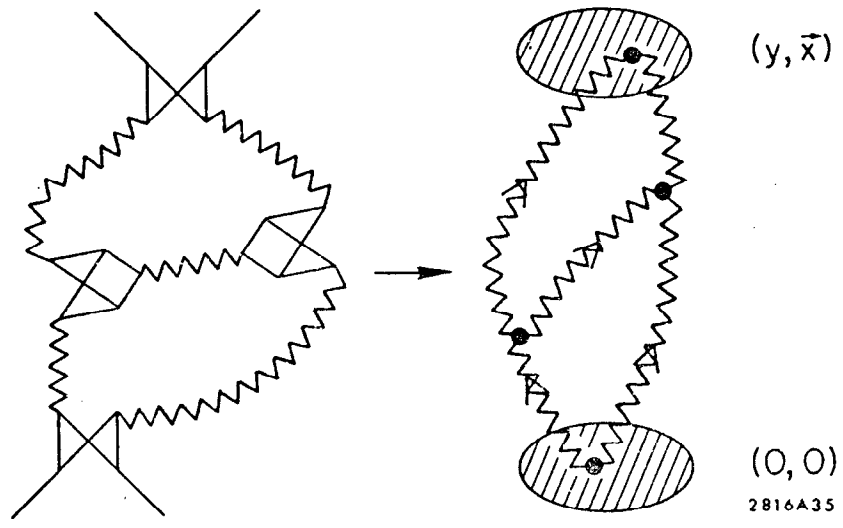


Fig. 43

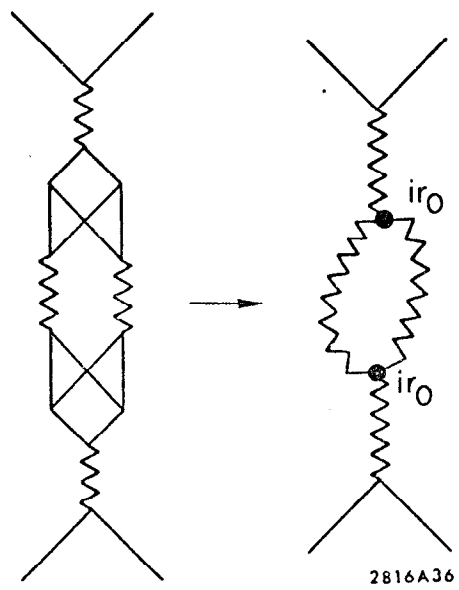
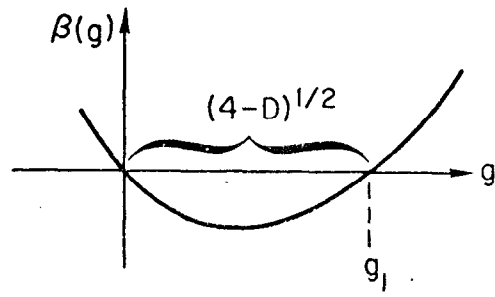
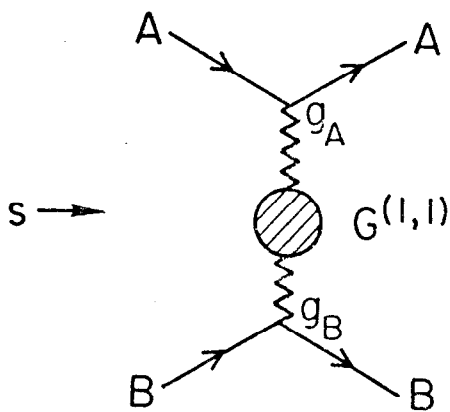


Fig. 44



2816A37

Fig. 45



$$\sigma_T^{AB}(s) \sim g_A g_B (\log s)^{-\gamma}$$

$$+1/4 \lesssim -\gamma \lesssim +1/2$$

2816A38

Fig. 46

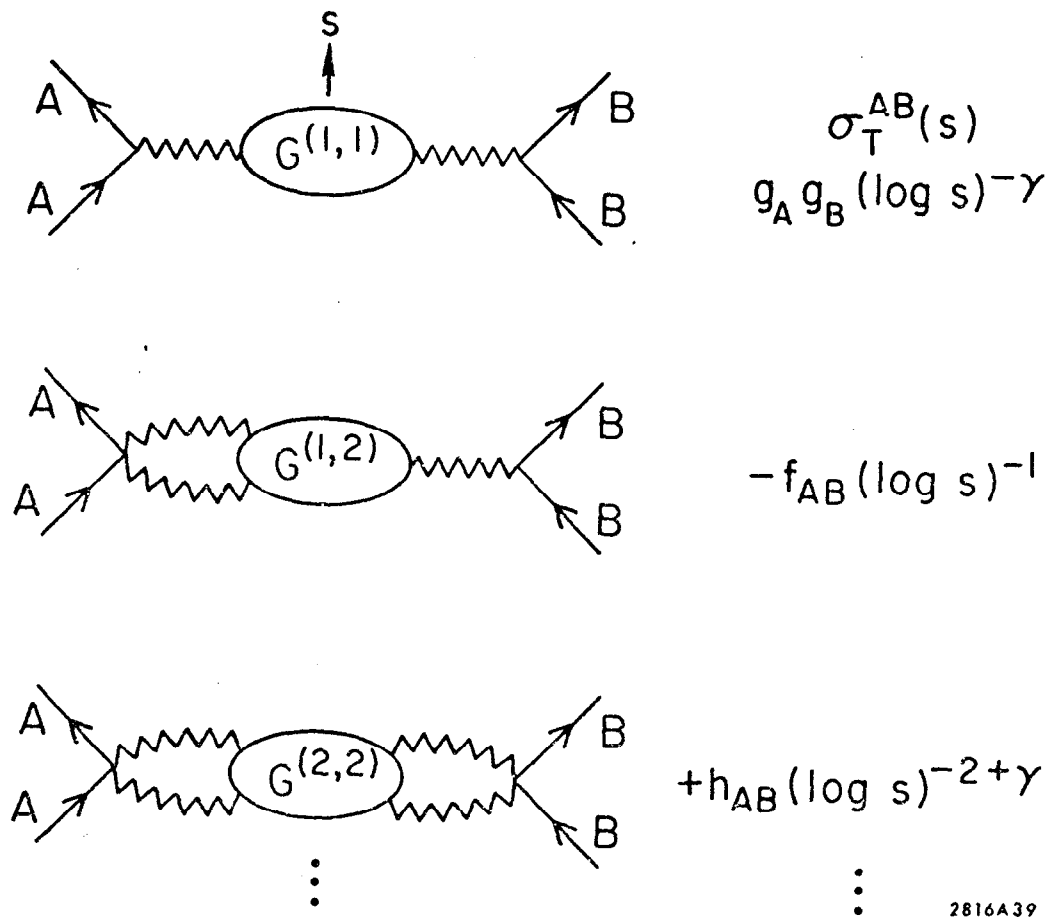


Fig. 47

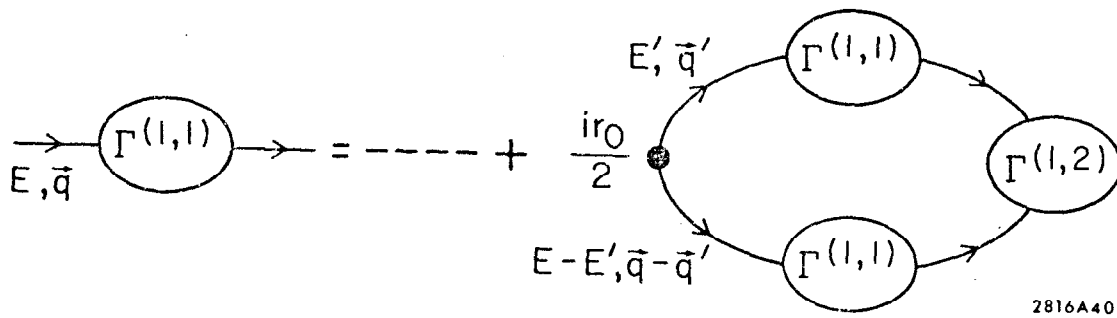
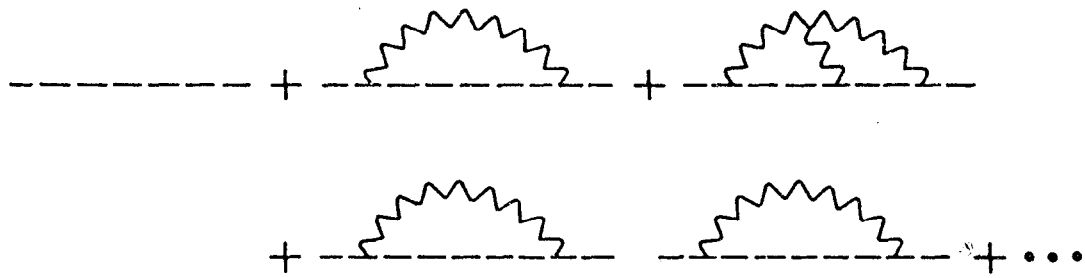
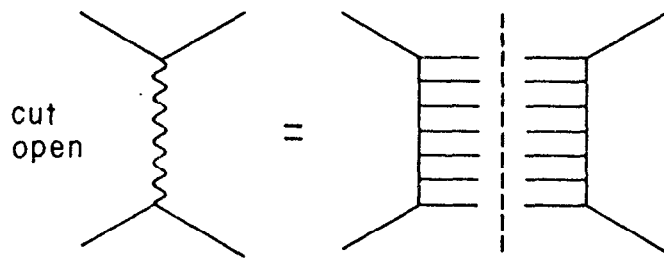


Fig. 48



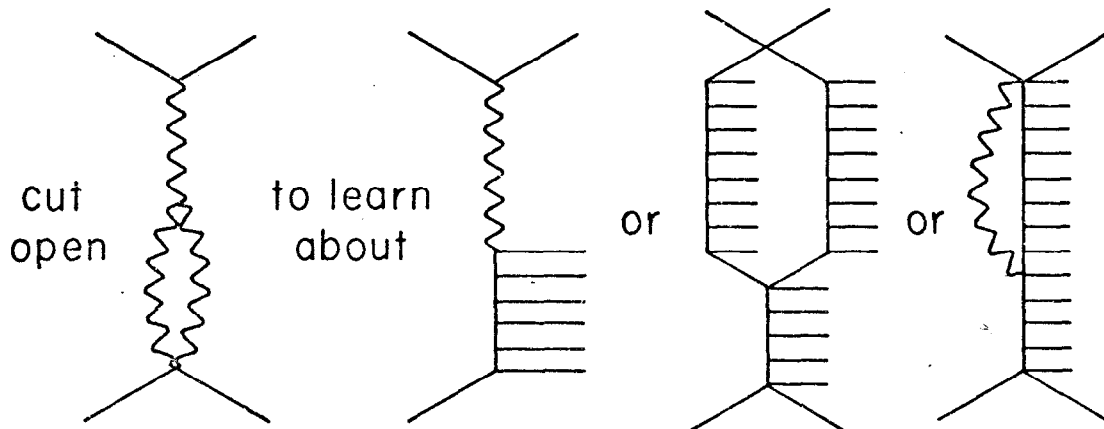
2816A41

Fig. 49



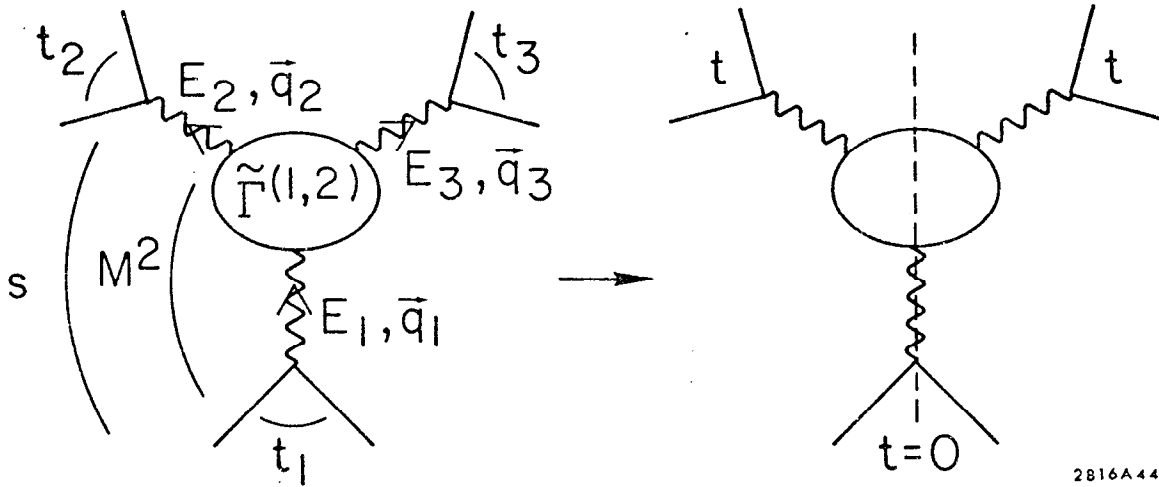
2816A42

Fig. 50



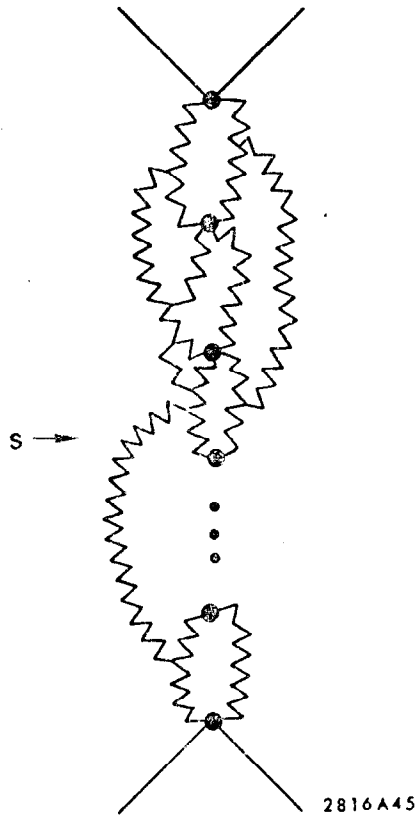
2816A43

Fig. 51



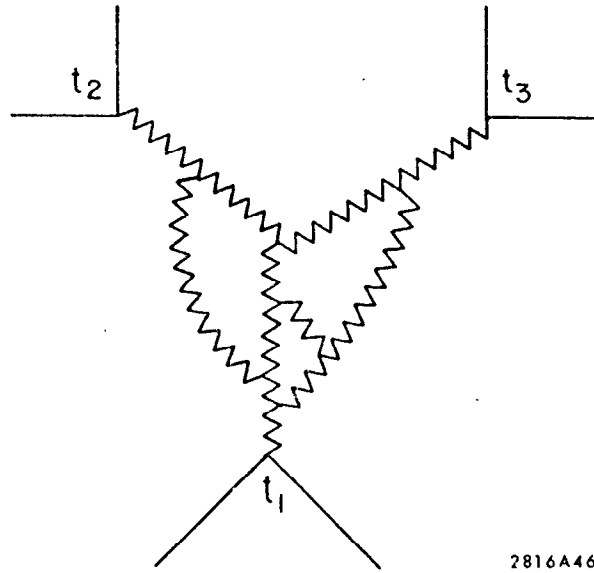
2816A44

Fig. 52



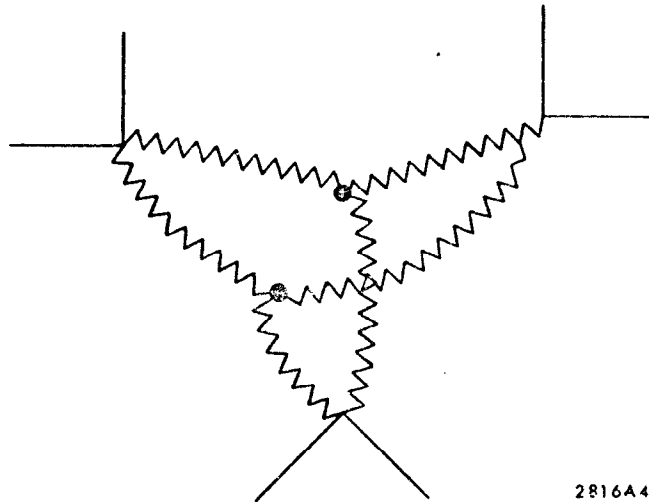
2816A45

Fig. 53



2816A46

Fig. 54



2816A47

Fig. 55

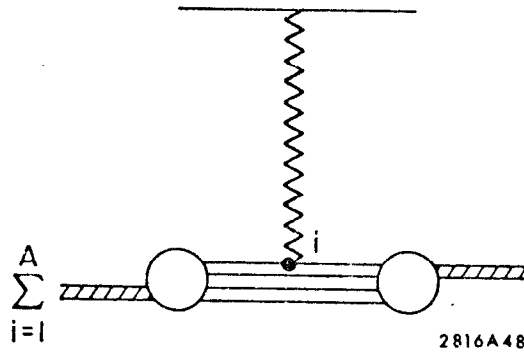


Fig. 56

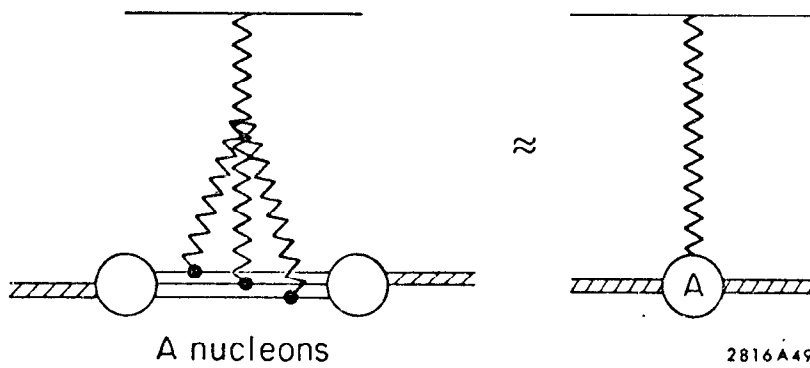


Fig. 57

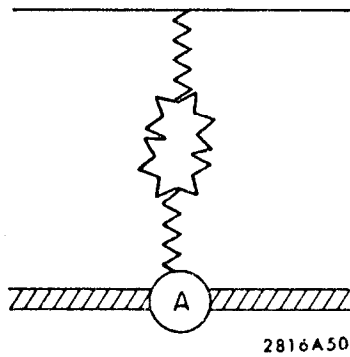
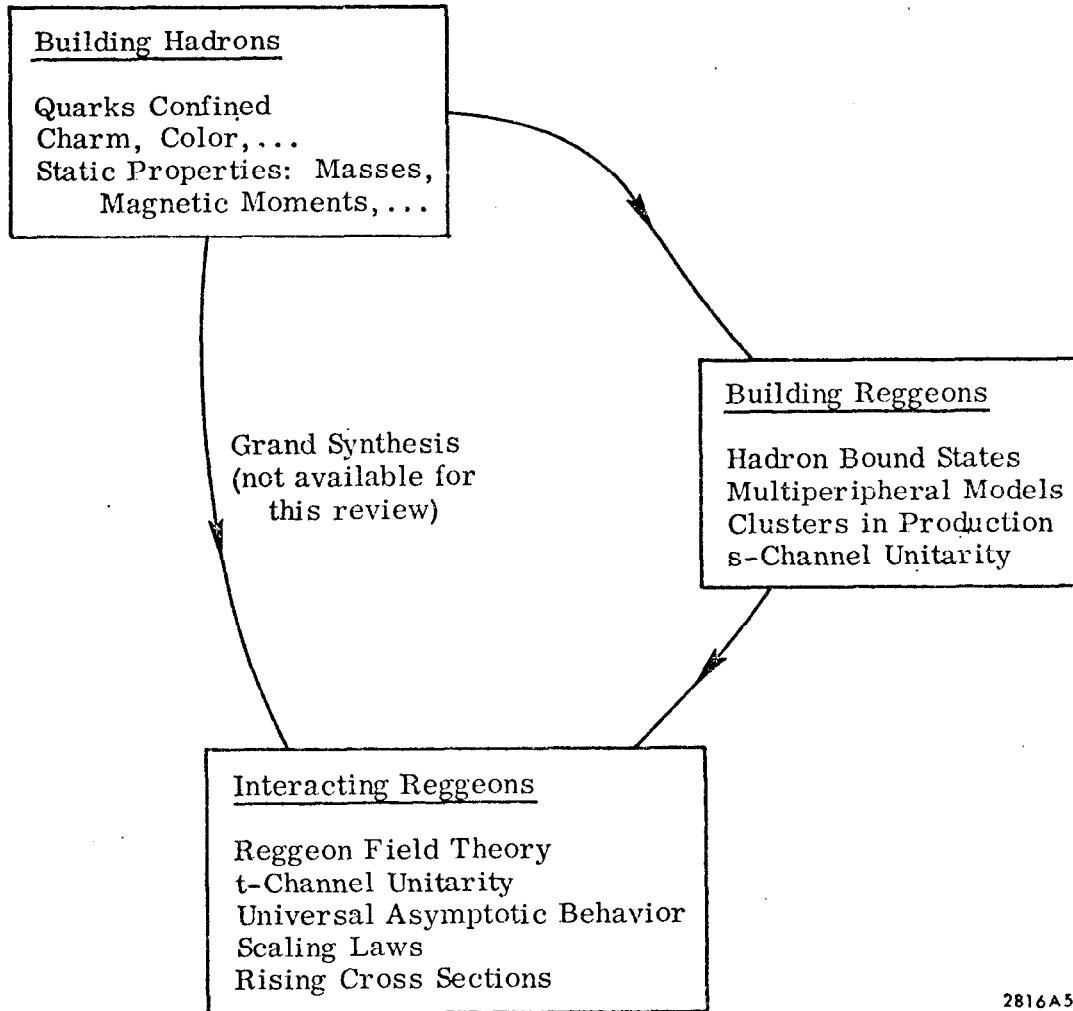


Fig. 58

HIERARCHY OF HADRON PHYSICS



2816A59

Fig. 59